KfK 5381
September 1994

The First Wall Test Facility FIWATKA

- Description of the Facility and Report on Commissioning Tests -

G. Hofmann, E. Eggert
Institut für Angewandte Thermo- und Fluiddynamik
Projekt Kernfusion

Kernforschungszentrum Karlsruhe

KERNFORSCHUNGSZENTRUM KARLSRUHE

Institut für Angewandte Thermo- und Fluiddynamik
Projekt Kernfusion

KfK 5381

The First Wall Test Facility FIWATKA
- Description of the facility and report on commissioning tests -

G. Hofmann
E. Eggert

Kernforschungszentrum Karlsruhe GmbH, Karlsruhe

Als Manuskript gedruckt

Kernforschungszentrum Karlsruhe GmbH
Postfach 3640, 76021 Karlsruhe

ISSN 0303-4003

ABSTRACT

The First Wall Test Facility FIWATKA

A facility for performing thermo-mechanical cycle tests (thermal fatigue tests) was designed and constructed. Such tests are in support of the design of first wall structures for fusion reactors.

The requirements necessary to achieve the test goals are outlined. The facility and its components are described; its upgrading capabilities are discussed.

The main commissioning tests are reported. It is concluded that the facility is ready to perform thermal fatigue tests; the capability of the facility includes the testing of specimens with high surface temperatures.

ZUSAMMENFASSUNG

Der Erste-Wand Prüfstand FIWATKA

Ein Prüfstand zur Durchführung thermomechanischer Zyklus-Tests (Versuche zur thermischen Ermüdung) wurde entworfen und aufgebaut. Solche Tests begleiten und unterstützen den Entwurf von Erste-Wand-Strukturen für Fusionsreaktoren.

Die Anforderungen, die zum Erreichen der Versuchsziele erfüllt sein müssen, werden umrissen. Der Prüfstand und seine Komponenten werden beschrieben; die Möglichkeiten für Prüfstands-Erweiterungen werden diskutiert.

Über die wichtigsten Inbetriebnahme-Versuche wird berichtet. Zusammenfassend wird festgestellt, daß der Prüfstand bereit ist für thermische Ermüdungs-Experimente; die besondere Fähigkeit des Prüfstandes liegt darin, daß Proben mit hohen Oberflächentemperaturen untersucht werden können.

Note

This work has been performed in the framework of the Nuclear Fusion Project of the Kernforschungszentrum Karlsruhe and is supported by the European Union within the European Fusion Technology Program.

CONTENTS

Figures

Tables

1. INTRODUCTION

In near-term fusion reactors of the Tokamak type operation generally consists of a sequence of alternating burn periods and dwell periods lasting only a few minutes each. Power is transferred from the plasma to the first wall (FW) and blanket structures during the burn periods only, while the structures are cooled continuously; this results in a periodic change of the temperature distribution in these structures, accompanied by corresponding stresses and strains which may limit the lifetime of the component by initiation and propagation of cracks (thermal fatigue), by ratcheting or by failure of protection layers. Since composition and a rather complicated geometry of the FW structures do not allow a reliable prediction of the performance and the lifetime with the existing analytical tools, tests with prototypic FW sections seem necessary.

These tests may aim at either producing data for strengthening the analytical tools or proving the performance of a specific design. The goal of strengthening analytical tools asks for a rather simple specimen geometry while the goal of proving the performance allows a high degree of complexity; in both cases very well known thermal and mechanical boundary conditions are mandatory.

In terms of the usual subdivision of tests into small scale, medium scale and integral tests this report describes a test facility capable of conducting tests of the medium scale type. The test facility named FIWATKA (First Wall Test Karlsruhe) was constructed at KfK as German contribution to and supported by the European Fusion Programme. The operation of the facility was started in 1992 with commissioning tests, was continued with R&D tasks for the Next European Torus (NET), and is now facing R&D work for the International Thermonuclear Experimental Reactor (ITER).

2. TESTING REQUIREMENTS AND LIMITATIONS

The test facility may be characterized comprehensively by describing some of the testing requirements and limitations.

Stress/Strain state:
Since the program aims at investigating the consequences of stresses and deformations in a FW component such prototypical stress/strain conditions at adequate temperature levels are required for the test specimens at least in locations of major interest. To be prototypical the stress/strain conditions must be composed of adequate portions of primary stresses, originating from coolant pressure and other mechanical loads, and secondary stresses, originating from nonuniform temperature distributions and thermal elongations.

In FIWATKA primary stresses may be generated by the coolant pressure in the cooling channels of the specimen; the pressure is limited to 15 bar.

Secondary stresses which are of major importance may be generated by applying thermal loads to the plasmafacing surface of the specimen in connection with the mechanical boundary conditions of the specimen's clamping to be chosen; thermal loads are limited to heat fluxes of approximately 80 to 120 W/cm^2 depending on the resulting surface temperature and on the emissivity of the specimen concerned.

In view of thermal fatigue and ratcheting failures the cyclic change of thermal loads reflecting the tokamak operation is an essential requirement of the tests and can be realized within wide limits, i.e. heat loads may be applied within 15 seconds and may last any time up to steady state operation. Internal heat sources in the specimen cannot easily be

simulated in the specimen; they seem of lesser importance for the FW zone since the temperature field in this front zone is dominated by the surface heat flux; if in addition the impact of large area temperature differences between the front and back zones of a thick specimen on local stresses has to be addressed an adequate temperature field may be generated by adjusting the local coolant temperatures.

Temperature level:
The temperature level at the specimen may be an important parameter for the properties of the materials concerned.
The temperature of the coolant is the basis on which any temperature profiles caused by the heat load will build up. The coolant temperature at the outlet of the specimen is limited to 120 °C with the present components of the water circuit. Local temperatures in the specimen may reach up to 1800 °C depending on the individual design and the heat flux applied.

Atmosphere:
For tests with high surface temperatures at the specimen a vacuum or inert atmosphere is necessary to avoid chemical reactions. In addition in cases where the FW includes protection tiles with radiative heat transfer between the tiles and the metal structure a vacuum atmosphere is necessary to avoid heat transfer by conduction and convection in the gap. In the test vessel the vacuum is limited to approximately 10^{-4} mbar.

Beryllium handling:
Some designs include Be as a protection layer on the FW or on the limiters. The FIWATKA facility is not equipped to handle Be since poisonous Be dust may be generated as Be faces the very high temperature heating elements or as the heater contacts Be at failure. The test vessel is not contained in a controlled atmosphere.

Specimen size:
The test facility was built for medium sized specimens; such specimens should be large enough to investigate technological questions including combined effects rather than purely fundamental tasks. In most cases they exhibit full size details but represent a section of the whole structural part only.
The specimen size for FIWATKA is limited by the maximum power of roughly 400 kW received by two specimens or 300 kW if there is only one specimen. It is also limited by the available space in the vacuum vessel which allows for a length and width of the heated surface of about 75 cm each and a specimen depth of roughly 40 cm.
The orientation of the heated surface needs to be vertical. More information on the possibilities of upgrading may be found in chapter 4.

3. DESCRIPTION OF THE FACILITY

3.1 General Setup

As shown in Fig. 1 there is a flat heater arrangement hanging vertically in the center of a vacuum vessel. FW specimens are facing this heater from both sides receiving their heat load by thermal radiation; if only one side of the heater should be occupied by a specimen there will be a dummy heat sink facing the back side possibly being separated from the heater by a radiation shield. Around the edges of the heater there is a water-cooled structure which together with the specimens forms a closed housing around the heater such that only a very small fraction of the heater power may reach the vacuum vessel through any gaps and instrumentation holes in the heater housing. The specimens and the remainder of the heater housing are water-cooled continuously while the power to the heater is turned on/off periodically to produce the cyclic heat load and the resulting stress/strain for the specimens. A vacuum vessel encloses the setup described so far.

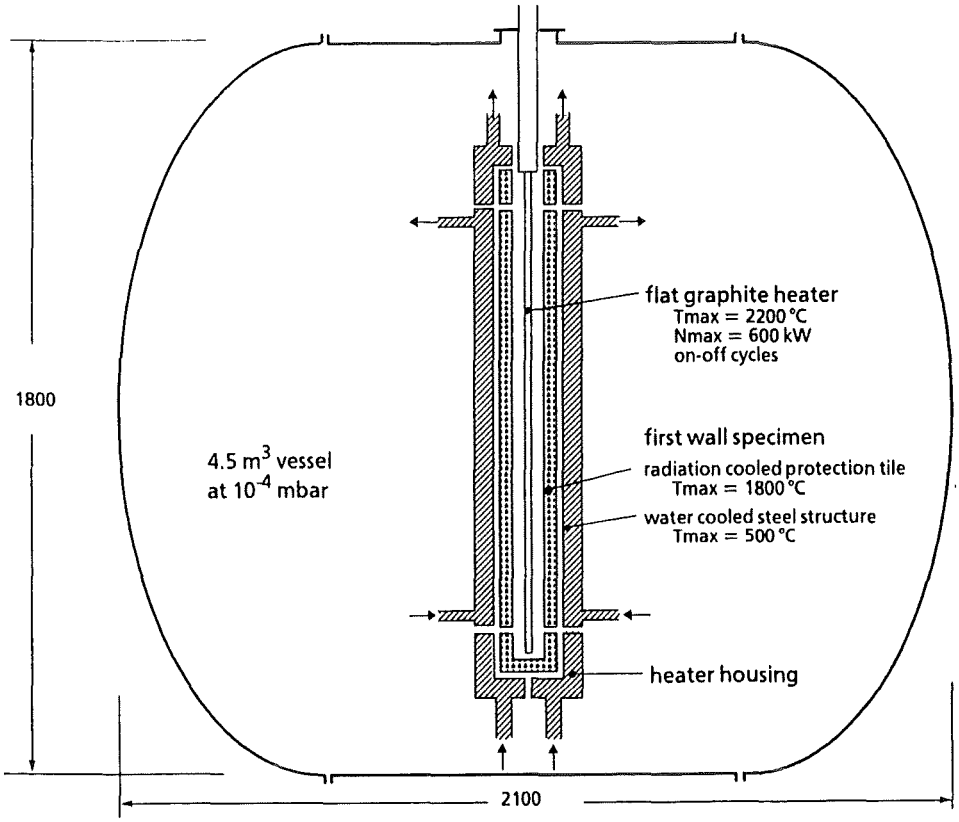

Fig. 1 Test Setup (schematic)

The simplified flow chart of Fig. 2 shows the peripheral parts of the facility:
- the cooling circuit I withdrawing the power received by the heater housing including the specimens
- the smaller cooling circuit II withdrawing power from the vacuum vessel and from the electrical power cables
- the electrical power supply
- the vacuum pumping system
- and, for safety reasons, an exhaust and a flooding gas system.

The facility operation is automated such that long-term tests with thousands of heating cycles are possible.
The main characteristics of the facility are summarized in Tab. 1; the components are characterized individually in the following chapters.

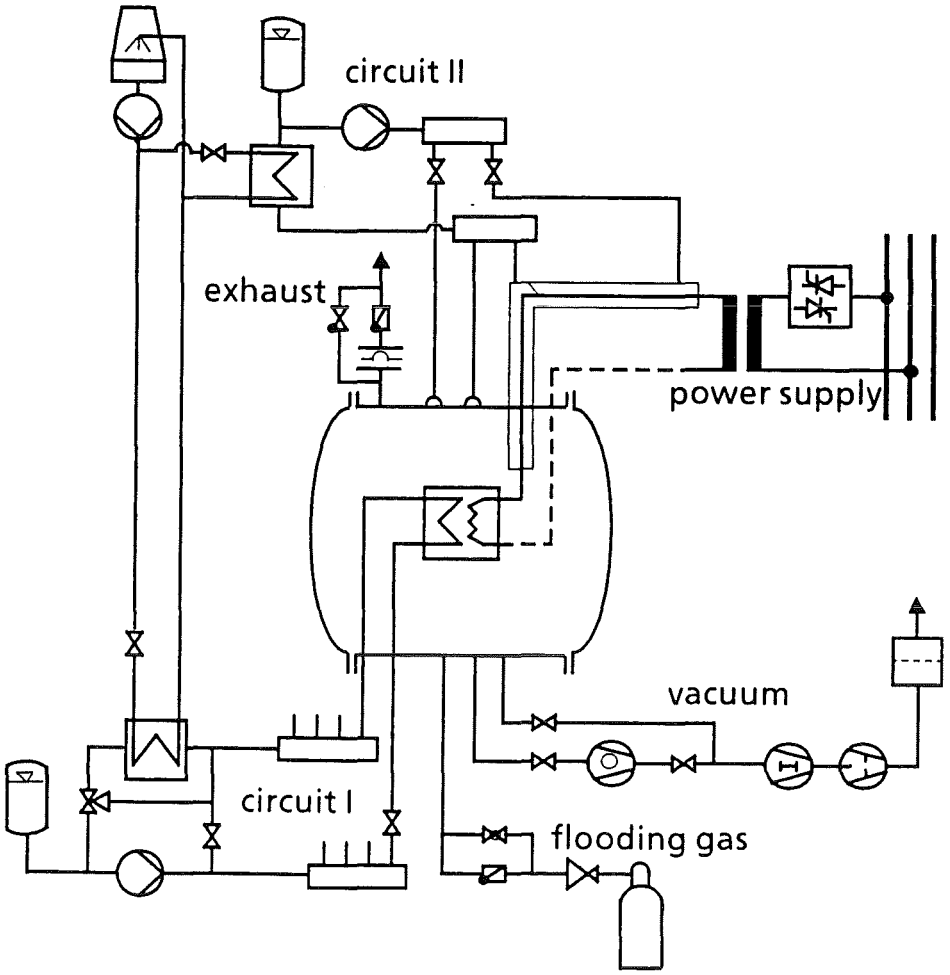

Fig. 2 Flow Chart (simplified)

Vacuum Vessel	Pressure Temperature Volume	$-1/+1$ bar 120 °C 4.5 m^3
Vacuum Pumps	Turbo Pump Backing Pumps	500 l/s at $<2 \cdot 10^{-3}$ mbar 400 m^3/h at 10^{-2} mbar
Cooling Water Circuit I	Pressure, max. Temperature, max. Flowrate, max. Power, nom.	16 bar 120 °C 80 m^3/h 600 kW
Cooling Water Circuit II	Pressure, max. Temperature, max. Flowrate, max. Power, approx.	7 bar 50 °C 4.8 m^3/h 90 kW
AC Power Supply (3 Phases)	Voltage, max. Current, max. per phase Power, max. per phase	180 V 3500 A 378 kW
Radiative Heater	Temperature, max. Area, each of two faces	2200 °C max. 0.25 m^2

Table 1 FIWATKA Main Characteristics

3.2 Vacuum Vessel

A stainless steel vessel (Figs. 3-5) provides the vacuum atmosphere and ample room (4.5 m^3) for test arrangements of variable sizes. The vessel consists of a cylindrical section (1.77 m ID and 1.14 m long with a horizontal axis) and of two vaulted covers connected to it by big flanges (Fig. 4); at the flanges there are two concentric 0-ring seals made of Viton with the possibility of vacuum pumping the gap. The covers are held with 12 easily removable clamp bolts each and since the covers hang on bracket jib cranes they may be easily swung open; this offers fast and full access to the internals of the vessel from both sides. Vessel feed-throughs are built into the cylindrical section only, namely

- for cooling water 8 stubs DN 100 on the diagonals (designated C on Figs. 4-5),
- for electric power 6+2 stubs DN 63 at the top (designated A),
- for vacuum pumping 2 stubs DN 160 and DN 100 to the south (designated D and E),
- for instrumentation cables 16 stubs DN 40 to the north (designated G),
- for inert gas inlet and water drainage 1 stub DN 63 at the bottom (designated H)
- for exhaust 2 stubs DN 150 and DN 25 at the top (designated B and N), and
- for extra use 2 stubs DN 63 at the top (designated H).

The two big removable covers do not carry any feed throughs except 3 stubs DN 160 (designated K, L. and M) for sight glasses. The vessel including the covers is slightly cooled by water passing through semicircular cooling channels which are welded to the vessel outside, they are spaced 115 to 215 mm one to each other and are designed for a pressure of 10 bar; this cooling may withdraw heat of some radiation leaking through the heater housing and hitting the vessel's inner surface.

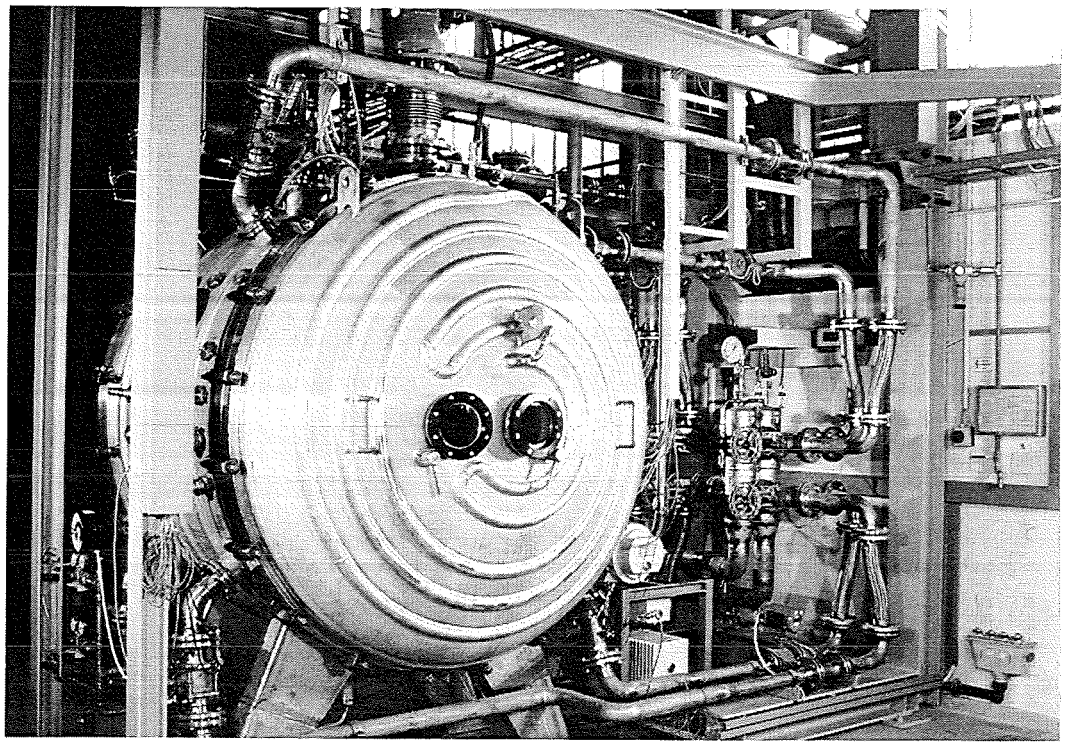

Fig. 3 FIWATKA Facility

The vessel is made of stainless steel according to material specification DIN 1.4301 and is designed to withstand internal pressures between vacuum and 1 bar gauge at a maximum temperature of 120 °C resulting in a wall thickness of 6 mm. Pressures above atmospheric may be encountered if the cooling system leaks into the vessel and/or the leakage is evaporated in contact with hot structures in the vessel; safety aspects are discussed in chapter 3.10.

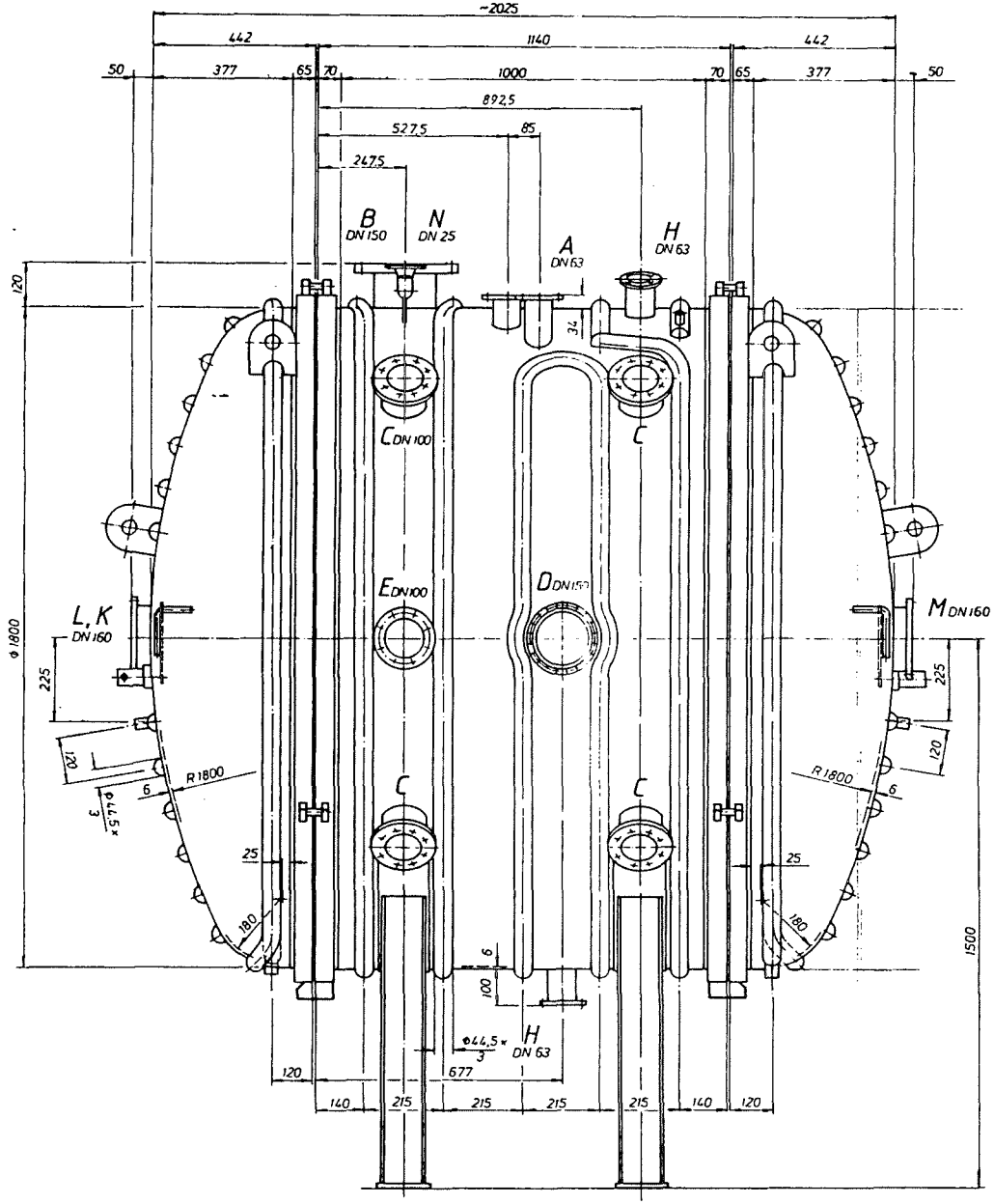

view from south

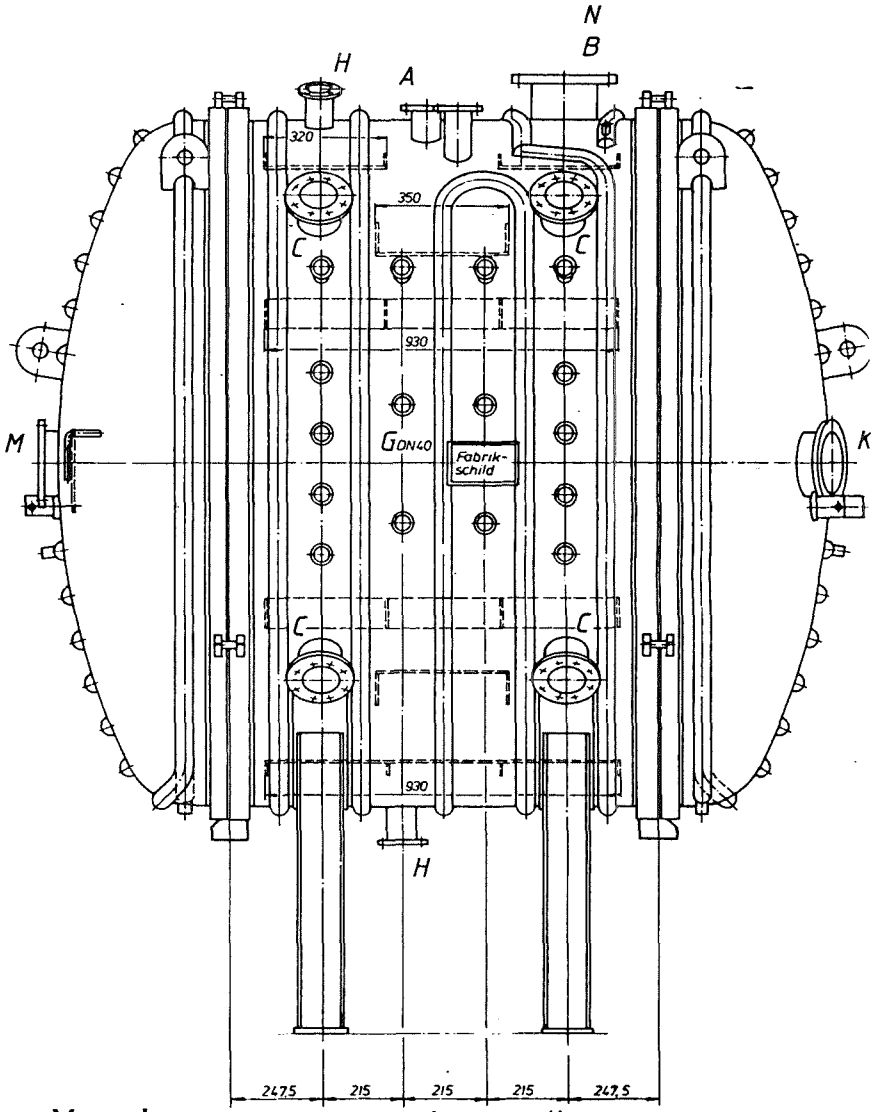

view from north

Fig. 4 Vacuum Vessel

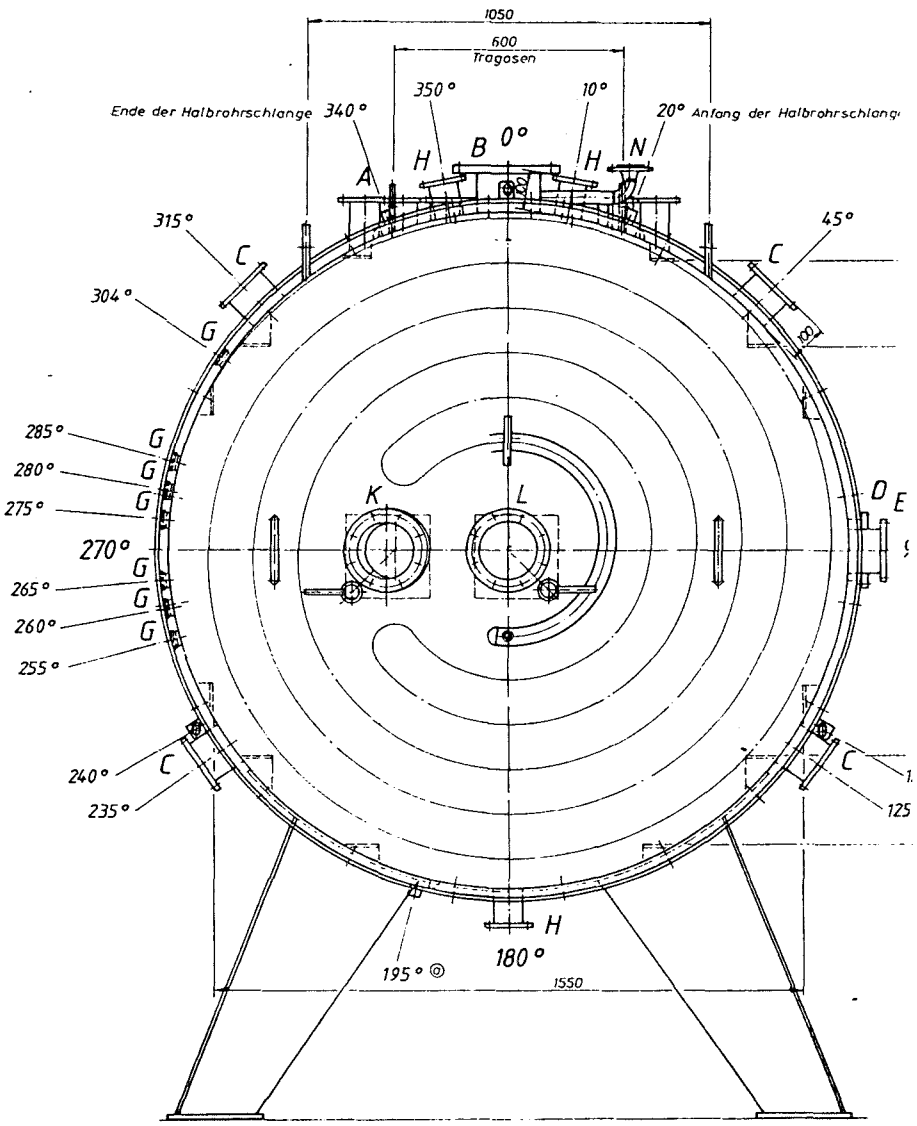

view from west

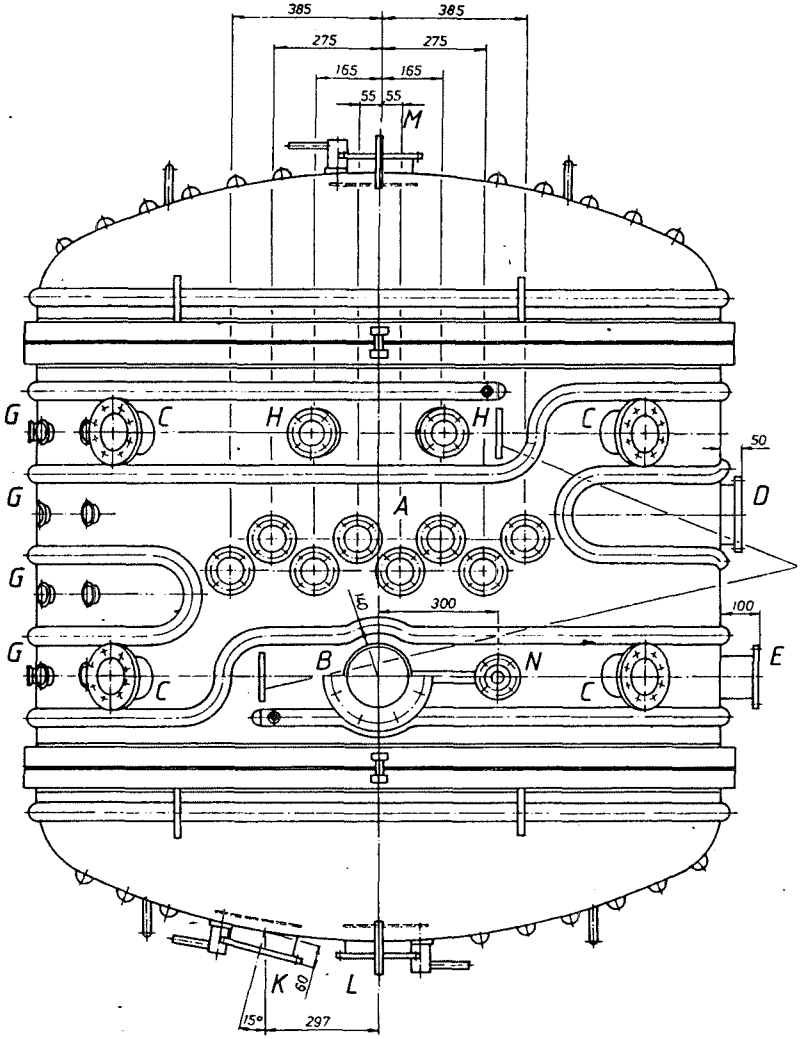

view from top

Fig. 5 Vacuum Vessel

The east and west covers of the vessel are equipped with one and two 150 mm ID sight glasses, respectively, positioned close to the center; the glasses may be covered with inside shutters handled from outside to protect the glasses from contamination. The sight glasses are also used for pyrometer measurements.

Welded to the inside of the cylindrical part of the vessel is a number of rails to support and fix the vessel internals.
The vessel inner surface was pickled and passivated and its roughness is $R_{max} \leq 20$ µm.

3.3 Radiative Heater

3.3.1 Heater Requirements

The heater as the key part of the test facility is required

- to transfer a uniform heat flux of up to at least 80 W/cm² to plane specimens of up to 0.25 m² in size which in case of protection tiles may have surface temperatures of up to 1800 °C,
- to be quick and allow cyclic operation with increases to full heat flux within less than 20 s,
- to be operated in vacuum
- to be long-lived to stand several thousands of high temperature cycles
- to be inexpensive to allow repeated replacement at long-term testing.

3.3.2 Early Design and Selection Decisions

Because of the rather large specimen size and rather moderate heat flux requirements an early decision was made towards trying to solve the problem with a thermal radiation heat source as a relatively inexpensive technology.

The heat flux requirement of 80 W/cm² together with the high temperature level of 1800 °C of the receiving surface asks for a heater temperature of roughly 2200 °C; this is true only if the emitting as well as the absorbing surfaces have high emissivities of between 0.8 and 0.9 and in addition if the specimen geometrically sees nothing else but the heater surface; this again means that the specimen must face a plane heater of a high and uniform temperature in a short distance in order to limit heat losses at the edges.

As heater materials for 2200 °C graphite and tungsten were under consideration and a preliminary decision was made for graphite because of the following reasons:

- uniform temperatures in the heater plane ask for plate-type elements for the resistance heater; tungsten sheet metal elements in contrast to graphite were not believed to stay flat.
- the first test specimens envisaged for testing included high temperature protection tiles made of graphite; in case of a tungsten heater the formation of brittle tungsten carbide with the danger of frequent heater failure was suspected.
- graphite offered the advantages of low cost and flexibility by laboratory manufacturing the heater elements

For the plate-type resistance heater elements it was also decided to have them hung from their electrical feed bars and to connect them such that they may freely expand downwards in order to avoid any mechanical loads.

On the basis of these decisions heater pretests were performed. They are summarized in Appendix A and resulted in the choice of laminated graphite (2mm thick) as the heater material.

3.3.3 Heater Design

Following the results of the pretests the heater consists of stripes of 2 mm thick laminated (flexible) graphite: The supplier of the material is Sigri Great Lakes Carbon GmbH, Meitingen; the grade used is Sigraflex L20010Z-LH additionally conditioned for outgassing. One pair of stripes in a vertical plane spaced by a gap of 3 mm forms a heater element. At its two upper ends this element is connected to thick graphite connection bars leading to the electrical power supply; at their two lower ends the stripes of an element are interconnected by a thick graphite traverse to close the electrical circuit. Usually the complete heater consists of three heater elements (six stripes) in one plane; they symmetrically load the three phases of the electrical supply grid.

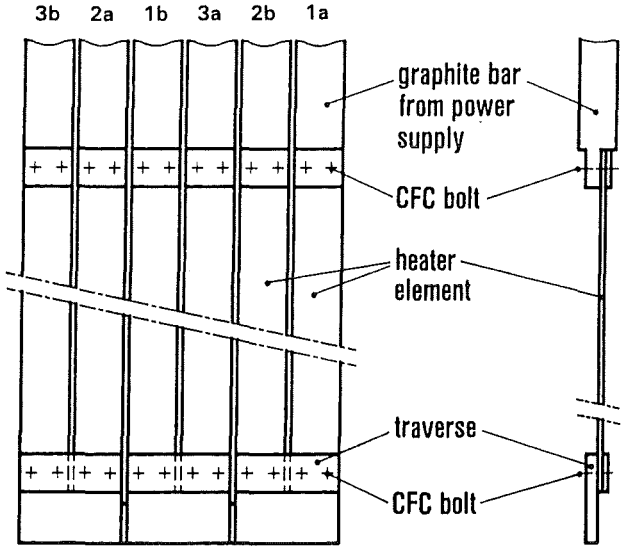

Fig. 6 Heater (schematic)

Details of the heater design are shown in Fig. 6. The high AC currents entering the vacuum vessel through water-cooled copper cables are transmitted to the upper ends of the heater element by connection bars made of fine-grained graphite roughly 17 cm long, 4 cm thick and adjusted to the width of the heater stripes; the purpose of this bar is to provide a low resistance connection for carrying the steep temperature gradient between the high temperature level of the heater stripe and the low temperature level of the copper cable; this avoids to face the hot heater directly with the cold cable and by those means reduces heat losses from and stresses in the heater. Contacting is by pressing the stripes to the bars by the aid of pressure plates and bolts both made of CFC (carbon-fibre reinforced carbon); an additional layer of laminated graphite under the pressure plate increases the flexibility necessary at thermal cycling. Contacting at the lower end of the heater stripe is made the same way; thus the heater stripe is a simple rectangular piece of laminated graphite which may be easily tailored in the laboratory by using an adequate paper cutting device and by drilling a couple of holes. The lower heater end traverse is a rather massive piece of fine-grained graphite; its functions are:

- to pass the current to the other stripe at a low current density (low internal heat sources)
- to radiate some heat from its surface to the surroundings in order to reduce the temperature level at the CFC bolts, and
- to act as a weight to keep the flexible heater stripes flat and vertical.

In the original design there were three traverses each connecting two neighbored stripes which belonged to the same power supply phase. In order to reduce the electromagnetic forces between the soft heater stripes (see chapter 5.4.3 for more details) any two associated stripes were taken apart and the three traverses were replaced by one coupling all six stripes as an electrical star point. The complete heater including the lower traverse is free to expand downwards and is only slightly centered at the traverse with horizontal alumina pins to avoid swinging.

The complete heater should always be larger by roughly 10 cm each in height and width to get a more uniform heat flux to the specimens by excluding the edge zones. Thus the necessary heater width determines the width of the six stripes after having taken the 3 mm gaps into account. Even rather wide stripes on the order of 6 to 8 cm implying high currents are possible since the power supply may be adjusted with different numbers of windings on the transformers' secondary sides. In case a total heater width of more than 40 cm should become necessary heater elements forming a W rather than a U should be considered in order to limit currents; but having the long heater dimension in the vertical direction is always preferable.

The resistivity of the laminated graphite (density ≈ 1 g/cm^3) is on the order of $\rho = 8\mu\Omega\cdot$m depending on the temperature with a minimum at roughly 1000 °C as shown in Fig. 7 taken from measurements during the heater pretests. Current and voltage necessary for a given heat flux to be transferred to the specimen depend on the individual width and height of the heater stripes chosen. As an example typical effective values for a given heat flux of 80 W/cm^2 are $I = 1000$ A for a stripe width of 5 cm and $U = 100$ V for a heater height of 60 cm.

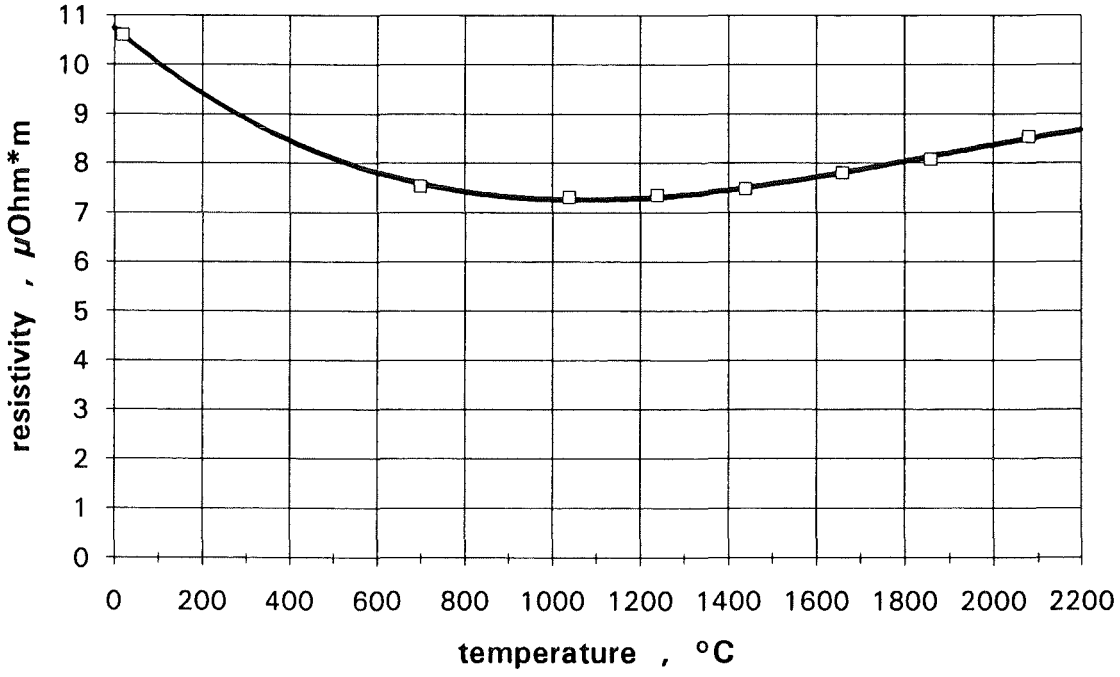

Fig. 7 Resistivity of Sigraflex LH ($\rho = 1$ g/cm^3)

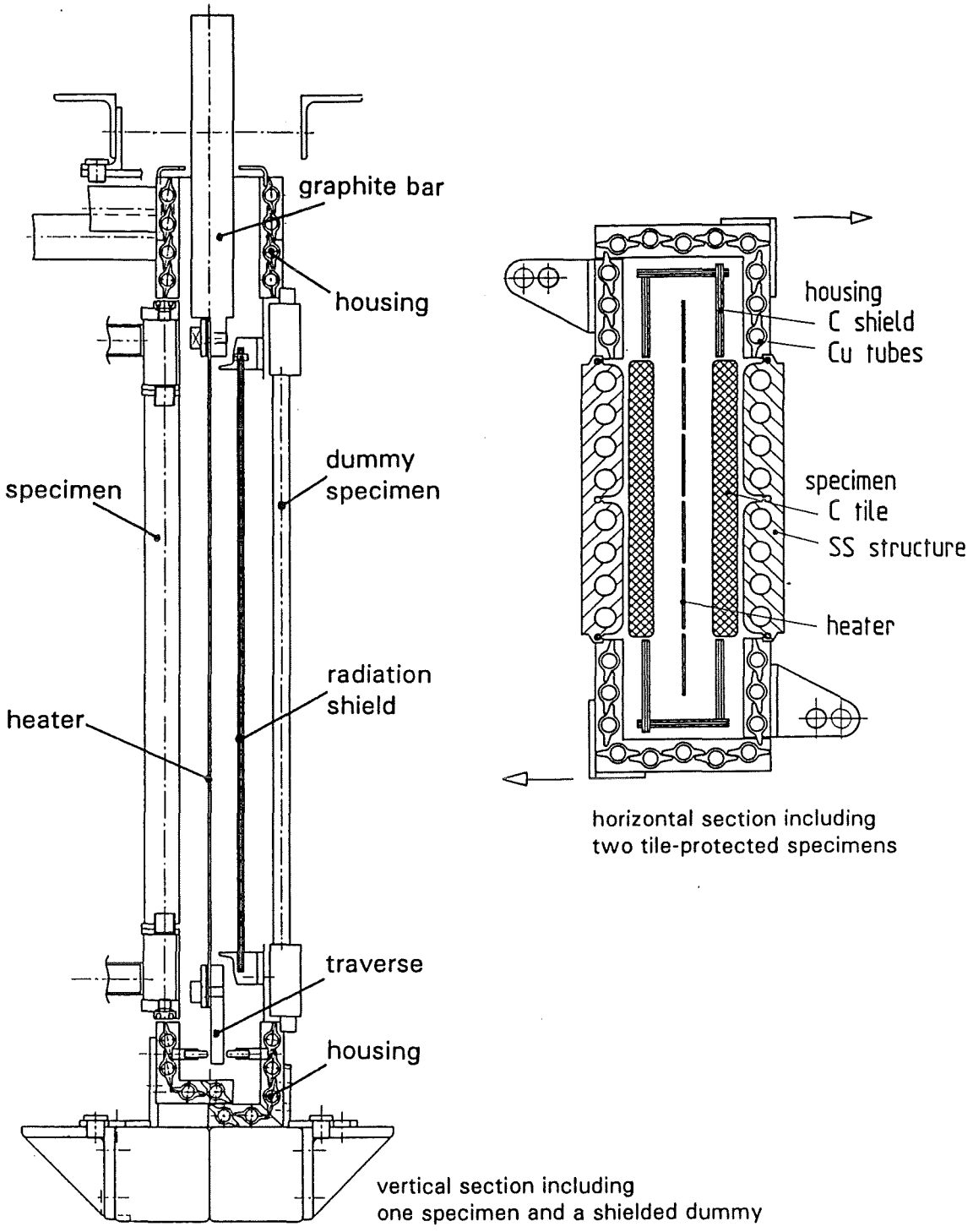

Fig. 8 Heater and its Housing Including Several Types of Specimens

3.4 Heater Housing

A water-cooled housing encloses the heater and absorbs almost all of the heat generated such that only a very little fraction may reach the vacuum vessel. The specimens on both sides of the heater (or specimens on one side and a dummy on the other) form parts of this housing by being placed into big windows which are cut into the large side areas of the housing; this means that the housing forms a frame around the specimens and together with them covers the heater not only at its useful central zone but also around its edges as shown in Fig. 8.

To make the housing insensitive against thermal fatigue (it receives the same cyclic thermal load as the specimen) it is built from an array of finned copper tubes; thus stresses in the housing are minimized by the high thermal conductivity of the copper and by the geometry. The fins of adjacent tubes overlap or at the corners of the housing they link the two adjoining sides together. This linkage with gaps is flexible and also blocks direct radiation from the heater from penetrating through the housing. The finned tubes turned out to be a handy constructional element since they allow building housings of different shapes; any holes in the housing for instrumentation or for fixing housing installations (like radiation shields) may be drilled into the fins without conflicting with the cooling channels.

It might be necessary to adjust the heat absorption of the housing to that of the specimen in order to avoid nonuniformities of the heater temperature. For high absorption (in case of a bare and black FW specimen) the housing is coated with a blackening color; for low absorption (in case of a FW specimen protected with radiation-cooled tiles) the housing is lined with a radiation shield consisting of laminated graphite.

Since the heater must be easily accessible for replacement the housing is designed as two half shells with hinges; the halves may be opened like doors after the specimens are removed. Both housing halves are connected to parallel paths of the water circuit I via metal hoses within the vacuum vessel. One half of the copper housing may be identified on Fig. 9 together with the heater which is visible through the window for the removed specimen.

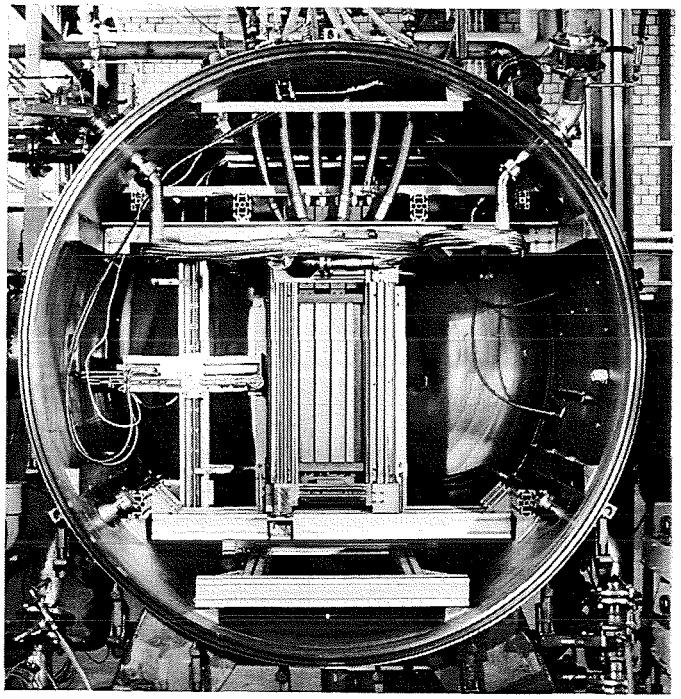

Fig. 9 Heater and Housing at the Center of the Vessel

3.5 Cooling Circuits

The cooling system consists of two separate water circuits. Circuit I is the main circuit and covers the heat withdrawal from the specimens and from the heater housing; circuit II cools the electrical high current cables, the vacuum vessel and some in-vessel instrumentation, if there is any.

3.5.1 Circuit I

As shown in Fig. 10 circuit I mainly consists of a pump, a heat exchanger, connecting piping and valves, an expansion tank, and a water degassing station with all components made of stainless steel.

The pump is a spiral casing pump type ZLNQ 65250/245 AB made by Sihi-Halberg. The device is capable of pumping 100 m^3/h at a total head of 7,5 bar or up to 60 m^3/h at a maximum head of 8 bar; it may be operated at up to 16 bar and up to 120 °C.

The plate heat exchanger type SIGMA 27 SC made by Schmidt, Bretten may be operated at a max. inlet temperature of 120 °C and at up to 16 bar; with its heat transfer area of 10 m^2 it is capable of transferring e.g. 1000 kW by cooling 30 m^3/h of primary water from 70 °C down to 40 °C by using 40 m^3/h of secondary water and heating it up from 15 °C to 37 °C. The ultimate heat sink is a wet cooling tower. The primary side pressure drop of the heat exchanger is 0.7 bar at a mass flow rate of 30 m^3/h.

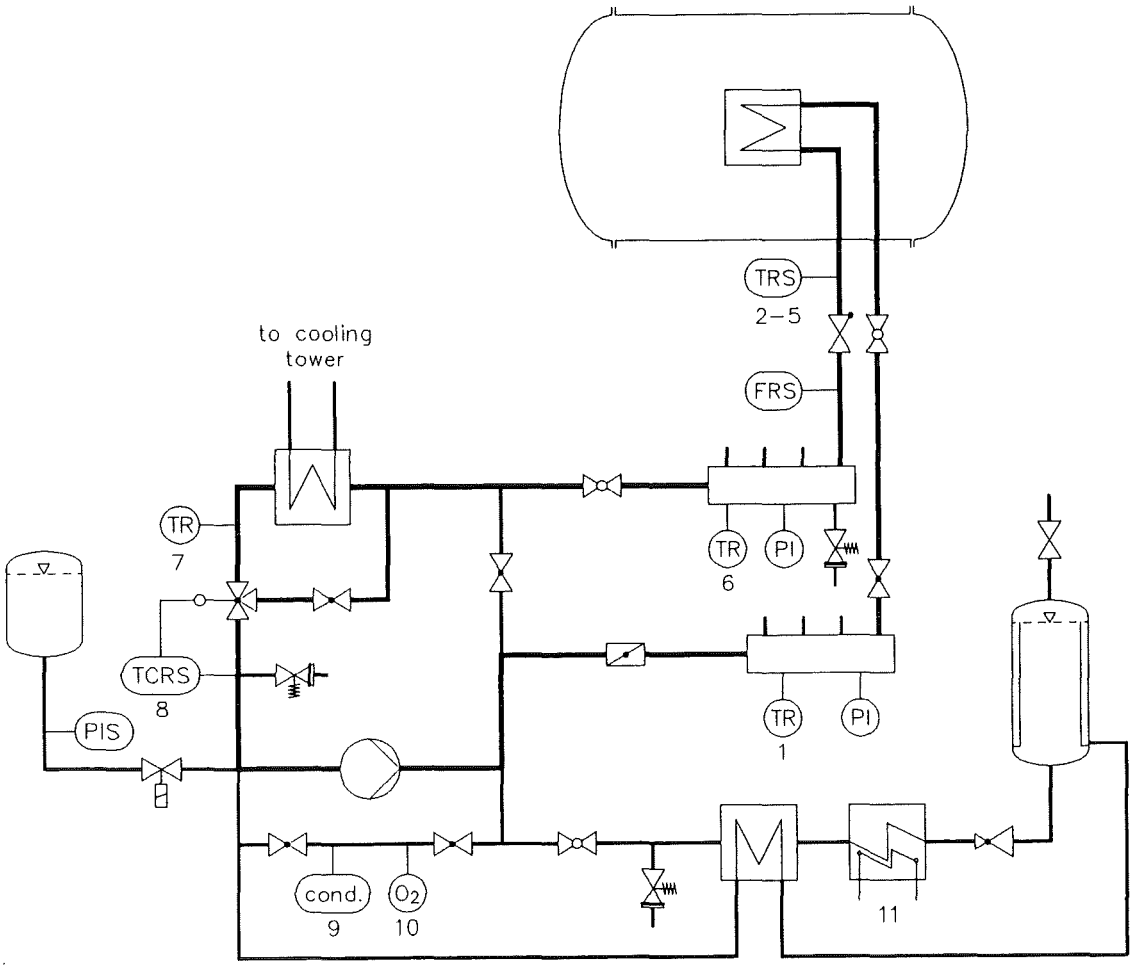

Fig. 10 Water Circuit I Flow Chart

Most of the connecting piping is DN 100 and it is again dimensioned for 16 bar and 120 °C. The safety valves limit the maximum pressure in the circuit to 14 bar.

The pump feeds water through a main throttle valve into an inlet manifold from which it is distributed into four parallel lines by adjusting four more throttle valves. The four lines at DN 65 enter the vacuum vessel and are connected one each to the specimen east, the specimen (or dummy) west, the housing-half east, and the housing-half west. After having received the heat the water leaves the vessel in four lines and after being individually measured with mass flow meters it is collected in a common outlet manifold.

When the water reaches the heat exchanger it may enter or bypass it depending on the position of a 3-way mixing valve behind the heat exchanger. This valve is operated pneumatically and is controlled by a thermocouple in the mixed water behind the valve thus trying to keep the temperature of the water at the inlet to the pump constant; this is important if tests are conducted with heating cycles delivering heat to the cooling system only during the heating phase; the test may nevertheless ask for a rather uniform inlet temperature for ease of interpretation.

At the location where the circuit is closed by feeding the water back to the pump an 80 l expansion tank with a rubber membrane is coupled ($p_{max} = 16$ bar, $T_{max} = 70°C$); it stores the expanding water when the circuit is heated up and it also allows to adjust the system pressure to a given level by filling its secondary side with compressed air. The expansion tank is separated from the circuit by a magnetic valve which is automatically closed if the pressure in the vacuum vessel should dramatically increase during operation, indicating a coolant leakage; this action is to avoid unloading the expansion tank's water into the vessel.

With the components described above the maximum operating conditions of circuit I are limited to 14 bar at the pump outlet and to 120 °C at the specimen outlet; the maximum pressure may be increased to 16 bar by replacing the safety valves.

Circuit I is filled with roughly 400 l of fully demineralized water. Its conductivity may be as low as 5 µS/cm corresponding to roughly 0,2 ppm remaining chlorides and the water is not degassed yet. Since the magneto-inductive flowmeters installed in the circuit (see chapter 3.9 for details) need a water conductivity of $\geq$ 20µS/cm some $CaCO_3$ powder is added to the water which increases the conductivity to roughly 40 µS/cm.

Degassing the water seems important in order to reduce its oxygen content and thereby reduce the danger of stress corrosion at specimen surfaces being in contact with the cooling water; thermal fatigue cracks as a test result should not be veiled by stress corrosion cracks. In order to exclude stress corrosion at the given chloride concentration of 0.2 ppm the oxygen content should be below 1 mg/l. Degassing to below 1 mg oxygen per liter water is achieved by a little degassing station coupled to circuit I and being passed by a small bypass stream. As shown in Fig. 10 this bypass stream is heated up to roughly 100 °C with a once-through electric household heater (11); it then is depressurized to close to atmospheric pressure and passed through a tank with a free water surface were undissolved gases are separated and released. The leaving hot water changes its heat to the incoming water and is then fed back into the main circuit at its point of lowest pressure (at the pump inlet). The solubility of oxygen in water decreases with increasing temperature and with decreasing pressure. At 100°C and at a pressure slightly above atmospheric an oxygen content of roughly 1 mg/l is reached at the outlet of the separator tank. This concentration is gradually extended to the whole circuit.

3.5.2 Circuit II

The auxiliary circuit II shown in Fig. 11 is similar to circuit I except that it is much smaller and that it does not have a degassing station.

The pump is a centrifugal pump type C70/45 made by Bavaria-Pumpen, Olching. It is capable of pumping 4.8 m^3/h at a total head of 5 bar; it may be operated at up to 8 bar and up to 40 °C.

The plate heat exchanger type 2L made by Rosenblads may be operated at a maximum pressure of 4 bar. With its heat-transfer area of $2m^2$ it is capable of transferring roughly 90 kW to the water of the wet cooling tower.

Circuit II is filled with roughly 120 l of fully demineralized water.

The pump feeds water through DN 40 piping into an inlet manifold where it is subdivided into ten parallel lines; each one may be individually throttled. Behind the flow meters the lines continue with plastic hoses.
Six lines are used to cool the electric power cables connecting the transformer outlets to the graphite heater connection bars inside the vacuum vessel. Their flow rates are usually set to 5 l/min.
Three lines are used to cool the vacuum vessel, one each for its cylindrical part and the two covers. Their flow rates are usually set to 11 l/min.
One line is provided for any in-vessel instrumentation that needs cooling; e.g. the heat flux probe used for the measurements reported in chapter 5.4 was connected to this line.

The water from the ten lines is metered and temperature-watched individually, is then collected in an outlet manifold, and is fed through the heat exchanger back to the pump inlet; coupled to the pump inlet is a 50 l membrane expansion tank ($p_{max}=4$ bar, $T_{max}=70$ °C). The expansion tank is separated from the circuit by a magnetic valve which is automatically closed if the pressure in the vacuum vessel should dramatically increase during operation, indicating a coolant leakage; this action is to avoid unloading the expansion tank water into the vessel. A safety valve at the outlet manifold is set to 2 bar.

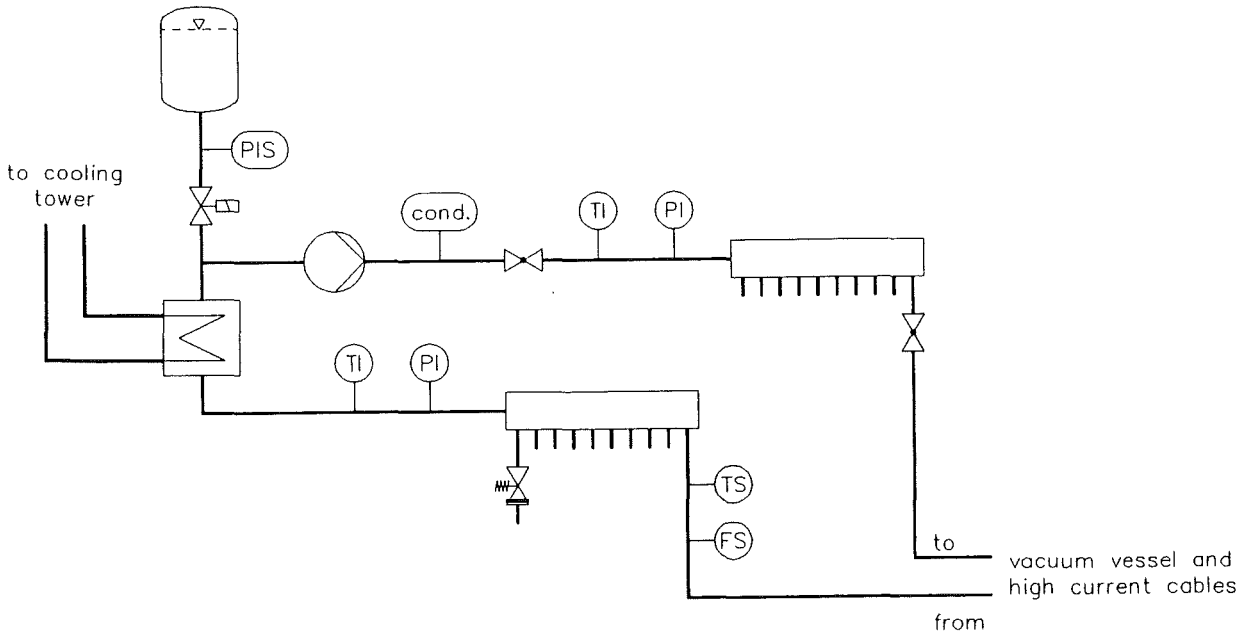

Fig. 11 Water Circuit II Flow Chart

With the components described above the maximum operating conditions of circuit II are limited to 7 bar at the pump outlet, to 50 °C at the outlet of the cable cooling lines, and to 70 °C at the outlet of the vessel cooling lines.

3.6 Vacuum Pumping and Control

The vacuum system is designed to pump the vessel down to a vacuum better than 10^{-4} mbar within a reasonable time of roughly 30 minutes and to cover the leaks through the numerous gaskets not only sealing the big vessel flanges and the 39 feed-throughs but also the coolant circuit connections inside the vessel.

The vacuum pumping system shown in Fig. 12 consists of a turbomolecular pump and two backing pumps (roots and rotary slide valve) in series. The vacuum components are manufactured by Balzers and specified as follows:

The turbomolecular pump (T) type TPU510 is capable of pumping 500 l/s at inlet pressures below $2 \cdot 10^{-3}$ mbar through a DN 150 inlet at a compression ratio for nitrogen of $8 \cdot 10^{8}$. It is air-cooled and is flanged directly to the vessel with only a valve in between. The back pumping device type WOD410B consists of a roots pump (R) type WKP500 and a rotary slide valve pump (D) type DUO60A capable of pumping 400 m^3/h at inlet pressures between roughly 10^{-2} and 1 mbar and of 60 m^3/h at atmospheric pressure. The backing pumps may either pump the vessel directly through a DN100 line in the beginning of the evacuation or back up the turbopump at pressures below $5 \cdot 10^{-2}$ mbar.
The pumps may be separated from the vessel by two pneumatically operated valves (V10) type SVP 160 P and (V11) type SVB100P; a third electromagnetic valve (V3) type EVA 040P allows to isolate the turbopump while it speeds up and while the vessel is still on a high pressure level.

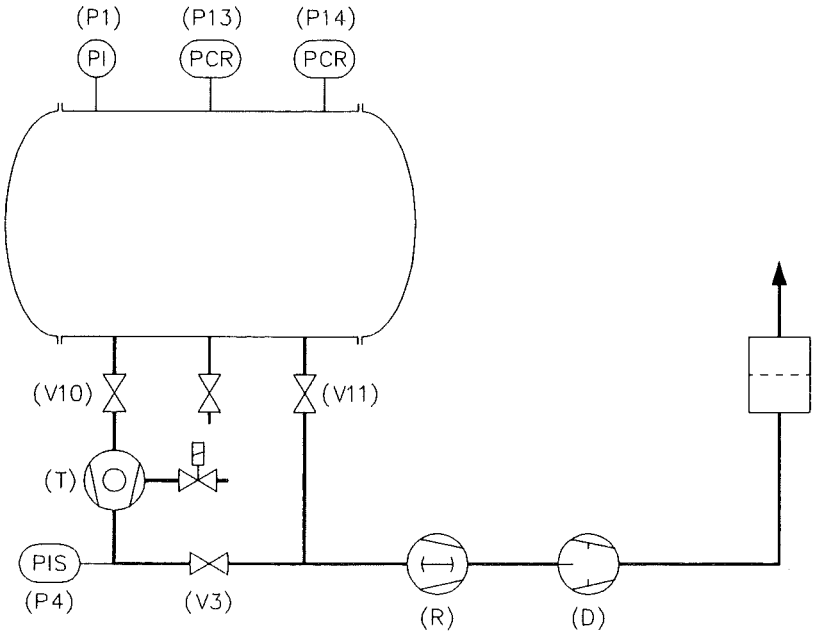

Fig. 12 Vacuum Pumping System

A control unit type TCS 1000 automatically activates the components for starting and shutting-down the pumping system:

- It starts all pumps with V10 and V11 closed to pre-evacuate the turbo-pump.
- It then isolates the turbo-pump by closing V3 and starts pumping down the vessel with the backing pumps after opening V11.
- The latter process is temporarily interrupted if the turbo-pump needs more pre-evacuation as indicated by the pirani sensor P4.
- After having reached a vessel vacuum of less than $5 \cdot 10^{-2}$ mbar as indicated by the pirani sensor P13 all three pumps are switched in series by closing V11 and opening V3 and V10.
- If a sufficiently low vacuum is reached and is indicated by the penning sensor P14 the turbo-pump may be automatically switched to run standby at reduced power.
- Stopping the pumping system results in automatically closing the valves, stopping the pumps, and after a delay time flooding the turbo-pump.
- Stopping is automatically activated if by some reason the vessel pressure increases beyond a preset value.

3.7 Power Supply

The heater is supplied with AC power taken from the grid, controlled by thyristor units, and transformed to an appropriate high current level as shown in Fig. 13. There are three parallel supply lines connected to two phases of the three-phase grid each. Each line is equipped equally.

The thyristor units (1) are of type M380-1000F made by AEG. Their voltage is 380 V and their nominal current is 1000 A. They may be operated either in the phase angle control or in the full oscillation strokes mode. Each unit includes a current measurement and a power control sub-unit which in this application is used only to watch overpower though.

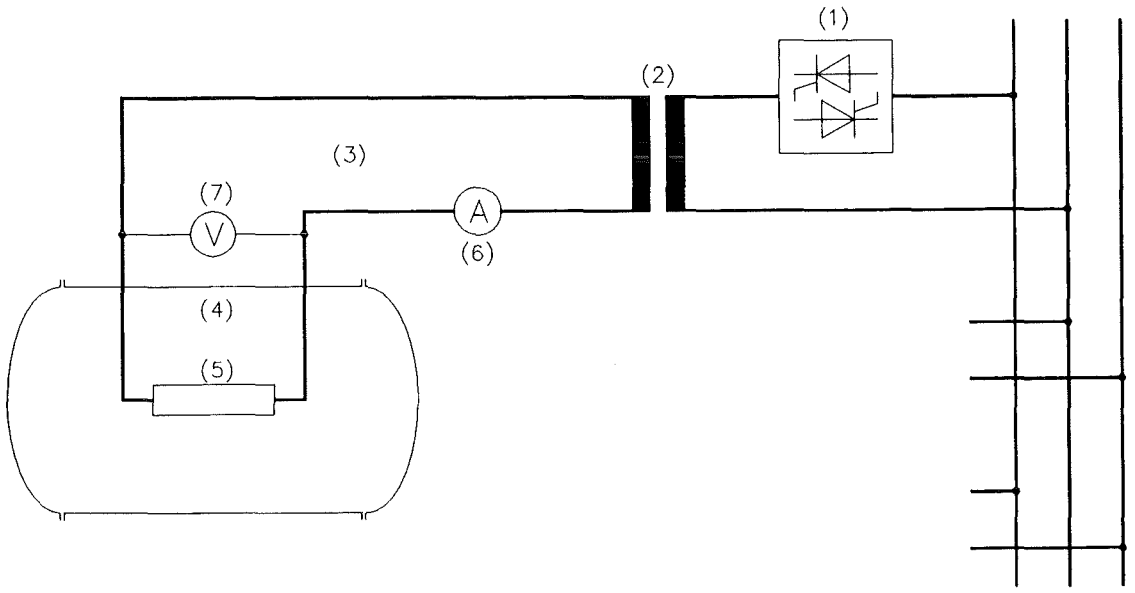

Fig. 13 Electrical Power Supply

The transformers (2) are special deliveries by AEG. The primary coil is for 380 V and 1000 A from the thyristor unit. The secondary coil is subdivided into four separated windings each one leading to a common switchboard. Two of the windings are dimensioned for 60 V and 1050 A, the two others for 60 V and 2100 A. Depending on the connections made on the switchboard the transformer's secondary side may be adjusted to three different pairs of nominal voltage and current:

180 V and 2100 A or 120 V and 3150 A or 60 V and 6300 A.

The transformers include air-cooling in case of reaching a temperature of 160 °C.

The six current leads from the transformers to the top of the vacuum vessel consist of water-cooled copper cables (3) type 3006/08 made by Homa, Mülheim-Ruhr. The cable has a total copper cross-section of 400 mm^2 consisting of 8 subcables positioned by a spiral around a central water duct; the cable arrangement is enclosed in a strong rubber hose. The electrical vessel feed-throughs (4) are water-cooled extensions of the cables made in a similar fashion except for the rubber hoses which are replaced by metal hoses; these feed-throughs are telescoping in order to be adjustable to varying positions of the heater connection bars (5). The current limit for the cables is 3500 A, which is sufficiently high for the applications expected for the test facility.

In each of the three lines the current I is measured by transformer-type transmitters (6) surrounding the cables. The current transmitter is type KSO361 class 0.2 for 2000A made by Ritz, Hamburg; it needs to be replaced if currents beyond 2000A should become necessary. There was some suspicion that such a regular current transmitter made for 50 Hz sinusoidal waves could produce errors when confronted with high harmonic contents of the current leaving the thyristor; this suspicion was eliminated by comparing the results to those gained with a LEM module; obviously the transformer and the load smoothen most of the harmonics out. The voltage U_o (7) measured at the vessel feed-throughs is typically about 5 % higher than the actual voltage drop U_H along the heater elements since U_o includes the resistances of the in-vessel electrical connections; this is tolerated because the measurement of the electrical power is used only for power control while for the test evaluation the power data are taken from calorimetric measurements of the power received by the specimen.

3.8 Power Control

The power control is the component responsible for generating adequate heating cycles at the heater and for the specimens. It consists of two microprocessor-controlled multifunctional units (MFE) type Teleperm D 6DR1520 made by Siemens. The two MFEs contain three separated power control circuits one for each of the three power lines. One such circuit is shown schematically in Fig. 14. The MFE receives the signals from the current and voltage measurements mentioned in chapter 3.7 after they have passed RMS converters; the signals are checked for overload and multiplied to result in the actual power of the heater element concerned. This actual value is compared to a desired value and the deviation is fed into a PID controller. The desired value may be preset time-dependently with the time-dependence consisting of any increase ramp, a first power plateau, a second ramp (upwards or downwards) a second power plateau, any decrease ramp, and a power-off plateau; this allows modelling of a large variety of time-dependencies including constant power or a short period of over-power in the startup phase to quickly reach the steady state temperature level at the specimen and also including the possibility of running the power-off plateau slightly above zero in order to avoid too low temperatures at the heater. Such a preset time-dependence is repeated until a given number of cycles is reached. All three power lines are supplied with the same desired value but they are separately controlled.
The output of the PID controllers are fed as inputs into the thyristor units.

It should be pointed out that the heater elements are not temperature- but power-controlled. If there should be a need to run the three heaters at different power levels there is a possibility to multiply the preset desired value of any power line by a constant factor.

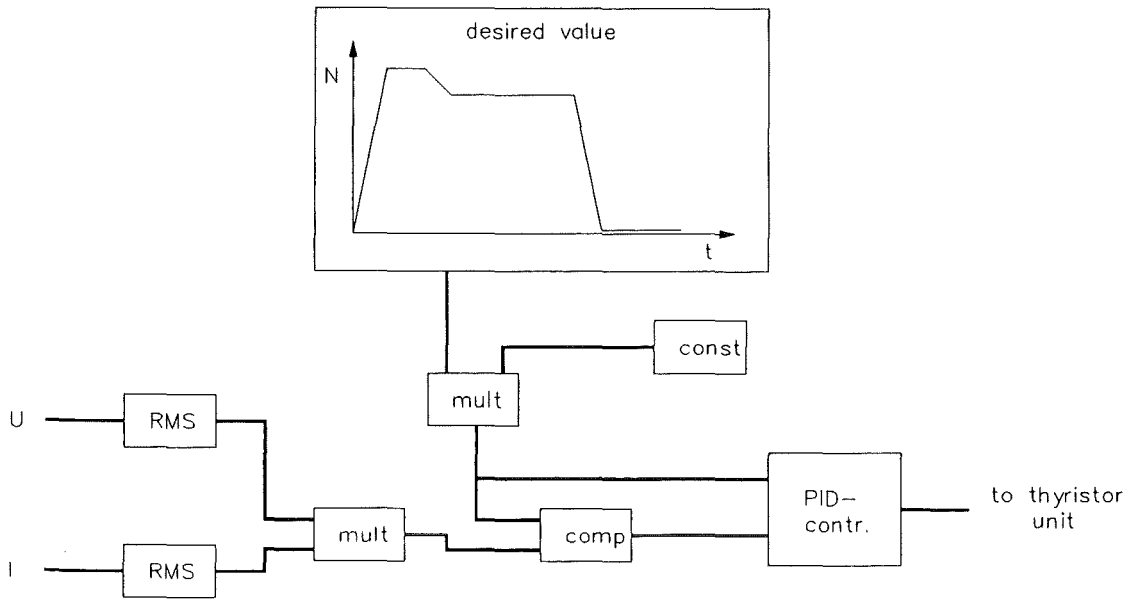

Fig. 14 Power Control Scheme of one Power Line

3.9 Operating Instrumentation

This includes all instrumentation necessary to run and automatically control the facility except for the specimen instrumentation which is typical for the specific goal of the test and is not discussed in this report. A simplified and more general description is given below subdivided into functional groups.

3.9.1 Vacuum Vessel Instrumentation

The vessel is equipped with pressure sensors for three overlapping ranges (see Fig. 12)

- a spring manometer (P1) covering +/-1 bar around atmospheric
- a Pirani gauge (P13) type TPR01 by Balzers covering $1 \cdot 10^{-3}$ to 100 mbar
- a Penning gauge (P14) type IKR020 by Balzers covering $5 \cdot 10^{-8}$ to $5 \cdot 10^{-3}$ mbar

The latter two gauges are part of the vacuum control system and their output may be displayed in the control room. Vessel temperatures may be watched with TCs as necessary if larger quantities of radiated heat can reach the vessel.

3.9.2 Water Circuit I Instrumentation

The instrumentation is indicated in Fig. 10. Three manometers are placed at the two manifolds and at the expansion tank. The one at the inlet manifold is a digital manometer; its signal may be input to the data logger. The one at the expansion tank is part of the safety system and watches the pressure to not fall below a preset value which would indicate water losses out of the circuit.

Water temperatures are measured with TCs at the inlet manifold (1), in the four outlet lines where they leave the vessel (2-5), at the outlet manifold (6), behind the heat exchanger (7), and behind the mixing valve (8). TCs (2-5) watch for overtemperature and are connected to the safety system. TC(8) controls the mixing valve as indicated in chapter 3.5.1. It is noted that additional TCs are installed in the in-vessel coolant lines serving the specimens; they are used for calorimetric measurements and they are part of the specimen instrumentation (see chapter 3.11).

Flow rates are metered in the four vessel outlet lines by magneto-inductive flow meters type Altoflux K480AS, DN50 made by Krone; their range is 2-84 m^3/h at an accuracy of +/-0.8 % of the actual value. For small flow rates an additional meter type IFM 4080 K, DN15 is available ranging to 7 m^3/h. The flow rates are locally displayed and the analog output of the meters is connected to the data acquisition and safety systems.

The conductivity of the water is measured at position (9) by a probe type XGPTC01 in connection with an instrument type LZW1 both made by Conducta GmbH, Gerlingen. The oxygen content in the water is measured at position (10) by a probe type Trioxmatic 600-7 in connection with an instrument type Trioxmatic 161-TR made by Wissenschaftl. Technische Werkstätten (WTW), Weilheim.

3.9.3 Water Circuit II Instrumentation

The instrumentation is indicated in Fig. 11. Spring manometers display the pressure at the inlet and outlet manifolds; in these places also temperatures are measured with TCs. A manometer at the inlet to the expansion tank is part of the safety system and watches if the pressure falls below a preset value which would indicate water losses out of the circuit.

Before entering the outlet manifold each of the ten lines are watched for overtemperature with thermal dry-reed contacts and for flow rates being too low by rotameters with dry-reed contacts; with preset values they all act on the safety system.

The conductivity of the water is metered as described for the water circuit I above.

3.9.4 Instrumentation of Electrical Power, Vacuum and Flooding Systems
See chapters 3.7, 3.6, and 3.10.1, respectively, for details.

3.9.5 Conversion and Display of Operating Instrumentation
All service temperatures are converted and displayed in the control room by utilizing control units type SIPART DR20K by Siemens; the outlet temperatures of circuit I are monitored for over-temperatures and possible yes-signals are fed into the safety system.

The mixed water temperature (8) signal of circuit I is input to a PID controller type DR20S by Siemens where it is converted, displayed, and compared to a set-point eventually resulting in the activation of the valve drive.

The power supply instrumentation signals are converted and displayed as currents, voltages, powers, and resistances by a three-phase precision wattmeter type 304B made by Infratek, Switzerland.

Vacuum sensor signals are converted and displayed within the vacuum control unit (see chapter 3.6).

Most of the operating instrumentation signals are connected to a switchboard where they may be checked and from where, in addition to any display, they may be transferred to the data acquisition system.

3.10 Safety Systems

There are two safety systems. The first one protects the vacuum vessel against excessive pressures and temperatures. The second one is tailored for a safe shutdown of the facility and for protecting the specimen in case of abnormal events.

3.10.1 Vessel Safety System
It may happen that there is a sudden ingress of water or air into the vacuum vessel. The water ingress could be the result of the failure of a coolant channel (e.g. at the expected failure of a specimen) or of a gasket. The air ingress could be the result of a sudden vessel leakage, e.g. through a broken observation window. In both cases a strong chemical reaction between water or air and the hot graphite materials of the heater and any other graphite parts like shields or tiles would take place. Reaction products would be gases like steam, H_2, CO, and CO_2 with the further potential of reactions between H_2 or CO and any entering air. Goals of the vessel safety system are to protect the vessel against pressurization beyond the design pressure of 1 bar gauge and against excessive burning of graphite and do this with a system containing passive components only. Details of the reactions to be expected and the system installed may be found in Ref. [1].

The passive system built up is shown in Fig. 15. It consists of an exhaust part on top of the vessel and a flooding part connected to the bottom of the vessel.

In the exhaust a spring-loaded back-pressure valve (3) of small size opens at 0.3 bar gauge to preserve the large size rupture disk in cases of over-pressurization with flooding gas. At nominally 0.8 bar gauge the rupture disk (2) type CDCVG-G, DN6" made by Continental Disc Corp., Kansas City, Missouri will break and release the gas over-roof to the atmosphere after it has opened and passed a weight-loaded back-pressure valve (1); the latter valve closes after the exhaust is finished and avoids the influx of air when the hot gas in the vessel contracts as it cools down.

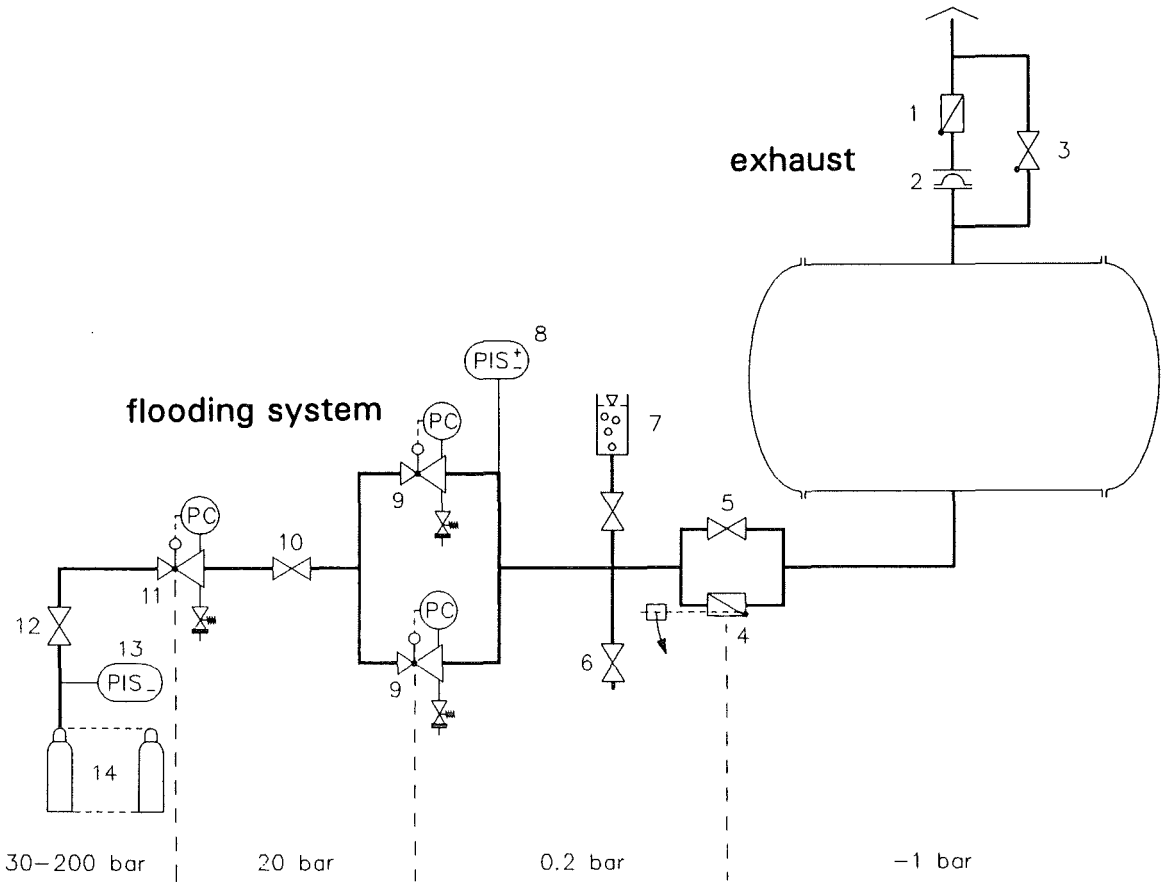

Fig. 15 Vessel Safety System

The flooding part of the system is to fill the vessel with nitrogen and avoid extended facing the possibly hot graphite with air. The influx of N_2 at a rate of 1.8 m^3/min is started as the weight-loaded nonreturn flap (4) opens at -0.5 bar gauge and connects the vessel with a room at +0.2 bar gauge behind two parallel pressure regulating valves (9); the pressure in this room is guarantied by a contact manometer (8) the output signal of which acts on the shut-down safety system; a percolator (7) helps checking that the valves in the supply line are open. Gas supply is from bottles and through another high pressure regulating valve (11); sufficient pressure in the bottles is watched by a contact manometer (13) again acting on the shutdown safety system.

3.10.2 Shut-down Safety System

This system shuts down a component or blocks starting it if not all requirements for a safe operation are complied with; the dependence is actually obtained by using stored-program controllers types Teleperm D 6DR1611-3AN13 and 6DR1612-ONN 13 by Siemens. The components concerned and the main functional dependencies are listed below.

- The heater power is cut if the preset limits of one of the following quantities are exceeded: current, voltage, or resistance of a heater element; flow rate or temperature in one of the lines of circuits I or II; pressure at the expansion tanks of circuits I or II; pressure in the vacuum vessel; temperature measured at the vacuum vessel; pressures in the flooding system; pressure of the compressed air activating various valves.
- The coolant pumps of circuits I and II are shut down also at the events listed above except that in most cases they are switched off only after some time delay to provide reasonable after-cooling.
- The expansion tanks of circuits I and II are disconnected during a test if the concerned flow rates pass lower limits indicating a major leak or if the pressure in the vacuum

vessel exceeds a preset value possibly indicating a coolant leak into the vessel; some of this is done only after a delay time.
- The vacuum system is disconnected by valves if the pressure in the vacuum vessel exceeds a preset value.

Some of the dependencies may be over-ruled by activating a start-up program, which is automatically reset as the over-ruled limits are satisfied for the first time.

In addition to this shutdown safety system covering the interactions within the facility, many of the components include individual safeguards that may result in shutting down this component separately.

3.11 Diagnostics

To be covered here are only the diagnostic methods that have relation to the specimen and to the test evaluation; operating instrumentation however is discussed in chapter 3.9.

As a rule for thermal fatigue experiments only a small amount of diagnostic methods must be applied and should be applied in order to not disturb the failure process at the specimen.

3.11.1 Temperature

The specimens may carry thermocouples of any type; if they are roughly 1.5 m long they may be connected directly to one of the multi-pin plugs of the vessel feed-throughs; there are up to 48 pins per plug. These plugs and the feed-throughs type RADV of different sizes made by LEMOSA, München are fast-connecting. The measurement lines are extended from the vessel to the data acquisition system by adequate extension leads; presently 20 lines are provided for type K TCs; more or others could be added. Where a very high precision in temperature measurement is not needed the presently available 40 copper lines may be utilized by using reference points provided at the feed-throughs.

Very high temperatures such as those of the heater or a FW protection tile may be measured with optical pyrometers through the observation windows in the vessel covers, provided that access through an adequately positioned 5 mm hole to the spot to be measured can be offered. There are two pyrometers available:
- a spectral (one-color) pyrometer type PB50 AF S17 made by Keller GmbH, Ibbenbüren-Laggenbeck measuring at a wave length of 0.85 µm within a temperature range of 800 to 2300 °C.
- a two-color pyrometer type PB07/PD05 AF 01/04 made by Keller GmbH, Ibbenbüren-Laggenbeck, which is a manually operated filament pyrometer used as a reference instrument. It measures at wave lengths of 0.546 and 0.645 µm and covers the temperature range between 650 and 3500 °C with a high accuracy above roughly 1100 °C.

3.11.2 Strain

The specimens may carry strain gauges. Like the TCs above the strain gauges are connected to multi-pin feed-throughs in the vessel wall. Wiring to the data acquisition system currently provided is sufficient for 32 three-wire strain gauges.

3.11.3 Displacement

The overall shape of the specimens as it changes with heat load and time may be metered with inductive displacement sensors (LVDTs). Currently 25 such LVDTs type 108/4 made by TWK Elektronic, Düsseldorf including supply, calibration, and conversion units assembled by Lamberz, Euskirchen are available and connected to the data acquisition system. The measuring range is $+/-2$ mm. The resolution is a few microns but because of time- and temperature-dependent instabilities of the system no accuracy below 10 µm should be expected.

3.11.4 Heat Flux

The heat flux received by the surface of the specimen is the main test parameter. It is therefore important to correctly measure the heat flux as an average value over the specimen surface as well as its local distribution; actually the practical way to go is to make sure that the uniformity of the heat flux on the surface is good and then evaluate test data with the average value which is easier to measure.

Supposing that the specimen and the heater surface each have uniform emissivities makes the local heat fluxes depending only on the temperature uniformity of the heater and on the geometrical situation. The heat flux uniformity may be determined by x/y-traversing a heat flux probe in the plane of the specimen surface (compare chapter 5.4 for measured results). A heat flux probe type C-1301-A-120-72-X2 made by Hycal Engineering, El Monte, California is available together with an in-vessel traversing mechanism. The water-cooled probe has a sensitive area of about 3 mm in diameter and is capable of measuring heat fluxes up to 140 W/cm^2. Even if its calibration should suffer due to changes in its surface emissivity the relative distribution measured should still be reliable.

The average heat flux to the specimen is determined calorimetrically by measuring the flow rate and the temperature increase of the coolant as it passes the specimen under steady-state conditions. In addition to precise flow meters the quality of the measurement is increased by making sure that the bulk temperatures of the coolant are measured and that as little heat as possible is picked up or lost through surfaces other than the heated specimen surface between the positions where the inlet and outlet temperatures are measured. Also a small flow rate resulting in larger coolant heat-ups and a calibration of the two TCs relative to each other at zero power steady-state conditions help improve the quality of the heat flux determination.

3.11.5 Gas Composition

For cases where the heater is attacked by evaporating constituents and others a mass spectrometer is available to analyze the remaining gas of the vessel atmosphere. The device is a quadrupol mass spectrometer type Data-Turboquad DTQ100DXS made by Alcatel for masses between 1 and 100 amu and for a smallest detectable partial pressure of $1 \cdot 10^{-11}$ mbar. The maximum operating pressure of the device may be reached with a pressure conversion unit type DW2 made by Leybold which may be positioned between the vessel and the spectrometer inlet.

3.12 Data Acquisition System

The data acquisition and display system consists of a data logger and a coupled PC.

The data logger is a Schlumberger type 3531 D device equipped for a maximum of 200 channels; it is operated at a scan rate of 40 channels resulting in an integration time of 20 ms, which seems important for avoiding errors due to 50 Hz pick-ups through the measuring lines. With 10 analog input modules type 35301A (with reed relays) the logger is ready for measuring and storing currents, voltages, temperatures from TC voltages, and with an additional transducer energization module type 35301D also resistances and strains from strain gauges.

The logger is capable of converting signals and of processing (combining) signals originating from different channels. Logging is performed according to pre-defined tasks.

The data may be stored on disk or transferred on-line via a parallel interface module (GPIB) type 35304A to the hard disk of the coupled PC. With the support of the software AXIS the logger's front panel may be manipulated from the PC and also up to eight channels may be displayed as on-line trend plots and a large number of channels may be listed as tables on-line on the PC's monitor.

Also with the AXIS software logger data files may be converted into EXCEL table files.

3.13 Long-Term Testing Capability

With the control safety and data acquisition systems described above the facility is equipped for long-term testing 24 hours a day. Depending on the type of test and on the cycle time inspection breaks are expected every few days or every week; these breaks may be used to renew the heater elements if necessary.

4. FACILITY UPGRADING CAPABILITIES

The facility, as it presently is, was built to the research needs that were recognized at the time of the facility's design in 1989. the main objective has been the performance of thermal fatigue experiments with medium-sized FW mockups; the facility was to allow testing of specimens protected with graphite tiles. Since one species of tiles, namely the so-called radiatively-cooled tiles, exhibit very high surface temperatures the facility had to be a high temperature device. Since long-term testing was expected the high temperature capability had to be combined with a sturdy construction for reliable operation at reasonable cost.

After some time of operation the question arises now whether the facility's capabilities could be extended beyond the goals originally envisaged. Some upgrading aspects are discussed in the following chapters.

4.1 Specimen Size

As presented in chapter 3.2 the vacuum vessel is a lying cylinder of 1.77 m inner diameter. The heater concept chosen asks for a hanging heater; it excludes a horizontal arrangement because hanging is the only possible support to the soft heater material and is the only way to keep the heater surface plane and to let it thermally expand without reaction forces. In addition the current feed-throughs are built into the top of the vessel.

A hanging heater means that its length is limited by the vessel's diameter after some space needed for the current feed-throughs and the connection bars as well as for the heater housing is subtracted. As mentioned in chapter 3.3.3 the specimen should always be about 10 cm shorter than the heater in order to avoid edge effects on the heat-flux uniformity. Based on the arguments above the maximum length for the heater is 100 cm and for the specimen is 90 cm; to achieve this a reconstruction of the present current feed-throughs would be necessary; otherwise the length of the specimen is limited to 75 cm.

With the feed-throughs as they are the width of the heater is also limited by the vessel diameter; this configuration should not be changed by rotating the heater plane parallel to the vessel axis since this would strongly reduce the maximum length and depth of the specimen, would conflict with the present concept of the heater housing, and would strongly restrict the heater's and the specimens' accessibility. In addition the heater width is limited by the way of subdividing it into stripes and by the maximum width of an individual stripe; as discussed in chapter 3.3.3 the maximum heater width of 40 cm of the present design could be extended by having four parallel stripes form a W-shaped heater element instead of the two parallel stripes forming a U-shaped element now; this would need development including some risk though.

Based on the aspects above the maximum width for the heater is 80 cm and, accordingly, for the specimen is 70 cm; to achieve this the development of a W-shaped heater would be necessary.

The maximum depth of a specimen is rather unlimited; presently a maximum depth of roughly 40 cm is possible, depending to some extent on the positions and sizes of the specimen's coolant connections, since the only limitation is the space provided under the cover of the vessel; if this space should be insufficient it could be enlarged by adding a cylindrical ring to the central part of the vessel.

In summary the maximum achievable size of a specimen seems to be 90 cm in height and 70 cm in width at any depth.

4.2 Power

Related to power actually the most interesting figure is the heat flux achievable at the surface of the test specimen. This heat flux depends on the temperature level and the emissivity of the specimen's surface and is limited by the maximum allowable temperature of the heater. At a reasonable maximum heater temperature of 2150 °C (see Appendix 1 for background information) and a heater emissivity of $\varepsilon_h = 0.7$ the achievable heat flux q_{max} is directly correlated to the properties of the specimen's surface, namely to its temperature T_s and its emissivity ε_s, as shown in Fig. 16. For convenience Fig. 17 in addition shows the heater temperature T_h that will be necessary to reach a certain heat flux q if the specimen temperature is T_s; this is plotted for the emissivities $\varepsilon_h = 0.7$ and $\varepsilon_s = 0.8$. Figs. 16 and 17 base on Stefan-Boltzmann's law for radiative heat transfer.

The maximum heat flux plotted may be increased only by increasing the maximum heater temperature beyond 2150 °C; this would be possible but would drastically shorten the lifetime of the heater.

The total power of the facility is limited by the maximum power of the heat source or the heat sink whichever is smaller. Presently both the source in form of the electrical power supply and the sink in form of the circuit I heat exchanger are designed for a nominal power of roughly 600 kW.

Whether this nominal power or more is available as radiative heat from the heater depends on the shape of the heater since the shape determines the relation of current and voltage; a power of 567 kW is available at any current/voltage relation; for some current/voltage relations the maximum available power reaches up to 1100 kW. Of the heater power only a fraction will reach the specimen positioned on one side of the heater since some of the power will go to the housing with the quantity depending on the specific dimensions, and a large fraction of the power will leave the backside of the heater; the quantity to the backside depends on whether there is a second specimen or a radiation shield. Of the heater power roughly 35 % is transferred to each of two specimens positioned on both sides of the heater or roughly 45 % is transferred to one specimen if there is a shield on the backside of the heater.

The power withdrawn in the heat exchanger depends on the operating conditions selected namely the coolant flow rate and temperature level. As indicated in chapter 3.5.1 the maximum capability of the heat exchanger is far beyond the nominal value of 600 kW, which was determined on the basis of a small temperature difference and of a low temperature level.

Both the powers of the electrical power supply and of the heat exchanger could be increased if there should be a need and provided that the increased power could be transferred from the heater to its surroundings. Upgrading the electrical power supply would be a major undertaking though, since the expensive transformers and thyristor units would have to be replaced. Upgrading the heat sink would be easier and much less expensive.

It seems, though, the power supply and heat sink are dimensioned generously enough to be not suspicious of needing upgrading.

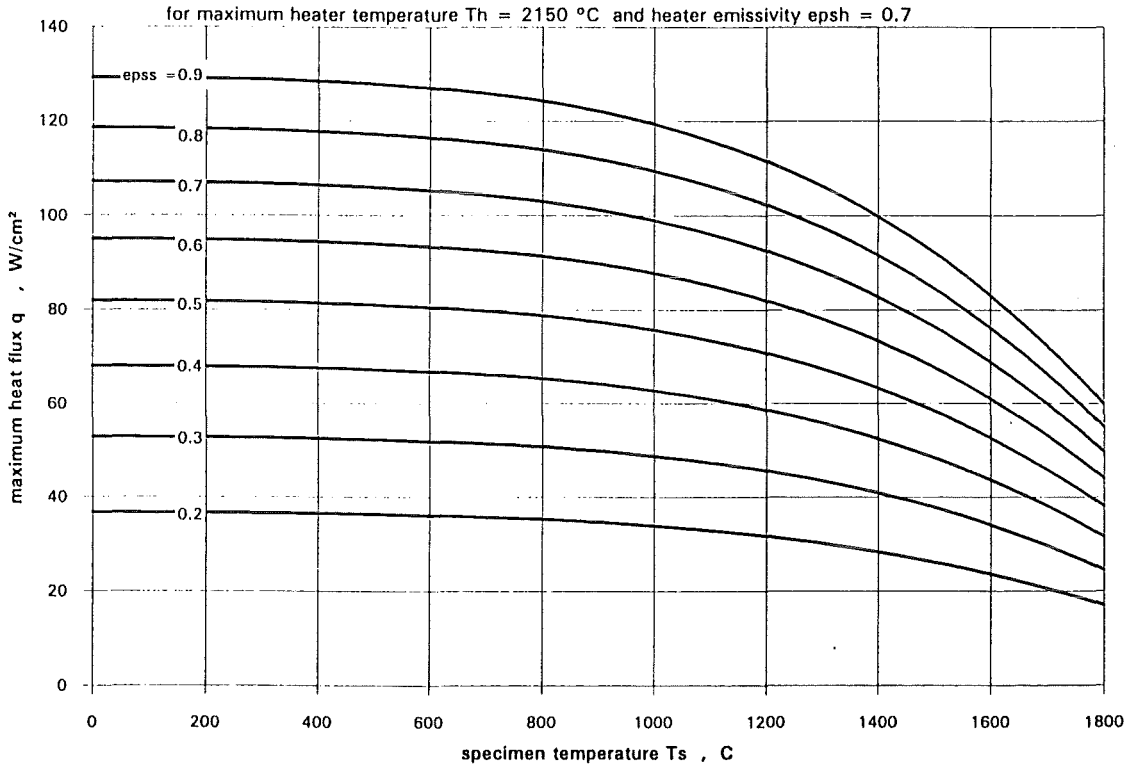

Fig. 16 Maximum Achievable Heat Flux

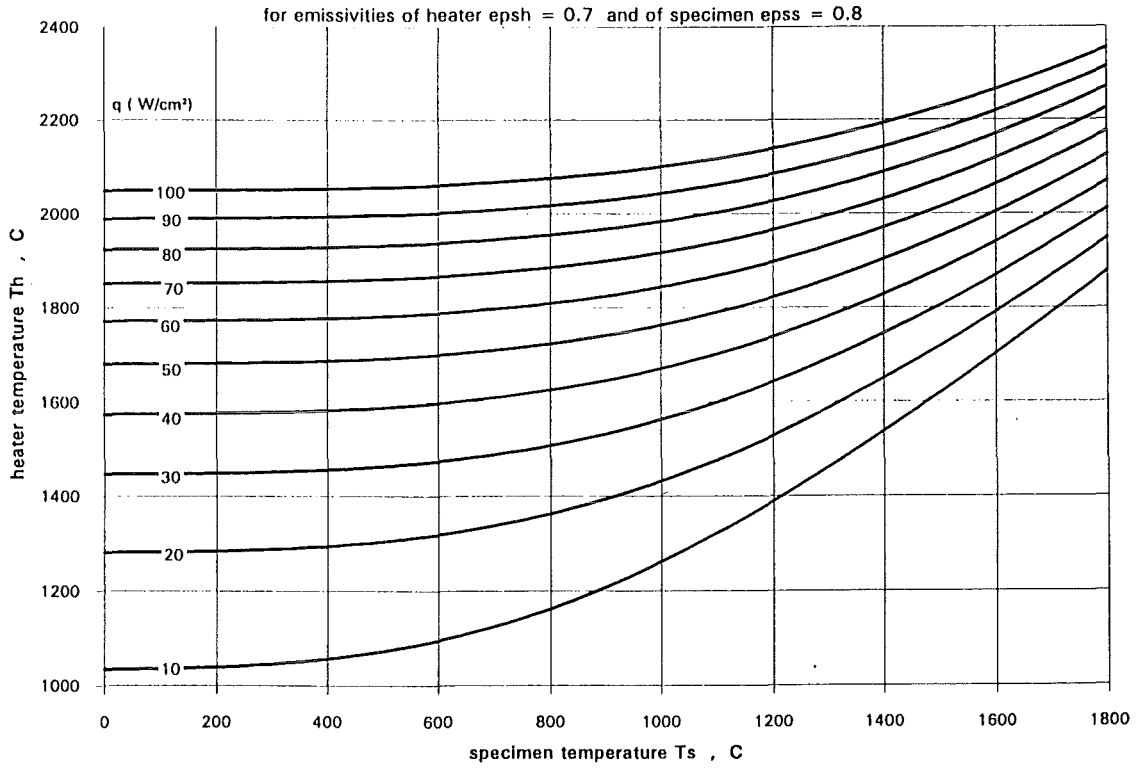

Fig. 17 Heater Temperature Necessary to Achieve Heat Flux q

4.3 Coolant

The conditions of the coolant for the specimens (cooling circuit I) are interesting test parameters since the coolant pressure causes primary stresses in the specimen and the coolant temperature is responsible for the temperature level of the specimen and thereby for the material properties.

Circuit I is presently constructed for a maximum of 16 bar and 120 °C. Upgrading the circuit to a higher pressure and/or temperature would mean a new construction of the whole circuit including all components mentioned in chapter 3.5.1. In case of a moderate temperature increase such a new circuit would probably again be a water circuit. In case of a strong temperature increase a new circuit could be a gas circulation loop.
Such a new circuit would not interfere with the present facility since the vessel feedthroughs for the coolant as the only points of intersection are designed such that high pressure/temperature lines could be built in. In such a case the present circuit I would be kept and would continue to serve the heater housing.

4.4 Diagnostics

The diagnostic presently available seem adequate and sufficient. If any diagnostic needs and possibilities should come up their inclusion needs to be checked.

4.5 Beryllium Handling

As indicated in chapter 2 the facility is not prepared to accept specimens wearing protection layers of Be on the heated surfaces, since when testing such specimens with the heating technique employed the formation and deposition of Be dust in the vacuum vessel could not be excluded.

At frequent openings of the large vessel covers an exposition of the possibly contaminated inside of the vessel to the open atmosphere cannot be tolerated.

An upscaling of the facility for Be handling would mean the building of a controlled area around the vacuum vessel with enough space to open the covers and handle the vessel internals including the specimens. Also controlled volumes would have to be supplied for the exhausts of the vacuum vessel and the vacuum pumps. Whether the general use of protection clothes would be necessary for the personnel when working at the open vessel would have to be decided from experience.

An upgrading for Be-handling is not envisaged presently.

5. COMMISSIONING TESTS

Several tests were performed during the construction of the facility and after it was finished; they aimed at proving to what extend the construction goals were reached. Most of these tests, which are reported in the following chapters were conducted with the first heater and housing setup installed in the vessel as shown in Fig. 9.

5.1 Tightness of the vacuum vessel

The tightness was first determined as part of the acceptance tests at the delivery of the vessel. At that time the vessel was empty; the feed-throughs were closed with blind flanges sealed with Viton O-rings. The tightness was measured by

- pumping the vessel down for several hours to below $1 \cdot 10^{-4}$ mbar
- wrapping the vessel up with a big plastic envelope
- attaching a helium leak tester to the turbo pump exhaust
- comparing the leak tester's output to the nominal value of a calibration leak
- filling the plastic envelop with helium
- reading the leak rate before the helium diffusion through the bulk of the viton O-rings became dominant

The leak rate measured was $1.3 \cdot 10^{-7}$ mbar·l/s; this was better than the $1 \cdot 10^{-6}$mbar·l/s specified.

The tightness was determined a second and a third time at different stages of mounting the electrical feed-throughs and the eight coolant lines. This time the measurement was performed by the method of watching the pressure increase after having separated the vessel from the vacuum pump; with this method the measured leak rate includes external leaks as well as outgassing of the vessel's inner surfaces (internal leaks).

After mounting most of the vessel internals including heater, heater housing, and the various metal hoses for cooling the total leak rate was determined to be $4 \cdot 10^{-4}$ mbar·l/s; gas analysis resulted in an oxygen content of only 1 % indicating that only 5 % of the measured leak rate is due to oxygen-carrying external leaks and the remainder is due to desorptions from the vessel's inner surface mainly consisting of hydrogen. This was satisfactory since the main goal of protecting the graphite heater from oxygen was reached to a reasonable extent.

In summary the tightness test was passed. Also, it was demonstrated that with the heater at room temperature a vacuum of $2 \cdot 10^{-5}$ mbar can be reached; later the operation of the facility showed that vacua of below $1 \cdot 10^{-4}$ mbar are reached even with the heater being at high temperatures.

5.2 Water Circuits I and II

For each circuit the pump was run with all main valves fully open. The resulting maximum flow rates and the pressures at the manifolds are listed in Table 2. For circuit I the numbers should be understood on the basis of a first set of vessel internals included in the circuit, i.e. two dummy specimens and two heater housing halves both fitting the size of a 23 cm by 68 cm specimen. The pressure at the pump inlet (expansion tank)was set to 0.2 bar.

	flow rates, m^3/h					pressure at manifolds bar	
	dummy east	dummy west	housing east	housing west	total	inlet	outlet
CIRCUIT I full flow through heat exchanger	17.2	17.3	15.6	15.2	65.3	8.2	3.5
heat exchanger fully bypassed	21.1	21.3	19.4	19.0	80.8	7.9	0.7
CIRCUIT II					3.7	4.4	0.6

Table 2 Flow Rates and Pressures of the Water Circuits

It should be noted that future design changes of the specimens and housing would change their flow resistances and the maximum flow rates correspondingly.

In circuit I the oxygen content of the water was reduced to or slightly below 1 mg O_2/l by running the degassing station for several hours after the circuit had been open to the atmosphere.

5.3 Safety Systems Responses

5.3.1 Vessel Safety System

For the system shown in Fig. 15 several functions were adjusted and tested:

- The facility is automatically shut down if at the gauges (8) or (13) pressures are beyond limits.
- At gauge (8) pressure goes beyond the limit, if valves (10) or (12) are closed.
- The nonreturn flap (4) was opened at a vessel pressure of 500 mbar.
- After flap (4) fell open the vessel was filled with nitrogen and reached atmospheric pressure within roughly 3 minutes.
- The back pressure valve (3) opens at 0.3 bar gauge.
- The function of the rupture disk has not been tested since a sample of the lot had been proven by the manufacturer to respond at 0.86 bar gauge.

5.3.2 Shut-down Safety System

The shut-down functions discussed in chapter 3.10.2 were tested by artificially exceeding the preset limits and observing the system's reactions. After some adjustments the system worked as expected.

5.4 Uniformity of the Heat Flux

From the beginning of the design of the test facility it was a major goal to make the heat flux received at the surface of a specimens as uniform as possible; any random and strong non-uniformities would result in unexpected and unknown local temperature deviations in the specimens that make the evaluation of thermal fatigue tests unreliable.

Since the received heat flux is by radiation heat transfer it depends on the temperatures and emissivities of the emitting surface (T_h and ε_h) as well as on those of the receiving surface (T_s and ε_s) and in addition on the geometrical configuration (shape factors); the uniformity of the received heat flux depends on the uniformity of these parameters.

For a bare specimen with its relatively low surface temperatures a non-uniformity of T_s has an insignificant influence on the heat flux; for a tile-protected specimen T_s is rather uniform because the tile equalizes any temperature differences that may exist at the steel surface.
ε_s should be made uniform when the specimen is manufactured; its uniformity should be watched since sublimated carbon may be deposited during the test.
The heater's emissivity ε_h is expected to be very uniform; only at very high temperature levels ε_h may locally increase somewhat as a result of the aging process of the heater; but then the heater will be replaced anyway.

The temperature of the heater is known to be nonuniform at all four edges; at the upper and lower ends the temperature is reduced by conductive heat losses into the connection bars; at the sides the temperature may be influenced by the housing characteristics. The shape factor of the configuration as a whole gives rise to the suspicion that the heat flux received at the specimen might be nonuniform since radiative heat transfer could be uniform only for infinite parallel surfaces; but actually there are finite surfaces and the heater surface includes gaps between the heater stripes.

So, non-uniformities of the heat flux will be mainly due to non-uniformities in T_h and to shape factors. A quantification of the non-uniformities in heat flux has been the subject of a series of commissioning tests which are reported in the following chapters.

5.4.1 Experimental Setup

The heater and its housing were installed in the vessel as shown in the horizontal cross-section of Fig. 18. Dummy specimens (cooled copper structures) were placed into the housing windows on both sides of the heater; the dummies were coated with a thin layer of heat-resistant black color. Between the heater and the dummy west as well as around the edges of the heater radiation shields made of laminated graphite (1 mm thick) were inserted as discussed in chapter 5.4.3; around the edges there were three parallel shields. In the space between the heater and the dummy east a movable heat flux probe was mounted such that the sensitive spot of the probe could be moved in a plane parallel to the heater; the distance between the heater and the probe was about 20 mm which is roughly the same as expected between the heater and any specimen surface in later tests. The heat flux probe was a water-cooled asymptotic calorimeter model C-1301-A-120-72-X2 made by HY-CAL Engineering, El Monte, California. The sensitive spot is 3 mm in diameter allowing a good spatial resolution; the absorptivity of the surface is 0.89 and the probe was calibrated between 0 and 120 BTU/(ft^2·s) equal to 136 W/cm^2. The probe could be moved horizontally (x-direction) and vertically (y-direction) to cover a space of 288 mm x 495 mm. It may be read from Fig. 19 that the area of the heat flux scanning has been a little larger than and included the area of the first specimen (called TS1) to be tested. Due to space limitations the scanned area did not cover the whole heater area though. In order to move the heat flux probe in two directions it was mounted on two carriages which were operated from outside the vacuum vessel.

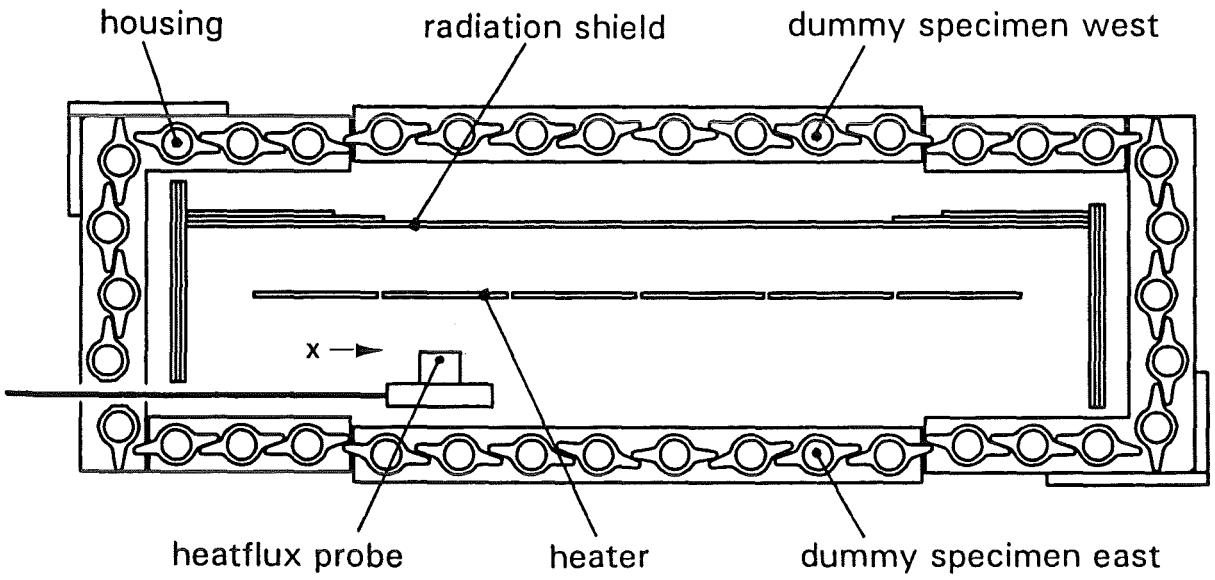

Fig. 18 Setup for Scanning the Heat Flux Uniformity

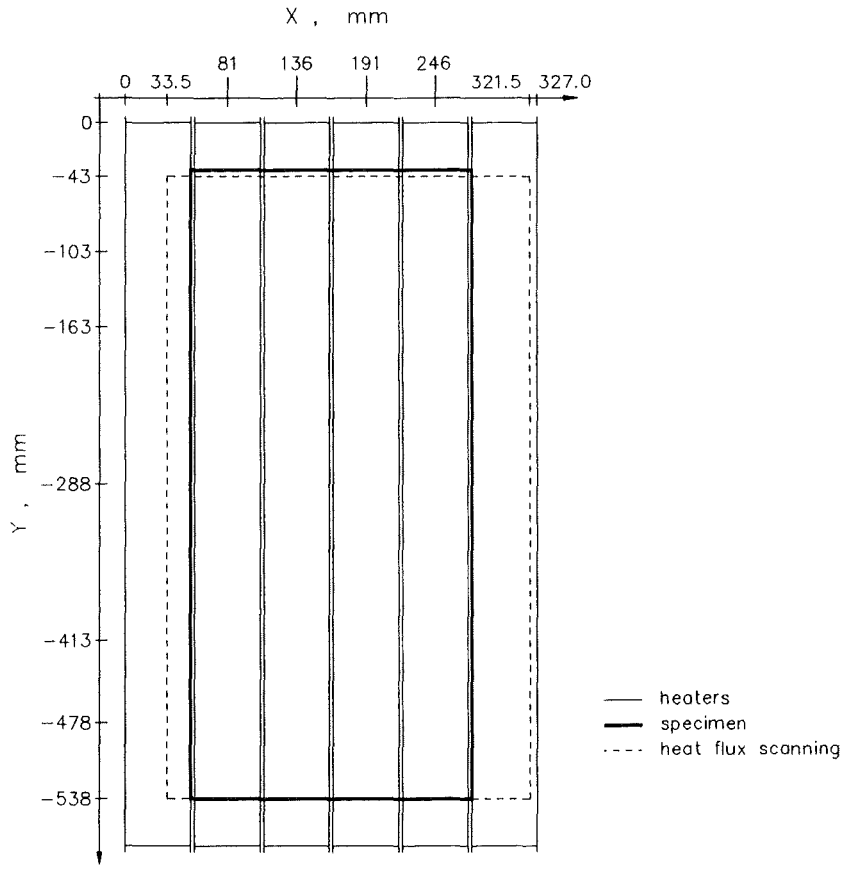

Fig. 19 Area Covered by the Heat Flux Scanning

In the x-direction a high spatial resolution was achieved by subdividing the space into 72 4-mm-steps and by taking measurements at each step. In the y-direction variations were expected towards both ends only and a coarse grid was chosen as indicated on the y-axis.

5.4.2 Measuring procedure

Heating was started by setting the desired value of the power at the controller; generally 50 kW or 90 kW per heater element were chosen resulting in total powers of 150 or 270 kW respectively. The heater was operated at steady state.

Heat-flux scanning was started with the x-traverse in the lowest position (−538 mm). Due to the fast response of the heat-flux probe stepping forward was possible every 7 seconds. After completing the x-traverse the probe was moved to the next higher y-position. It took almost about two hours to do one complete scan; during this time the heater power and the heater temperature were watched to run steadily with no noticeable deviations.

5.4.3 Lessons learned and Improvements made

When starting heat-flux scanning with the first heater configuration the results proved a high resolution of the method but the data showed that the heat flux uniformity was not satisfactory. As an example Fig. 20 shows a scan of the poor uniformity in x-direction at a power level of 50 kW per heater element. The slightly more than five heater stripes in the scanned area may easily be identified around the curve's maxima as well as the heater gaps next to the minima. The non-uniformity is on the order of +/−7% of the average value; this seemed to be not acceptable.

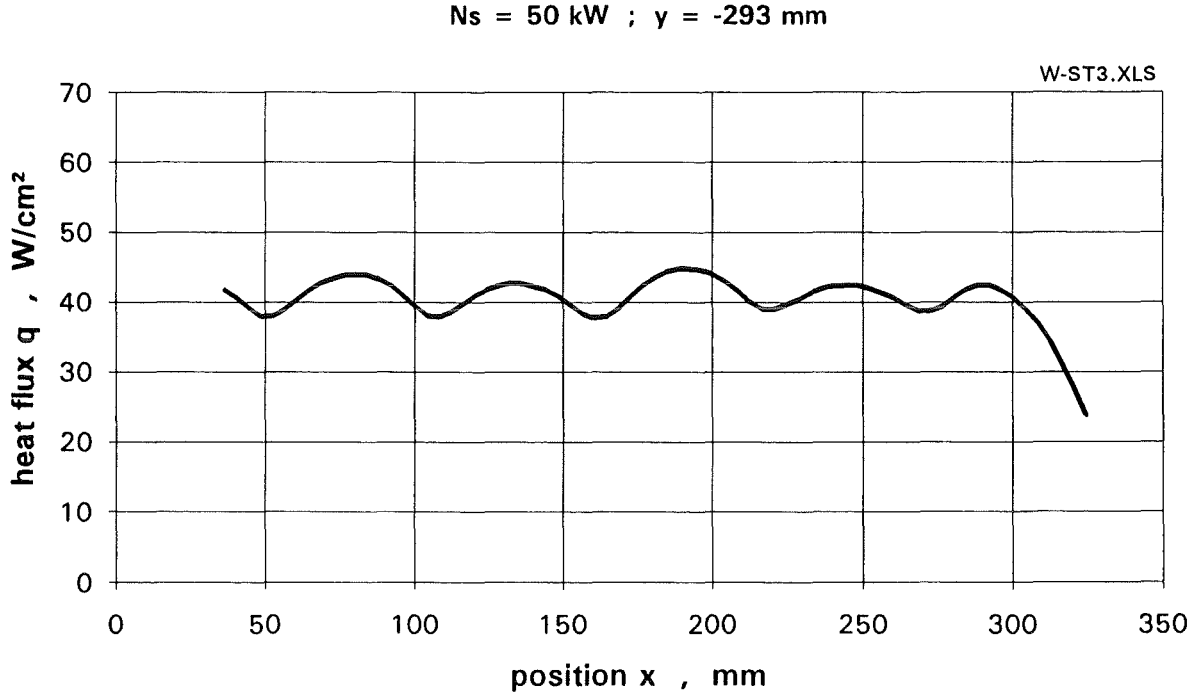

Fig. 20 Heat Flux Distribution with Poor Uniformity

Four reasons were found and eliminated to a large extent by several measures:

The first reason was the width of the gap between the heater stripes; at this stage the gap has been 5 mm as taken from the heater pretests. The gap could easily be reduced to 3mm.

The second reason was an opening up of the gaps as a result of the magnetic forces between two adjacent stripes. It was noticed that the uniformity of the heat flux was poorer in the middle than towards the upper and lower ends of the heater; also the stripes appeared to be bowed out of the plane into different directions after the test. At this time each transformer was connected to a pair of adjacent stripes. The close neighborhood of two parallel conductors leading currents in phase and in opposite directions resulted in magnetic forces on the order of a few newtons; obviously this was enough to bow the stripes apart. The forces were reduced by as far as possible separating the stripes that belong to the same electrical circuit; in fact the row of stripes within the heater was changed to the sequence indicated by the stripe numbers in Fig. 6.
As a consequence of doing this the originally three separated traverses at the lower ends of the three heater element had to be united into one. This long traverse connecting all stripes forms a star point for the electrical circuits. By this measure stripe bowing was strongly reduced even though, as a side effect, the heater now could expand only as a whole and not as three individual elements anymore.

The third reason for the non-uniformity was the cold background which the probe saw through the gaps in the heater, since in the beginning of the tests there was no radiation shield on the backside of the heater and the probe looked at the cold dummy directly. Building-in the radiation shield shown in Fig. 18 smoothed the heat-flux distribution considerably. It should be noted that the radiation shield may be included only if there is no specimen on the backside of the heater; but this seems to be a normal situation since the number of FW specimens available is very limited.

The last reason was responsible for the strong heat-flux decrease towards the side edges of the heater; it consisted of a reduced angle under which the probe sees the hot surface of the heater when approaching the heaters's edge. This effect to some extent was compensated by putting a three-layer shield around the edges as shown in Fig. 18; the compensation is partly by slightly increasing the temperature of the outermost heater stripes and partly by replacing the cold housing by the hot shield as a radiation partner to the specimen.

5.4.4. Heat Flux Distributions
After all improvements mentioned in chapter 5.4.3. were made the heat flux was scanned again. The results are reported in detail in Appendix B. As an example Fig. 21 shows a distribution that was taken at the same heater position and at the same heater power as the one of Fig. 20; in both cases the power per heater element was 50 kW the distance between the heater and the probe was 18 mm and the measurements were taken on a x-traverse at $y = -288$ mm (at the middle of the heater).

It is obvious that most of the earlier non-uniformities are smoothed out. The gaps in the heater can hardly be identified anymore.

The heat flux decrease towards the heater edge is reduced but still exists; it cannot be avoided but it can be made ineffective by not facing that portion of the heater with the specimen; this is the reason why, as a rule, the size of the heater should always be about 5 cm wider and 6 to 7 cm longer than that of the specimen at all edges.

The small remaining non-uniformities are probably due to minor differences between the powers of the heater elements and to the existence of the heater gaps which locally may open up a little more during operation.

Except for the edges the uniformity achieved is better than $+/-2\%$ of the average value. This uniformity is judged adequate for testing FW specimens.

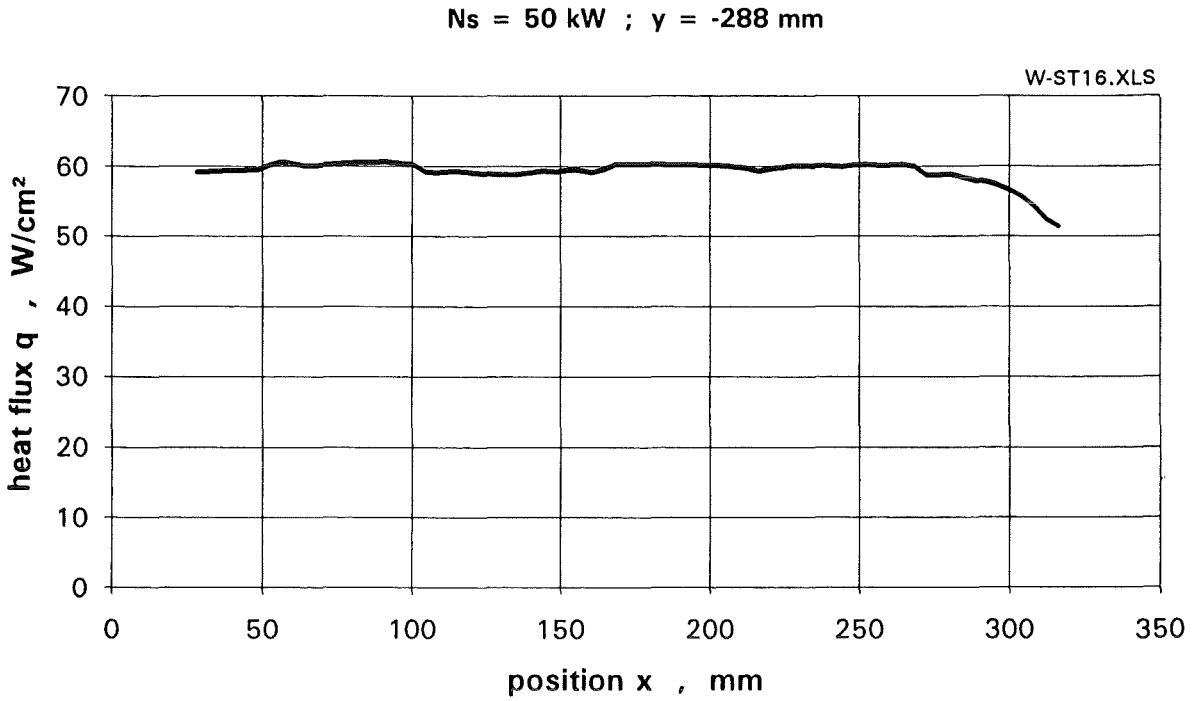

Fig. 21 Heat Flux Distribution with Improved Uniformity

5.5 Heating Cycles

As the main goal the facility should be capable of running adequately shaped heating cycles as a thermal load for the FW specimens. Therefore, as a final commissioning test, typical heating cycles were run and some of their transient data are reported.

Figs. 22-24 show some measured quantities for two cycles of such a test. The preset desired values for the power cycle consisted of a first power plateau at 92.5 kW/heater element for a total time of 3 s and a second power plateau at 90 kW/heater element for a total time of 87 s adding up to a power-on time of 90 s followed by a power-off time of 45 s (note that at power-off the power was actually set to 1 kW in order to keep the heater on an elevated temperature level).

In Fig. 22 is plotted how this desired power setting was converted into actual heater power. The same figure shows how the heater temperature reacted to the power transient; the temperature curve measured by the spectral pyrometer indicates a fast temperature increase to a plateau level without overshooting; this shape of the curve is due to the choice of the first power plateau. After a period at constant temperature the heater temperature fell down below the measuring range of the pyrometer.

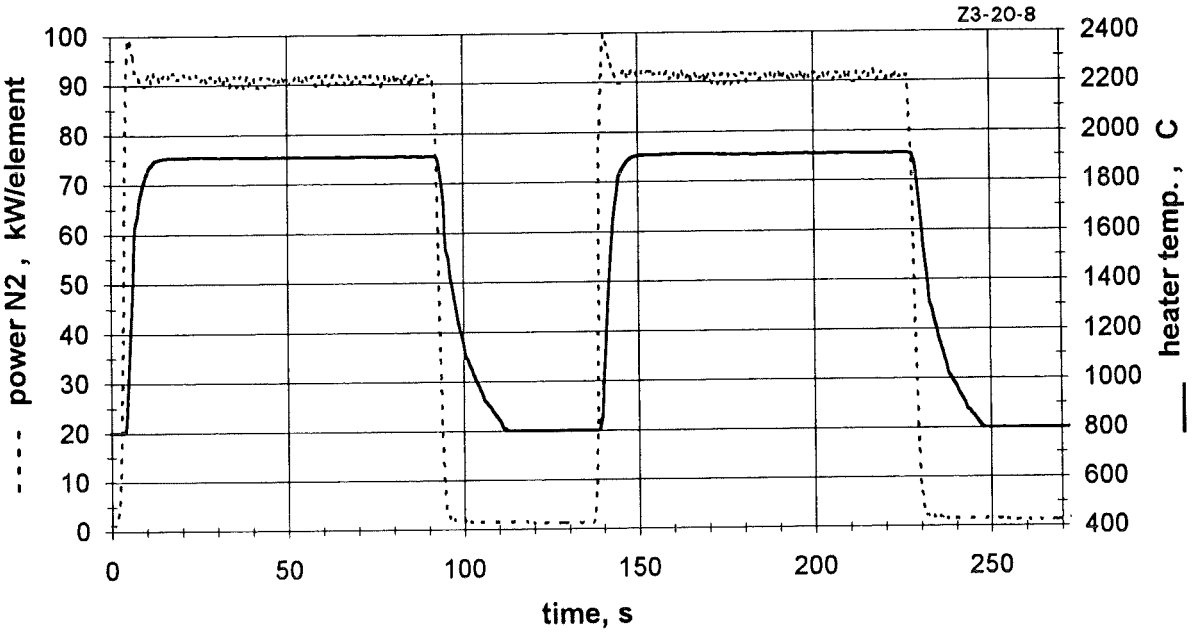

Fig. 22 Heater Power and Heater Temperature during two Cycles

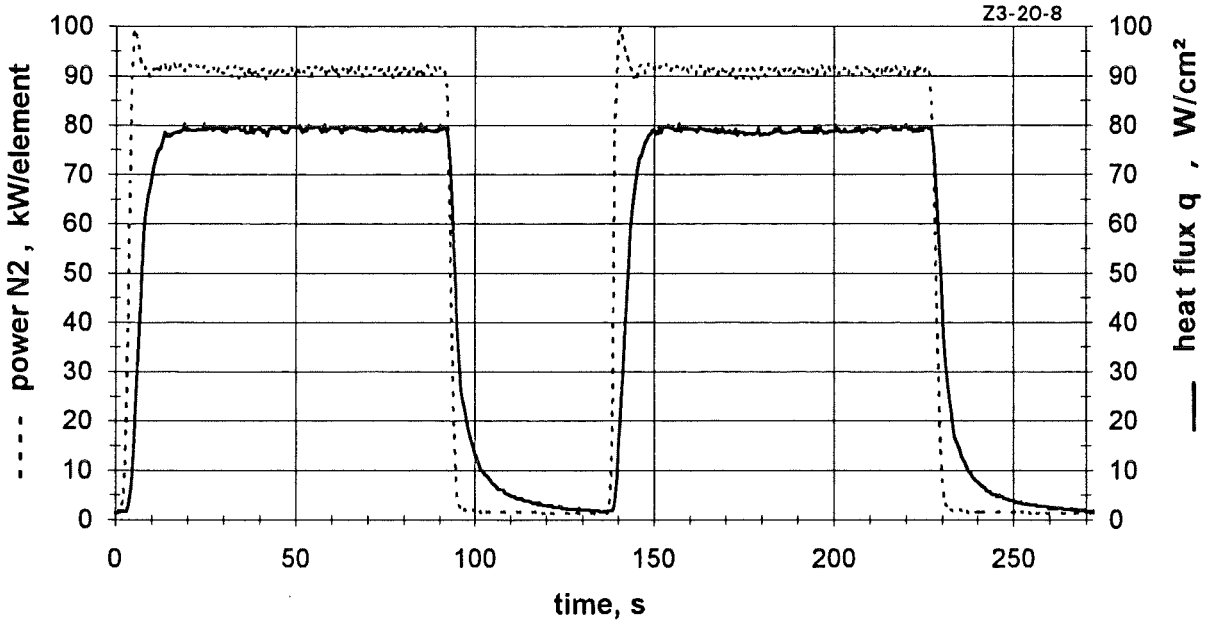

Fig. 23 Heater Power and Heat Flux at Specimen during two Cycles

Fig. 23 repeats the power transient as a reference and compares it to the heat flux transient as measured with the heat-flux probe in a x=81.5 mm and y=−478 mm position; the time response of the heat-flux probe is 80 ms. It is obvious that due to the power cycle and the fast response of the heater the heat flux increased fast to a constant level; this had been a design goal in order to realize well defined boundary conditions for the thermal fatigue tests and to not waste much experimental time on slopes.

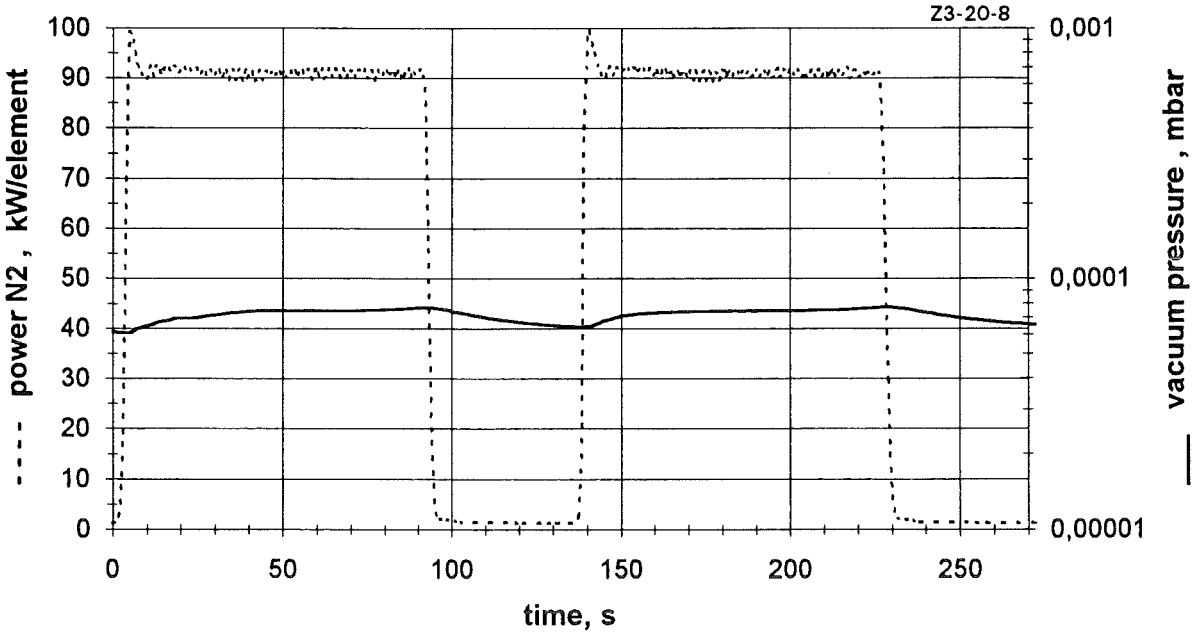

Fig. 24 Heater Power and Vacuum Pressure during two Cycles

Fig. 24 shows the pressure in the vacuum vessel again together with the power transient; there is a small cyclic change of the pressure with the heater temperature.

As a preliminary result it can be stated that the heating cycles that may be run with the test facility seem to satisfy the needs.

6. CONCLUDING REMARKS

The FIWATKA facility for thermal fatigue tests is outlined in this report. It is located at the Institut für Angewandte Thermo- und Fluiddynamik (IATF) of the Kernforschungszentrum Karlsruhe (KfK).

After completion of the commissioning tests the facility is operable since October 1, 1992. Tests with the first FW specimen provided by the NET team started in January 1993. Since then several tests on the performance of protection tiles in front of a FW specimen have been conducted. During these tests the facility performed well including long-term testing over several days.

The facility may be adjusted to any type of specimen if the limits given in this report are observed; in addition it should be mentioned that any parts of the specimen must not protrude beyond its heated surface and that, for the sake of a good calorimetric determination of the heat flux, it should be possible to have the housing start with its edge-fins very close to the edges of the specimens. Considerable effort is necessary to fit the housing to new dimensions of a specimen. Therefore, wherever possible the fitting needs should be considered at the design of a specimen already.

7. REFERENCES

[1] G. Hofmann; unpublished report, IATF, Kernforschungszentrum Karlsruhe (Sept. 1989)

Appendix A Heater Pre-Tests

In the beginning of the project it was not clear whether a resistance heater of graphite could stand the large number of fast temperature transients that would be necessary.

An extended test program was conducted in order to qualify and select a graphite quality suitable for the specific service conditions of the heater, i.e. power cycles with steep ramps up to selected high temperature levels. These tests aimed at investigating by long term cycling

- the integrity and shape stability of the heater
- the stability of the electrical contacting chosen
- the uniformity of the temperature distribution as a result of local current densities and of conductive heat losses in the vicinity of the contact points
- the lifetime of the heater with respect to uniformity of heat generation

The graphite materials investigated ranged from fine-grained graphite and carbon fiber reinforced carbon (CFC) to laminated graphite; the graphite grades and heater dimensions are listed in Table A-1 and Fig. A-1 respectively.

graphite grade	no.	type	manufacturer	number of specimens tested
fine-grained	1	EK 96	Ringsdorff, Bonn	3
	2	FE 219	Schunk u. Ebe, Gießen	2
CFC	3	CC 1001 G	Sigri, Meitingen	1
	4	CF 322	Schunk u. Ebe, Gießen	3
laminated	5	Sigraflex L200 10 Z	Sigri, Meitingen	1
	6	Sigraflex LH, perfor.	Sigri, Meitingen	13
	7	Papyex N	Le Carbone Lorraine,	9
	8	Papyex NT	Gennevilliers, France	0

Table A-1 Graphite Materials Tested for the Use as Heater Materials

The test heaters were machined or cut from graphite plates; they were U-shaped with a gap of 5 mm between the two legs as shown in Fig. A-1; at the two top ends they were electrically connected to an AC power supply. The samples were resistance-heated in a vacuum of roughly 10^{-4} mbar. The test apparatus mainly consisting of glass is shown in Fig. A-2.

The heaters were tested by running a large number of heating cycles. Each cycle started with a fast temperature increase up to a preset temperature level of between 2100 and 2200 °C; in many of the tests this temperature was kept for some time (plateau) as a balance between the electrical power and the heat losses to the surroundings; the cycle was completed by cutting the power and letting the sample cool down to roughly 1100 °C, before the next cycle was started. During cycling changes of the heater resistance were monitored; in larger intervals the samples were inspected visually and the remaining uniformity of the heat generation was determined by taking black and white photographs of the heater during the heat-up phase and by scanning the gray densities on the films.

Besides the variation of the graphite material and some minor changes of the design the main test parameter has been the maximum heater temperature.

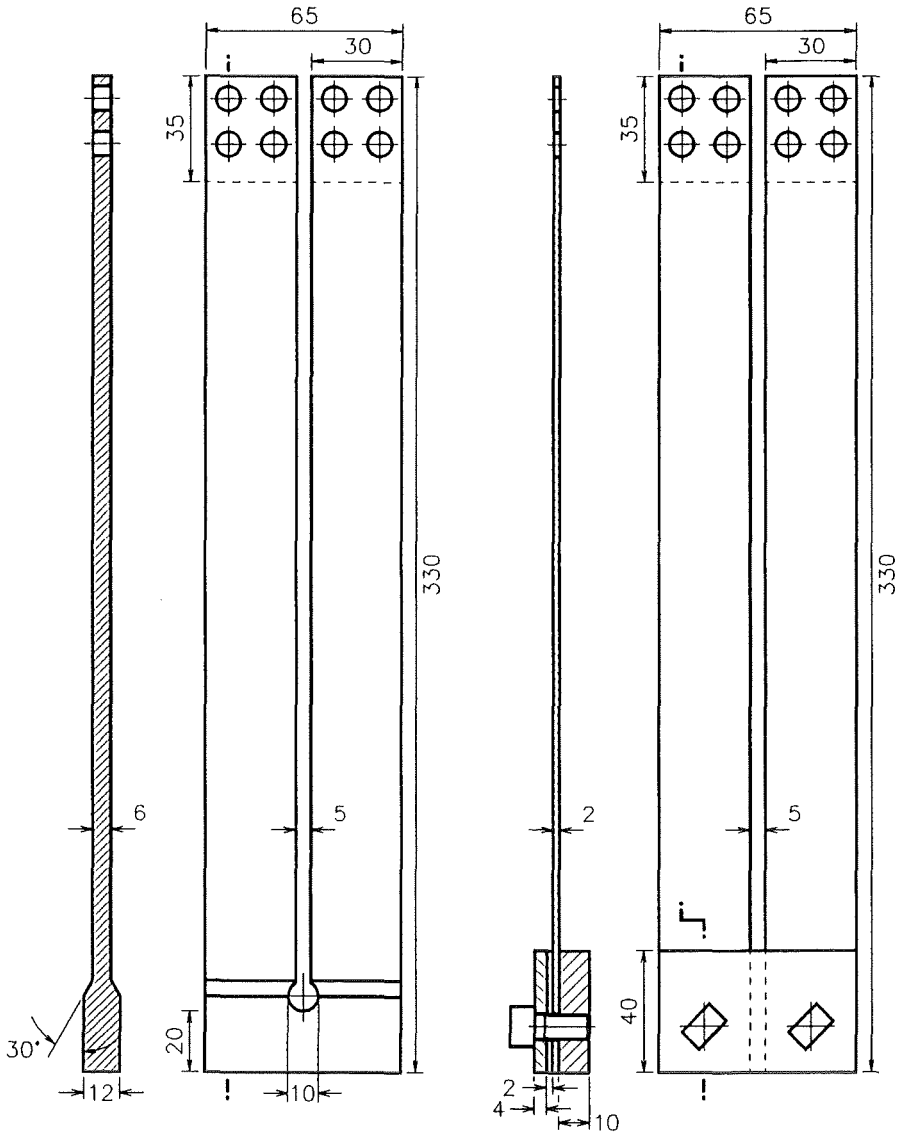

Fig. A-1 Specimens for Heater Pre-Tests

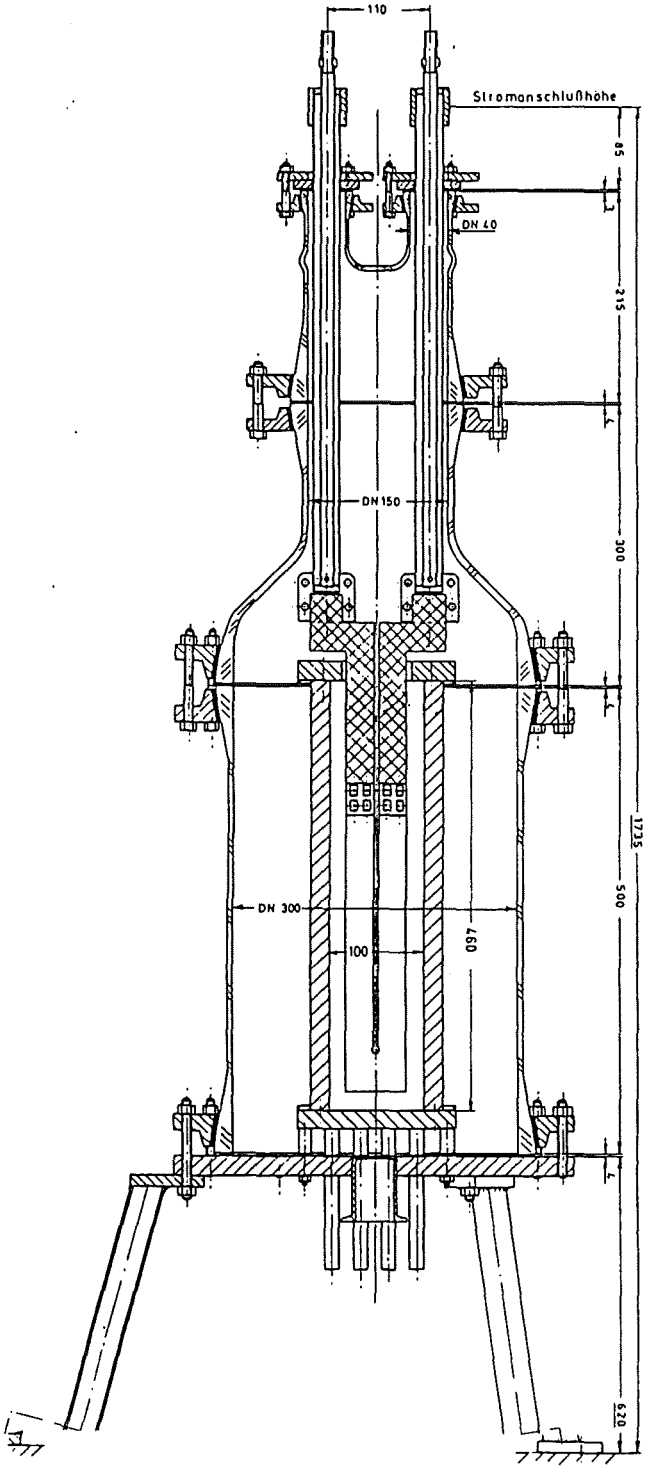

Fig. A-2 Test Apparatus for Heater Pre-Tests

A total of 32 heater pretests were conducted; the results may be summarized as follows:

- Screening test showed that all graphite materials tested seemed suitable for the purpose intended.

- Laminated (flexible) graphite offered several advantages; that led to performing most of the pretesting with only this material: its low mass (thickness 2 mm and density 1 g/cm^3) makes it fast reacting to power changes, it is inexpensive, and the in-laboratory tailoring of heaters is easily possible.

- There was no bowing or buckling of the heater elements.

- The uniformity of the temperature distribution as indicated by the photographs was very high; this was supported by a later heat flux scanning reported in chapter 5.4. The zones of lower temperature in the vicinity of the upper and lower electrical connection bars are on the order of 5 cm each.

- There was no indication of any contacting problems between the heating elements and the connection bars for the contacting design chosen (for details see 3.3.4).

- For the current turn-around at the lower end of the heater elements it proved preferable to provide an enlarged material cross-section in order to avoid hot spots due to current non-uniformities.

- Some electrical discharges between parts of the heater or the connection bars and the grounded test section housing were observed but happened without impact on the integrity of the heater. They were associated with pollution of the vacuum atmosphere and were minimized by reducing the voltage differences between closely neighbored parts where possible.

- The only failure mode encountered during the pretests was a kind of localized aging of the graphite. By some sublimation and restructuring mechanisms, not investigated in detail, the heater in its hottest zone (in the center) starts to uncouple, electrically as well as heat-conductingly, surface layers of graphite from the bulk of the material, i.e. a layer of flakes or dust develops at the surface. This causes a local increase of the heater resistance as well as a thermal shielding of the heat generating bulk material, resulting in a temperature increase in the bulk of the heater material. Since the aging is strongly temperature dependent the process is self-escalating. The early indications of this process are an increasing total resistance of the heater and the development of a cold spot on the heater surface; after some exponential growth the local temperature increases dramatically and the heater is destroyed.

- This failure mode is started and largely supported only at very high temperatures and the aging (formation of layers) needs time to develop; this is the reason why we observed a strong dependence of heater life time on heater temperature. Fig. A-3 shows the end-of-life data for heater specimens made of laminated graphite; the accumulated time at maximum temperature is plotted versus the maximum heater temperature; since only the highest temperature portions of the heating cycles will add to the aging process only these portions (usually a time plateau at maximum temperature) were included into the accumulated time. The points in the figure represent the testing status when the heaters having been run at the indicated maximum temperatures were judged to be at the end of their life; in the pretests end-of-life was assumed at an indication of temperature nonuniformities on the heater photographs usually coinciding with an increase of the total heater resistance by 2 %. The figure shows that there is a steep decrease of the heater life time with the temperature in the range above 2100 °C where the addressed aging process is dominant.

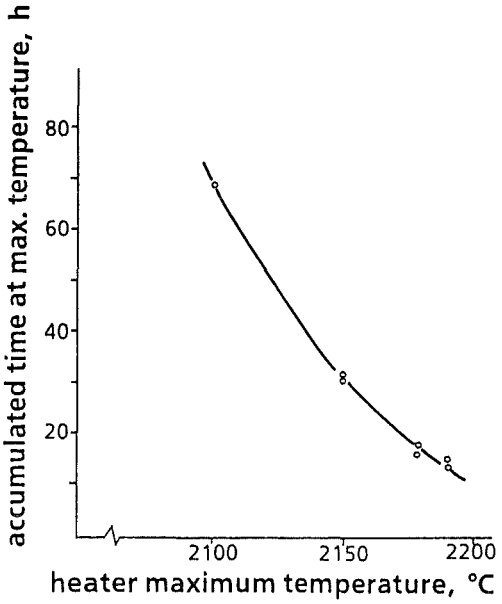

Fig. A-3 End-of-Life Conditions for Heaters of Laminated Graphite

- Fortunately it turned out that extensive aging happens only beyond the limits necessary for running the FIWATKA tests since in most cases the heater temperatures necessary are below 2100 °C and even above this level in many applications a sufficient number of cycles is possible since only those time portions add up during which the heater is at maximum temperature.

- It was decided that from a lifetime point of view the graphite heaters are adequate for the tests since, if necessary in long term tests at extreme temperatures, the heaters may be replaced every few days.

- Regular grade laminated graphite of both suppliers (materials 6 and 7 listed in Table A-1) tended to develop blisters during the first heat-up except when the first heat-up was very slow up to temperatures of roughly 1600 °C; the reason was an outgassing of ingredients of the material which were not analyzed in detail. These blisters could not be tolerated but they could be avoided, when the outgassing rates were small by running sufficiently low heat-up rates, and when outgassing was supported by a pattern of needle perforations into the material's surfaces. The material no. 8 from Table A-1 that was offered high temperature treated by the supplier turned out to delaminate during heater tailoring; since no better lot was available at that time this material was discarded from the pretests.

Blistering was avoided by buying the perforated material from Table A-1 and have it high temperature treated with low heatup rates in vacuum (conditioning).

It was concluded from the pretests that a plane resistance heater of 2 mm thick laminated graphite (material 6 from Table A-1 with additional conditioning) could stand the large number of high temperature transients necessary for conducting the FW tests.

Appendix B Results of Scanning the Heat-flux Uniformity

As reported in chapter 5.4 both the heater and housing arrangements have been changed in several steps in order to approve the uniformity of the heat flux received in the specimen plane. This appendix contains the data which were measured with the last arrangement that was judged satisfactory.

The data were taken as horizontal x-traverses with 4-mm-increments in x-direction; a total of seven such traverses were measured distributed over the length of the heater as indicated in Fig. 19. For each of these traverses the heat-flux distribution is plotted in Figs. B-1 through B-7 for a power setting of 50 kW per heater element. At the bottom of each figure the data curve is related to the spatial arrangement of the heater stripes and of the radiation shields; the distance between the 3 mm sensitive spot of the heat-flux probe and the heater was 18 mm.

The next four figures show the uniformity in y-direction; these y-traverses plotted in Figs. B-8 through B-11 are taken along the centerlines of each of the four inner stripes (see Fig. 19 for x-positions). It should be noted that because of the coarse measuring grid with only seven points along each y-traverse the slopes towards the upper and lower ends seem to start earlier than they actually do.

Fig. B-12 shows all data for the 50 kW condition on a 3-dimensional plot.

Another set of 2-dimensional and 3-dimensional plots for a higher power setting of 90 kW is shown in Figs. B-13 through B-24.

Fig. B-1 Heatflux distribution on the x-traverse for y = - 43 mm at Ns = 50 kW/heater element

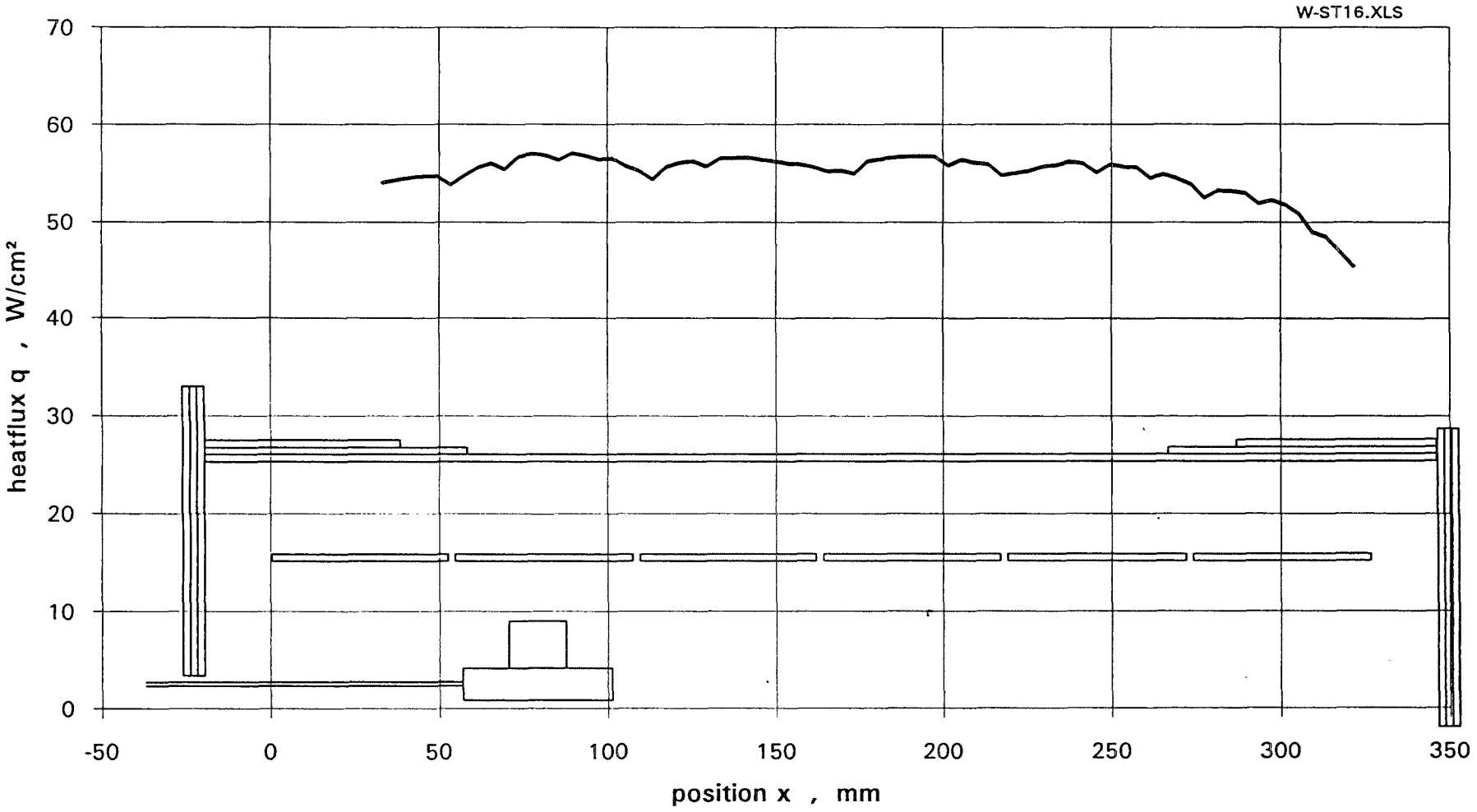

Fig. B-2 Heatflux distribution on the x-traverse for y = -103 mm at Ns = 50 kW/heater element

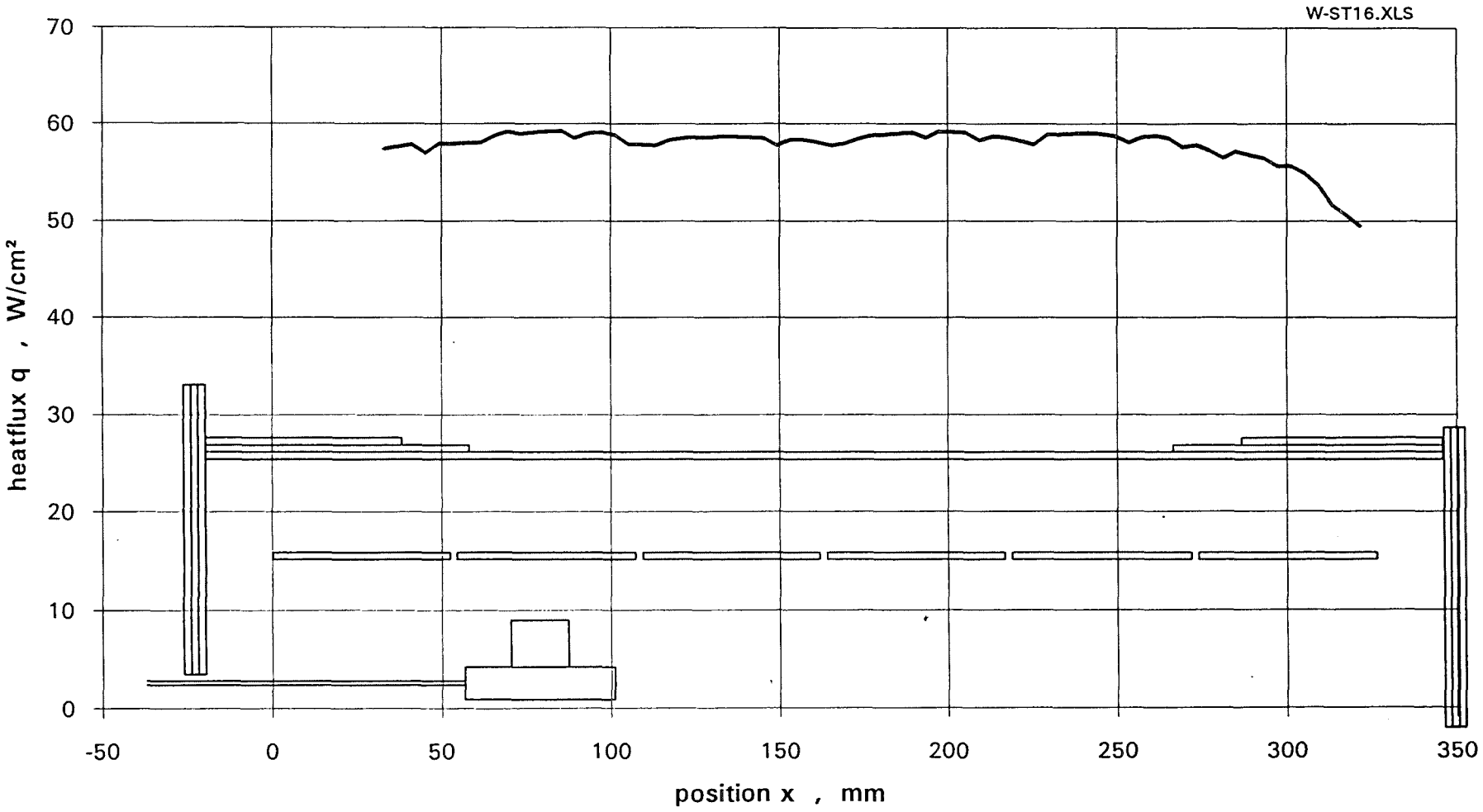

Fig. B-3 Heatflux distribution on the x-traverse for y = -163 mm at Ns = 50 kW/heater element

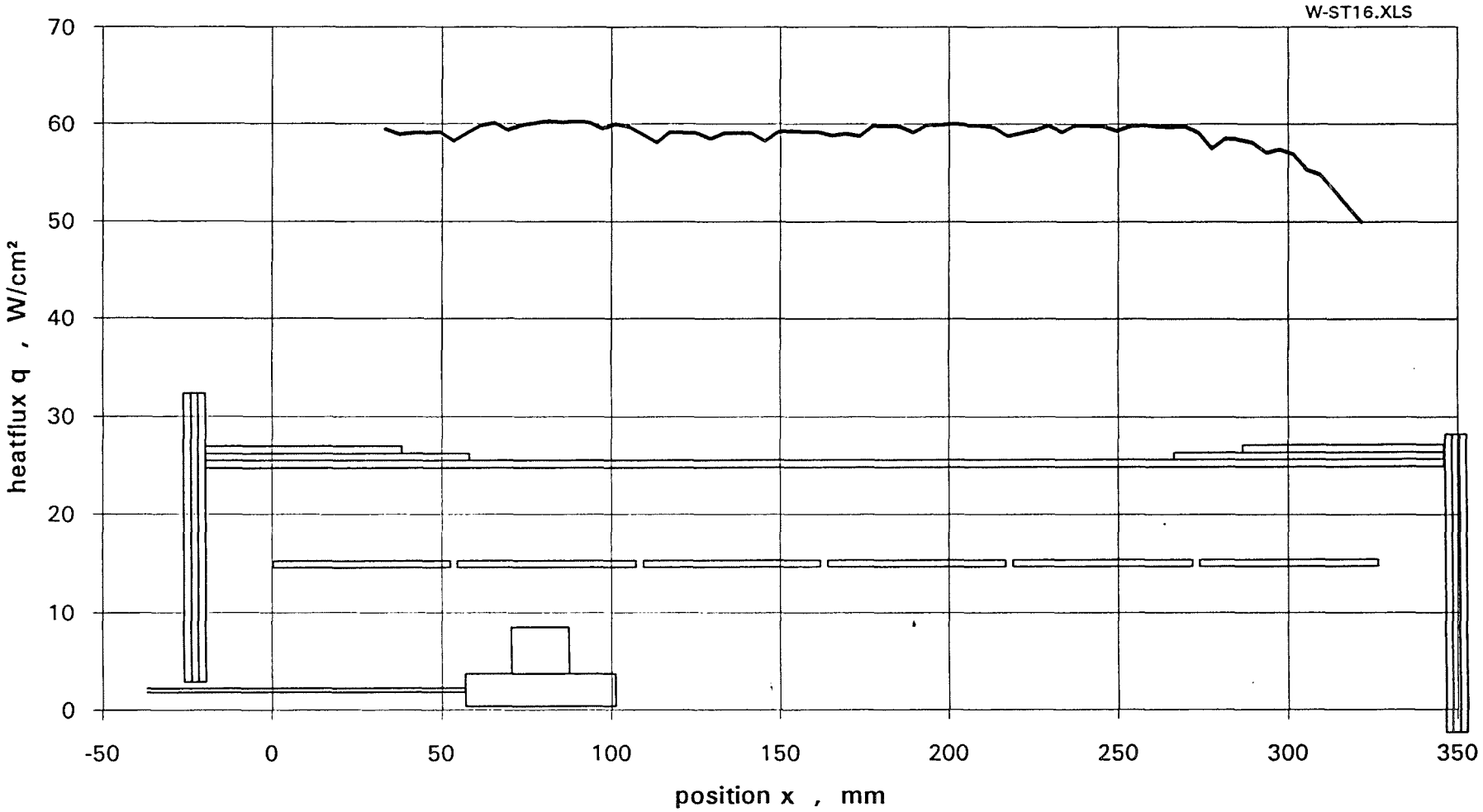

Fig. B-4 Heatflux distribution on the x-traverse for y = -288 mm at Ns = 50 kW/heater element

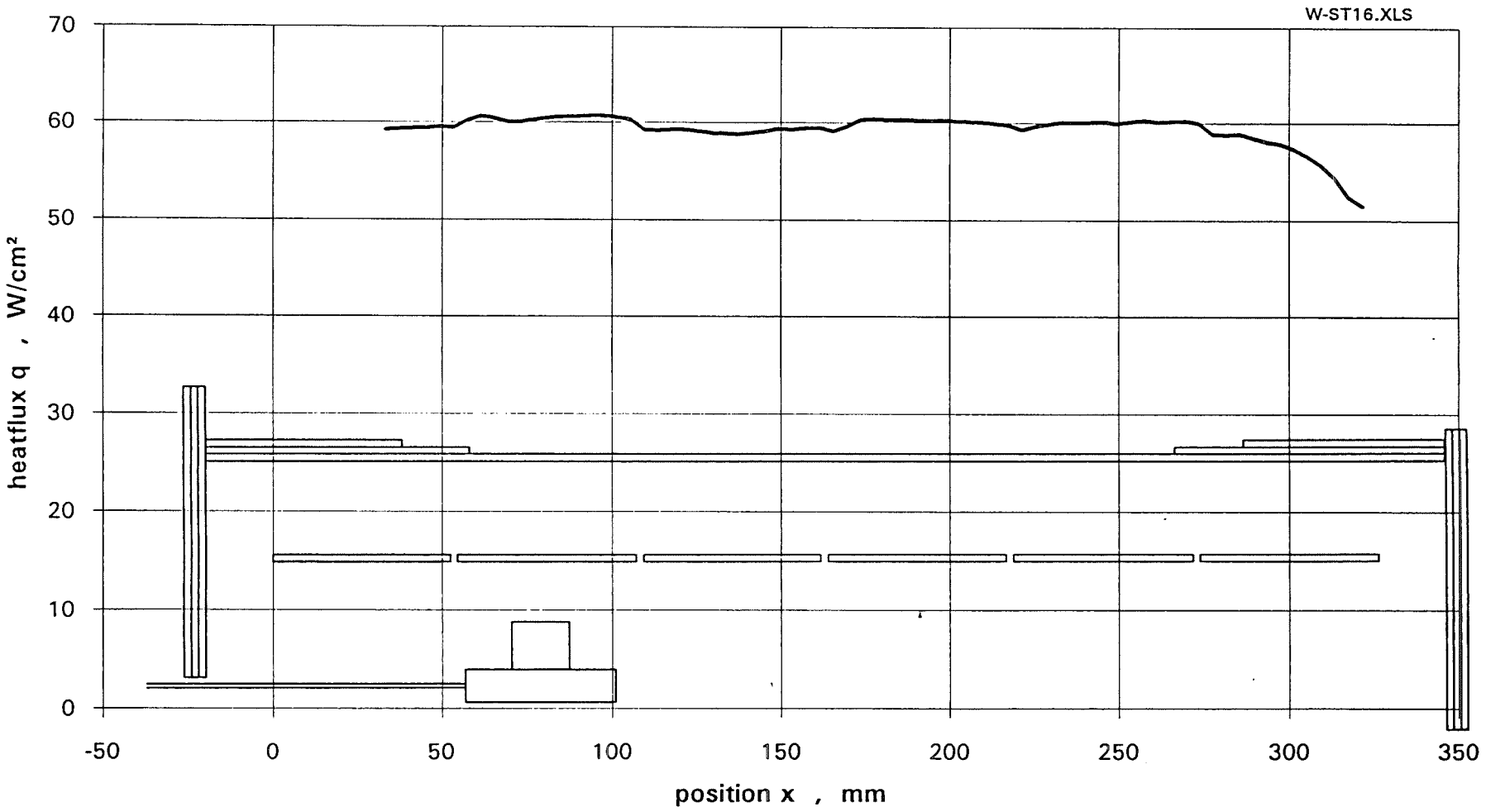

Fig. B-5 Heatflux distribution on the x-traverse for y = -413 mm at Ns = 50 kW/heater element

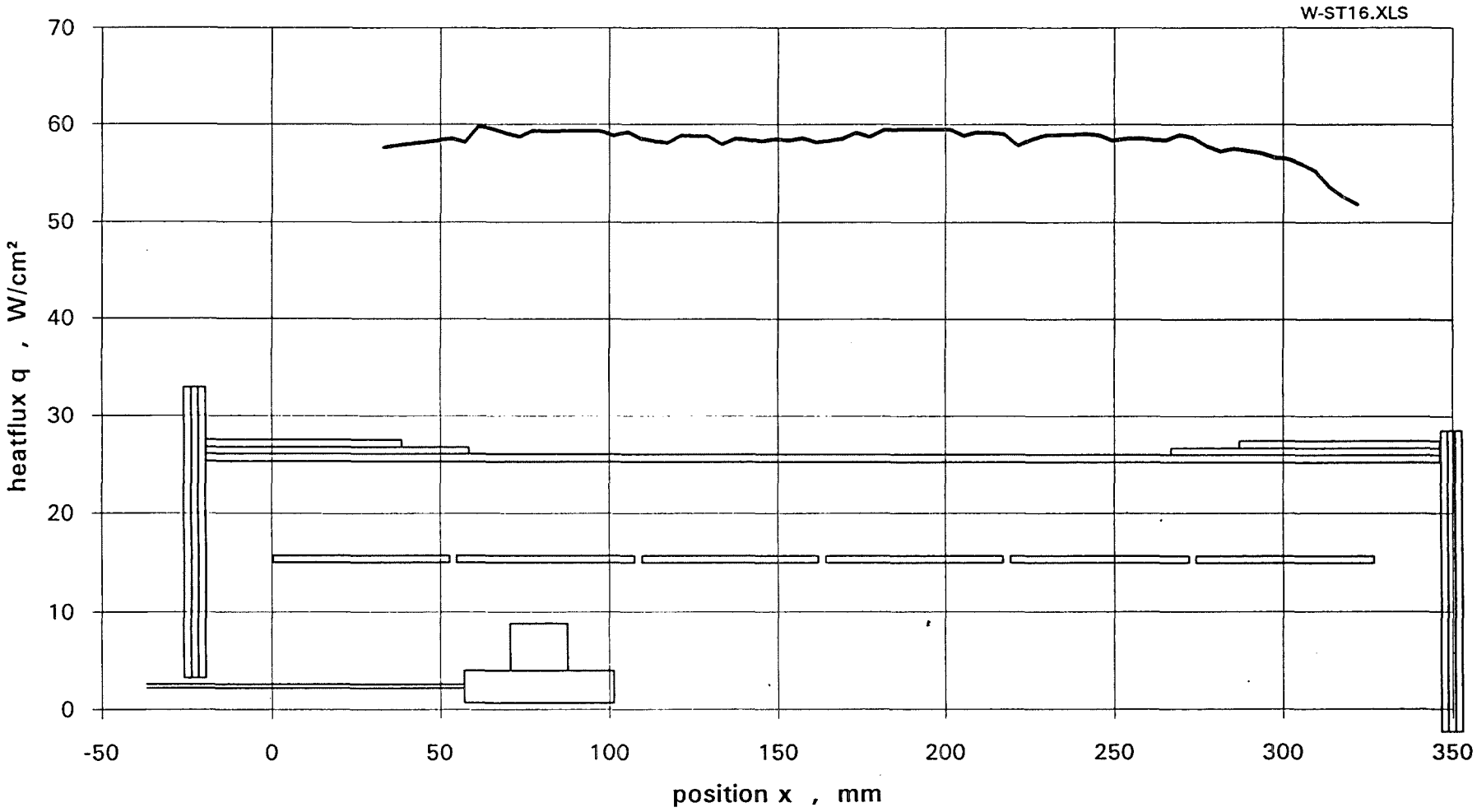

Fig. B-6 Heatflux distribution on the x-traverse for y = -478 mm at Ns = 50 kW/heater element

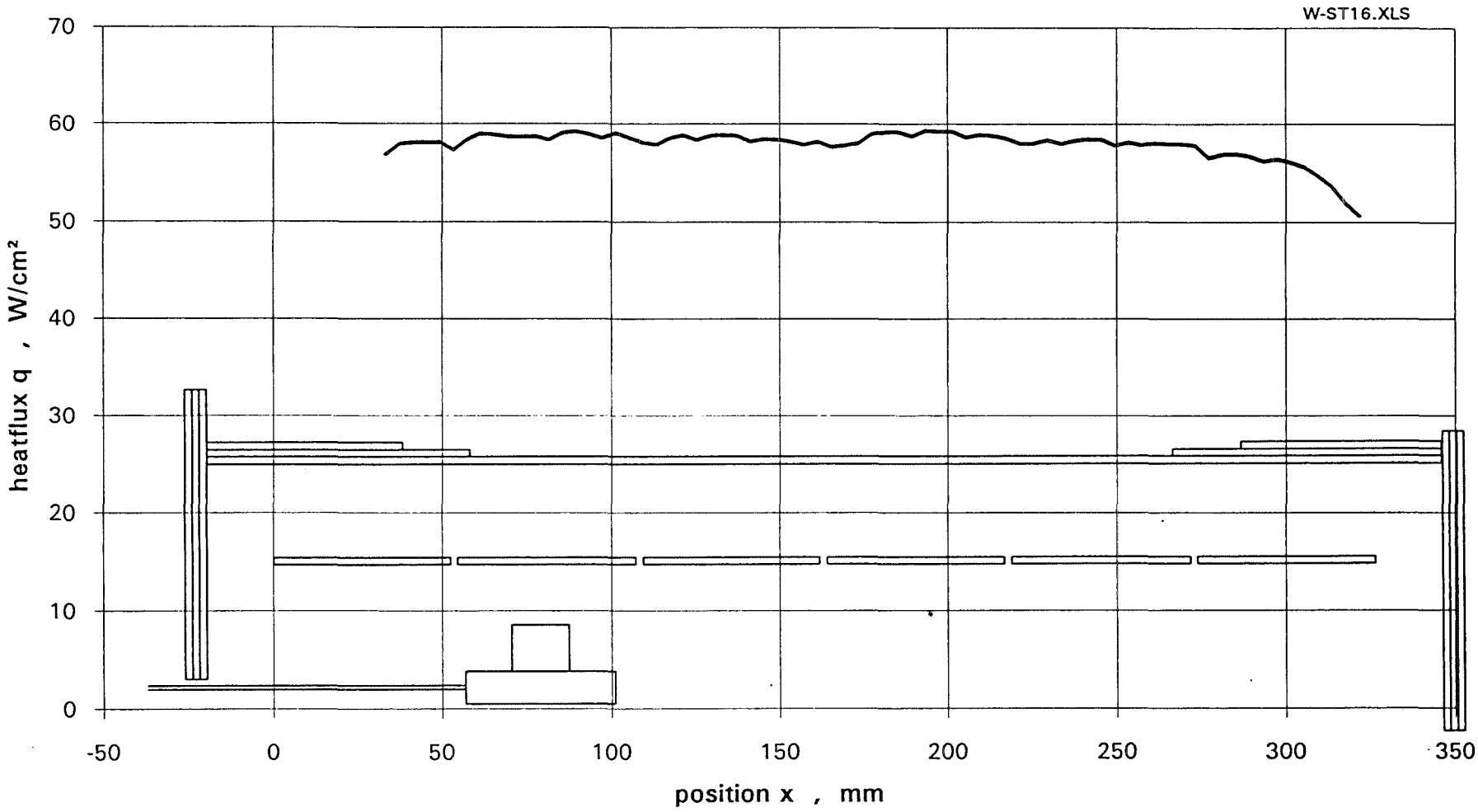

Fig. B-7 Heatflux distribution on the x-traverse for y = -538 mm at Ns = 50 kW/heater element

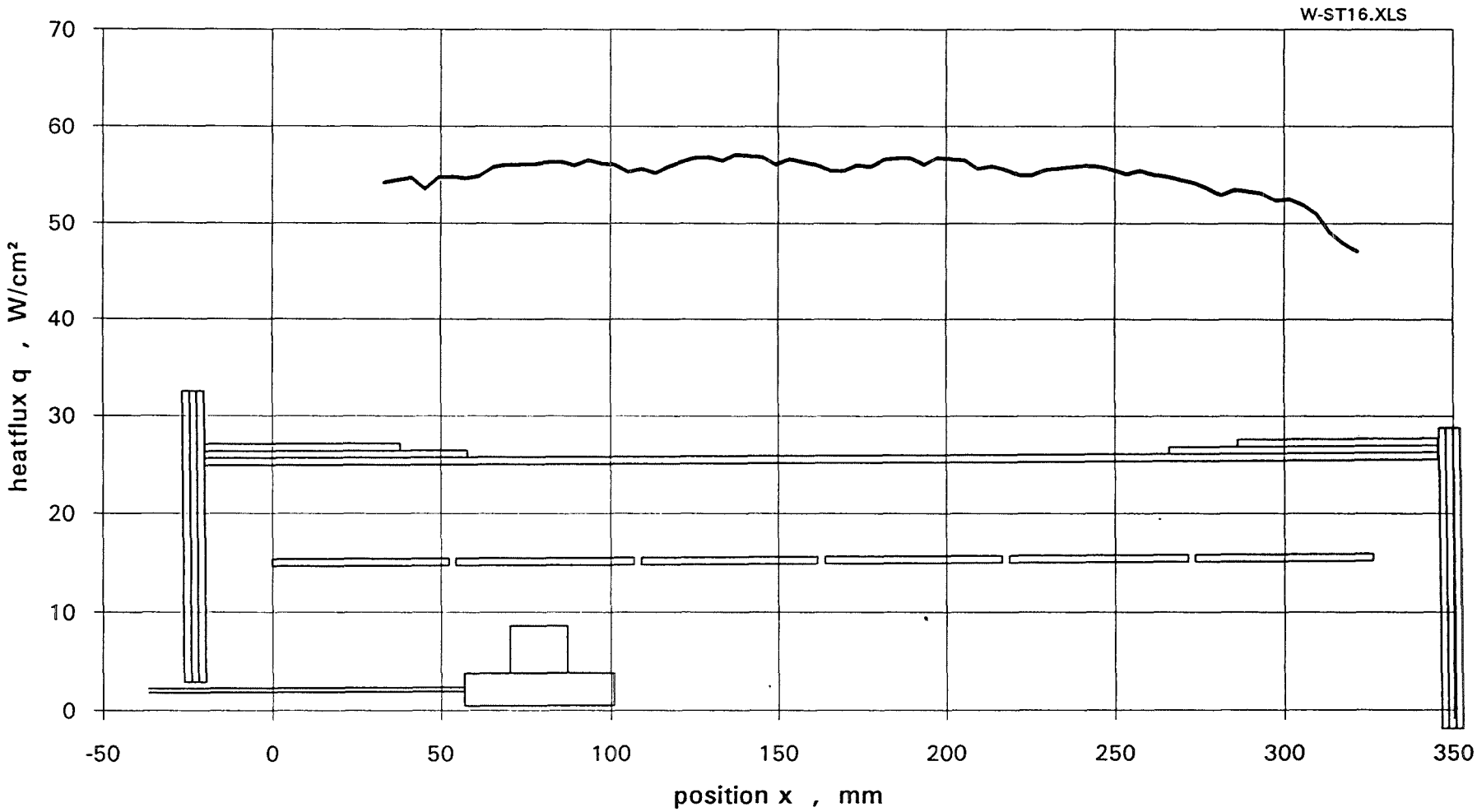

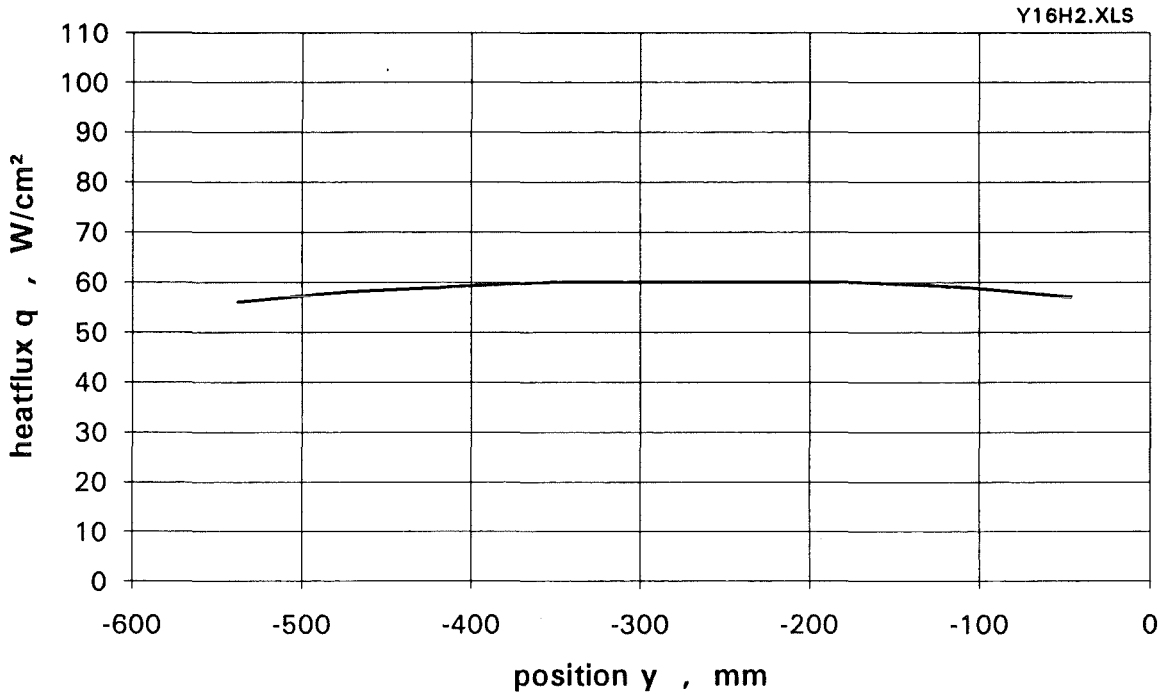

Fig. B-8 Heatflux distribution on the y-traverse for x = 81 mm at Ns = 50 kW/heater element

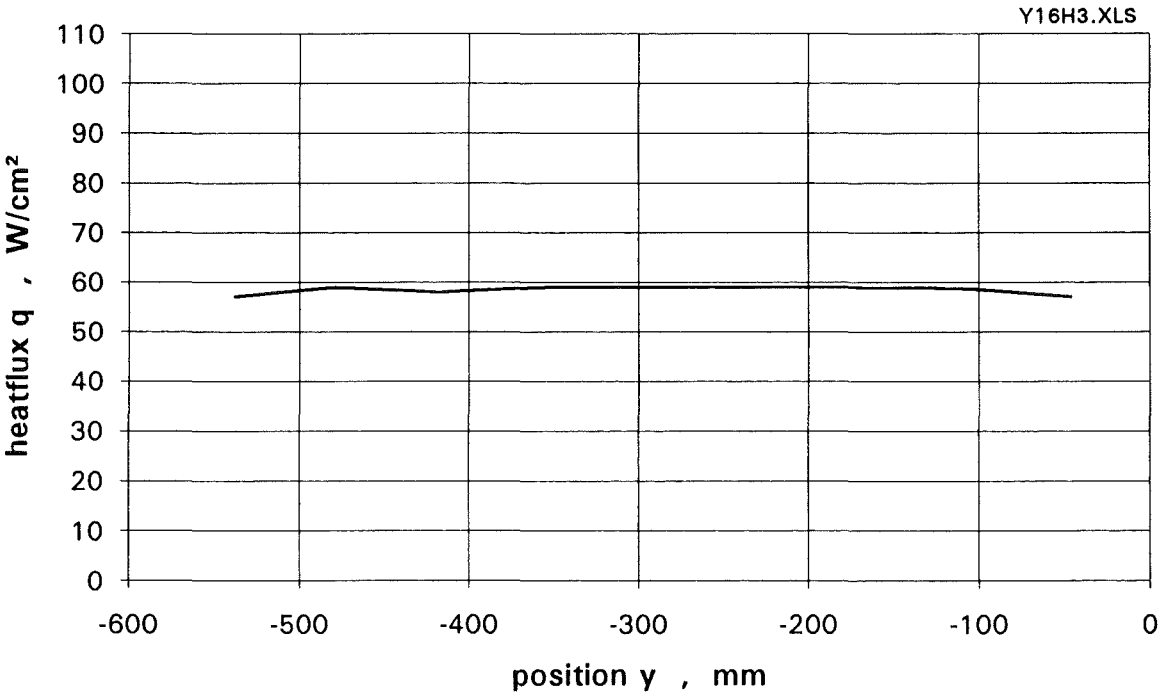

Fig. B-9 Heatflux distribution on the y-traverse for x = 136 mm at Ns = 50 kW/heater element

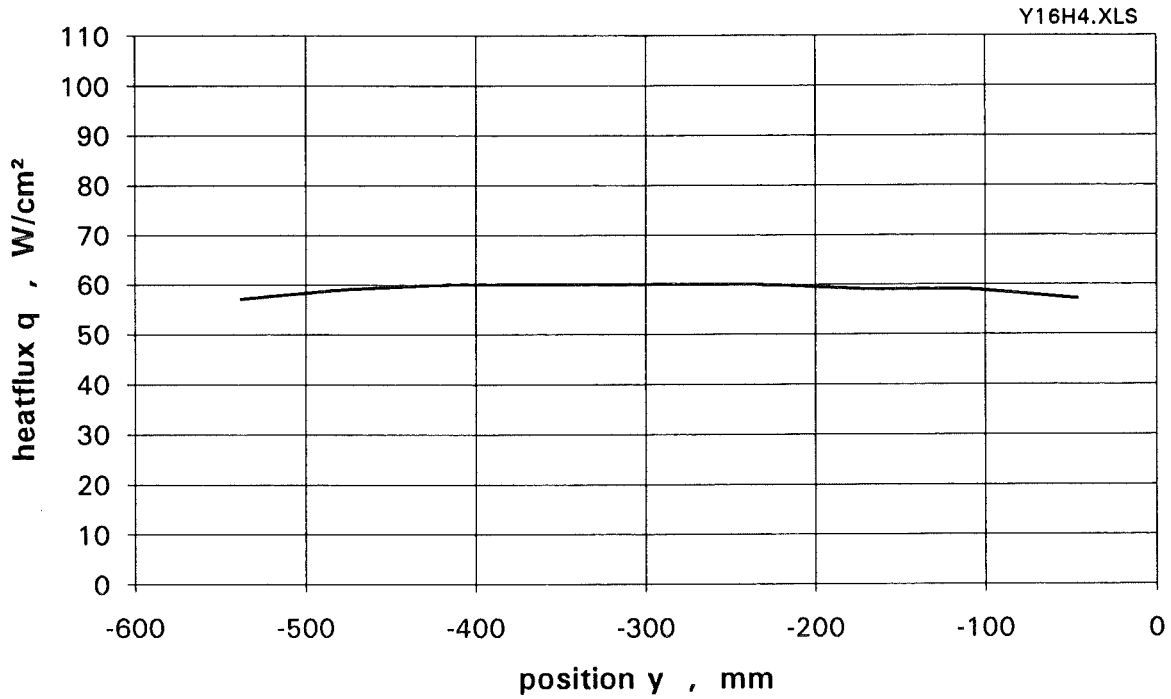

Fig. B-10 Heatflux distribution on the y-traverse for x = 191 mm at Ns = 50 kW/heater element

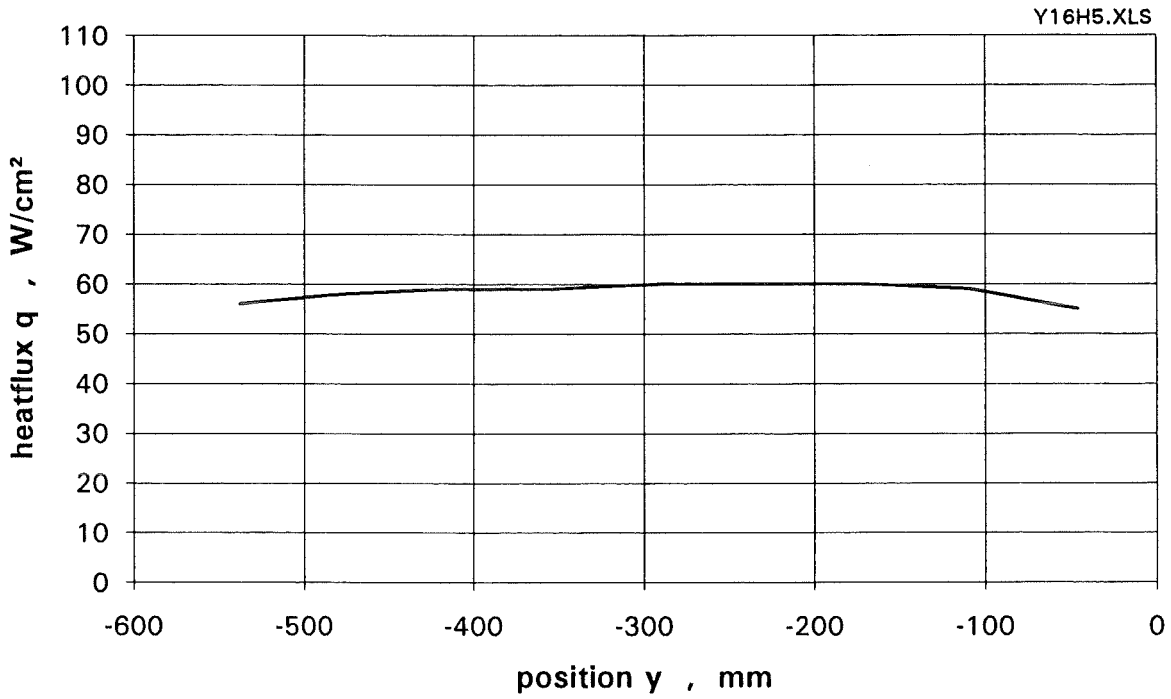

Fig. B-11 Heatflux distribution on the y-traverse for x = 246 mm at Ns = 50 kW/heater element

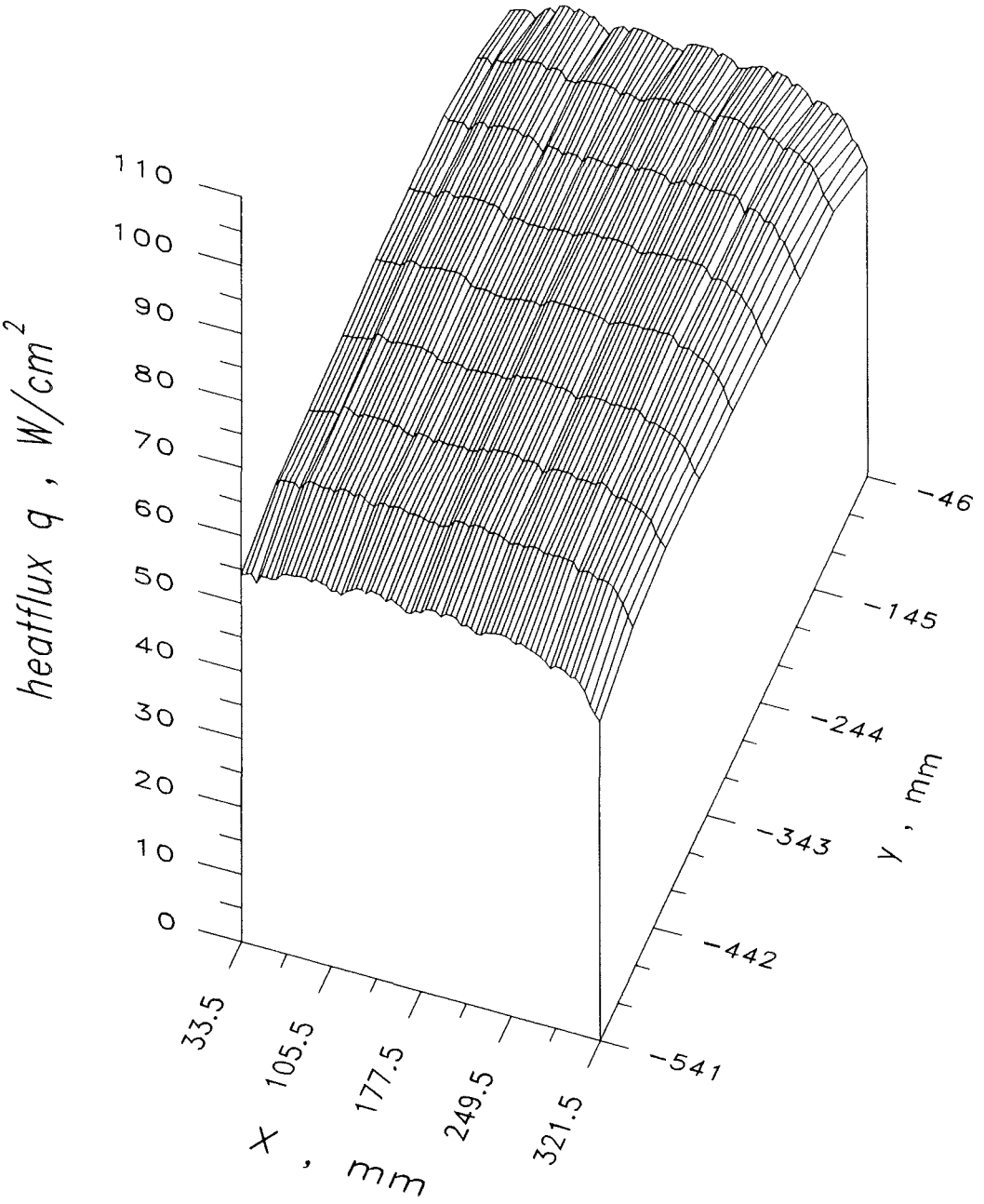

Fig. B-12 Heatflux distribution across the heater at Ns = 50 kW/heater element

Fig. B-13 Heatflux distribution on the x-traverse for y = - 43 mm at Ns = 90 kW/heater element

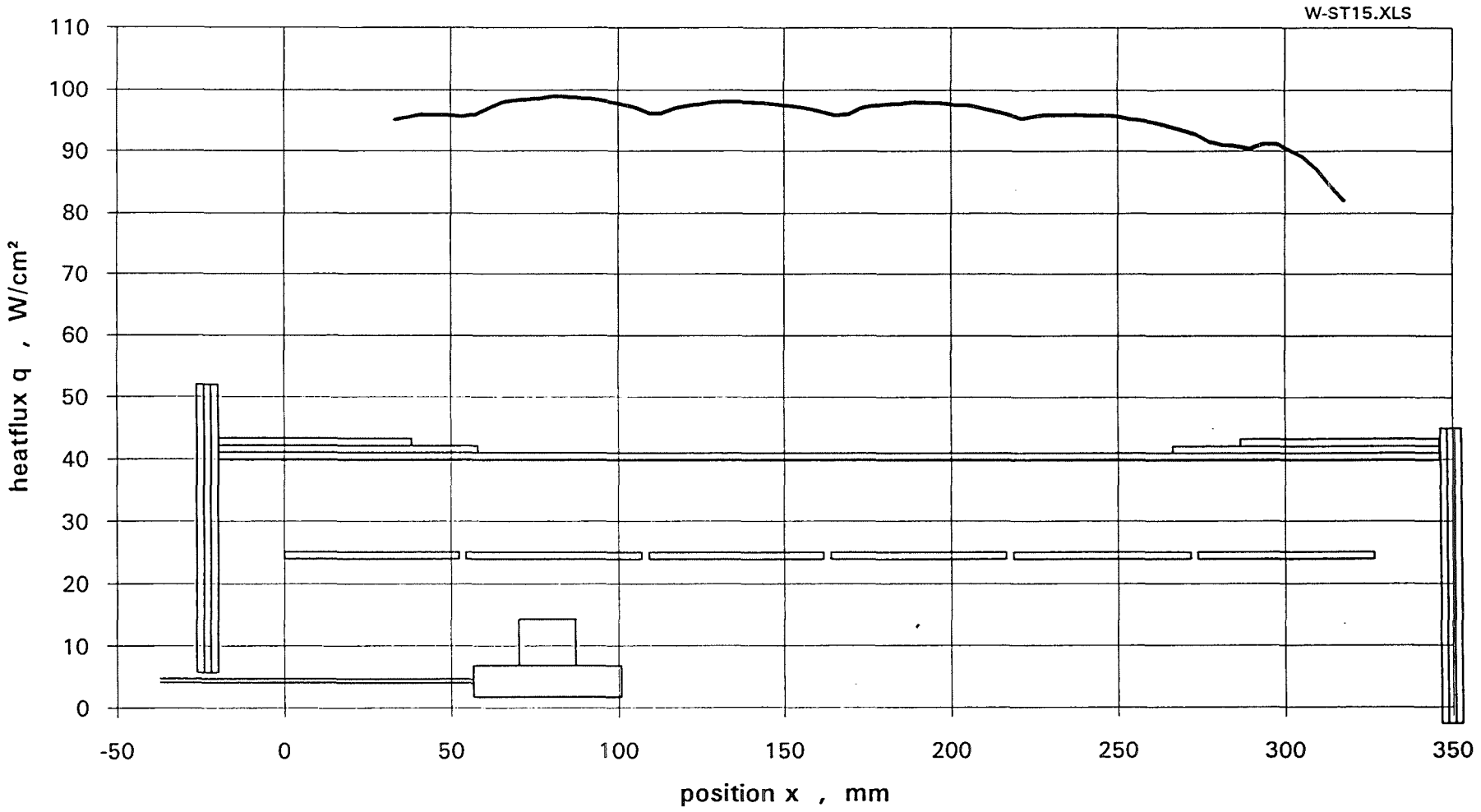

Fig. B-14 Heatflux distribution on the x-traverse for y = -103 mm at Ns = 90 kW/heater element

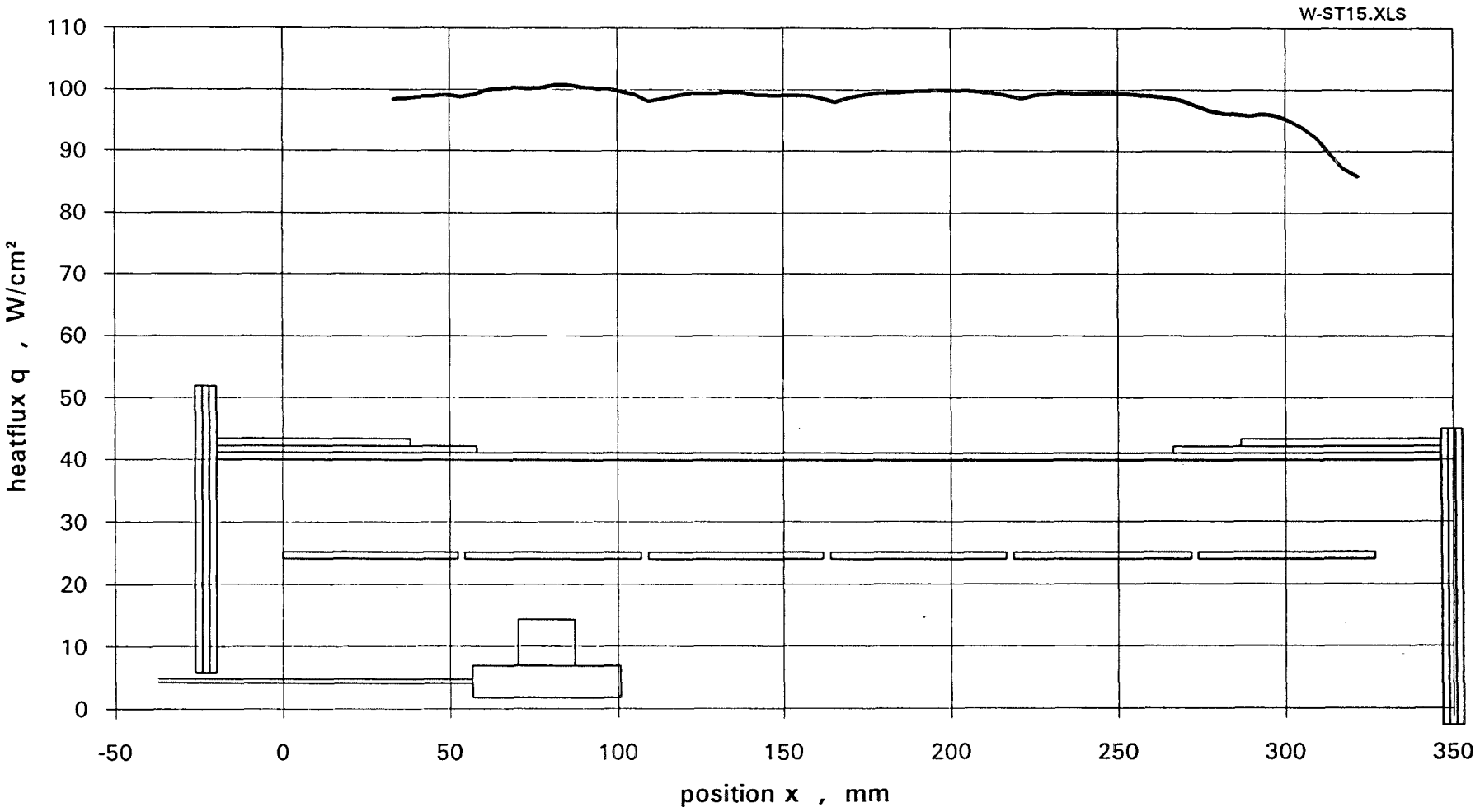

Fig. B-15 Heatflux distribution on the x-traverse for y = -163 mm at Ns = 90 kW/heater element

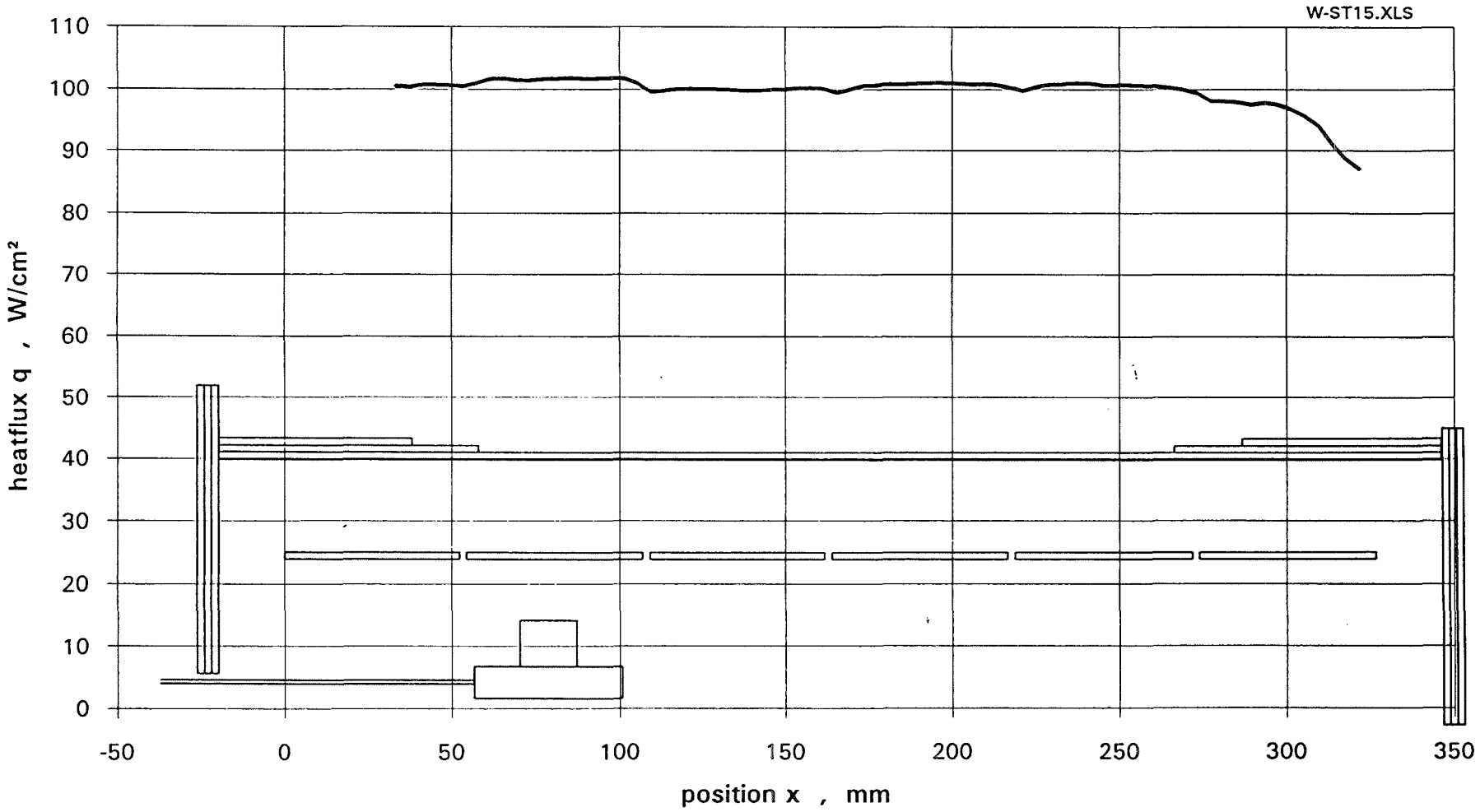

Fig. B-16 Heatflux distribution on the x-traverse for y = -288 mm at Ns = 90 kW/heater element

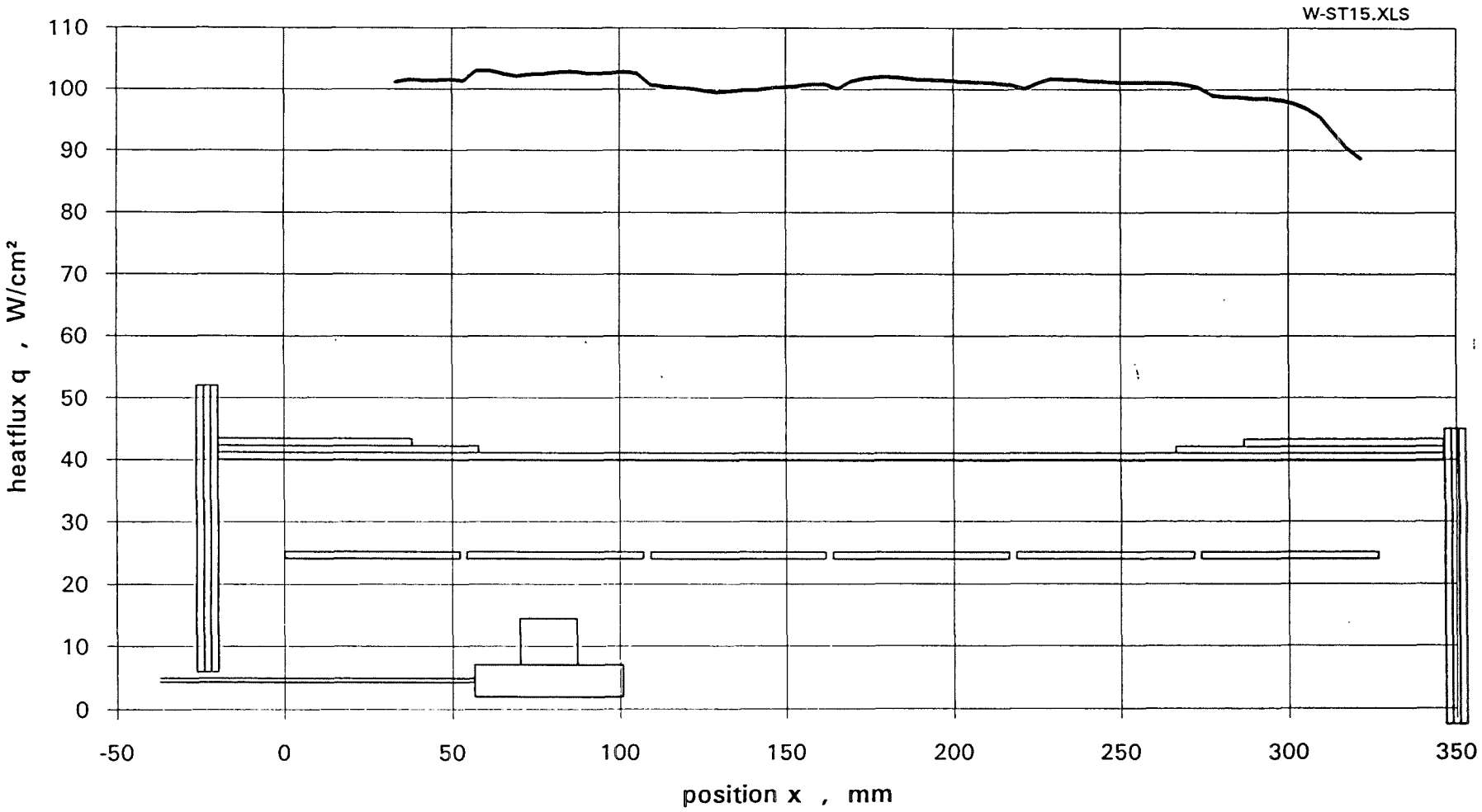

Fig. B-17 Heatflux distribution on the x-traverse for y = -413 mm at Ns = 90 kW/heater element

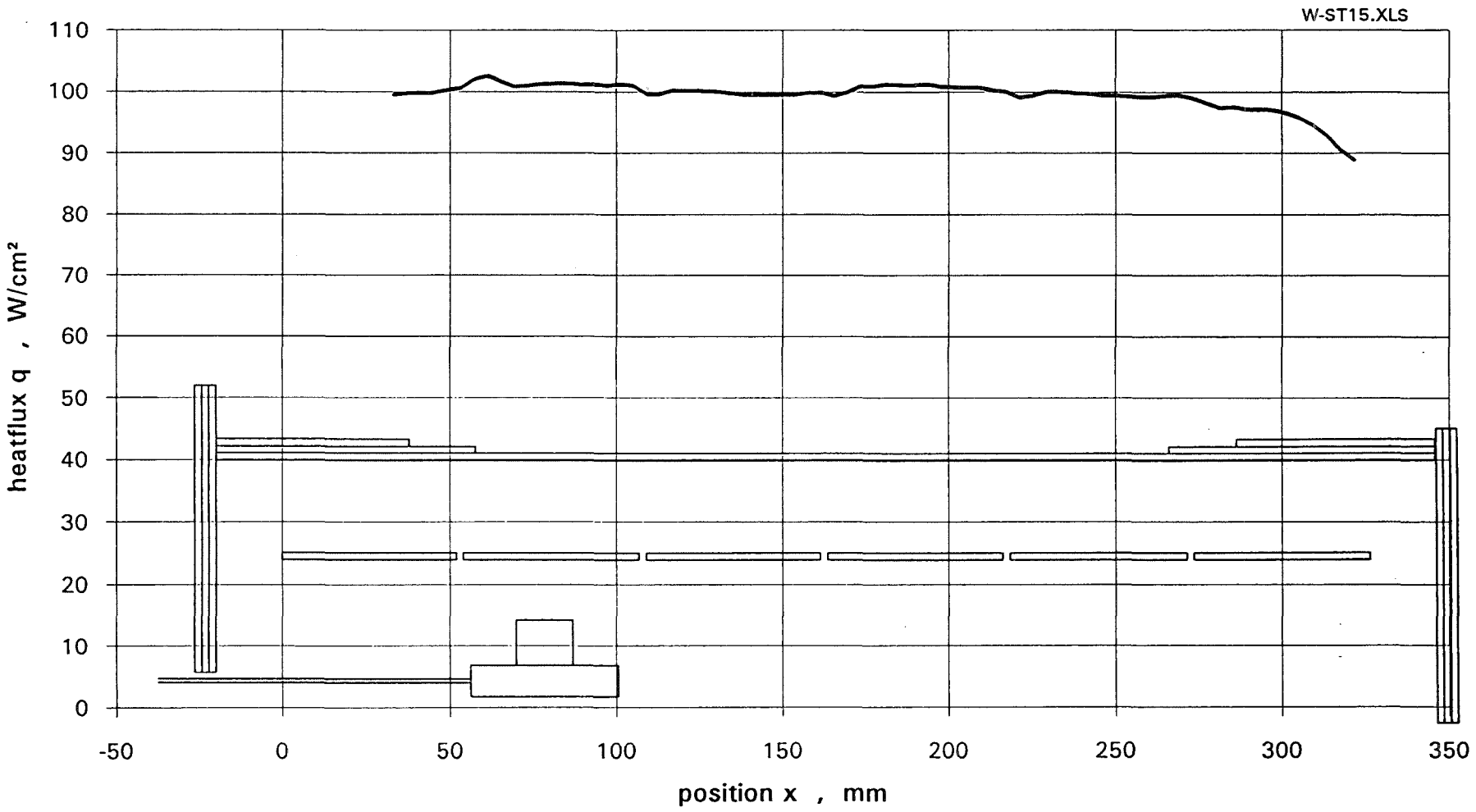

Fig. B-18 Heatflux distribution on the x-traverse for y = -478 mm at Ns = 90 kW/heater element

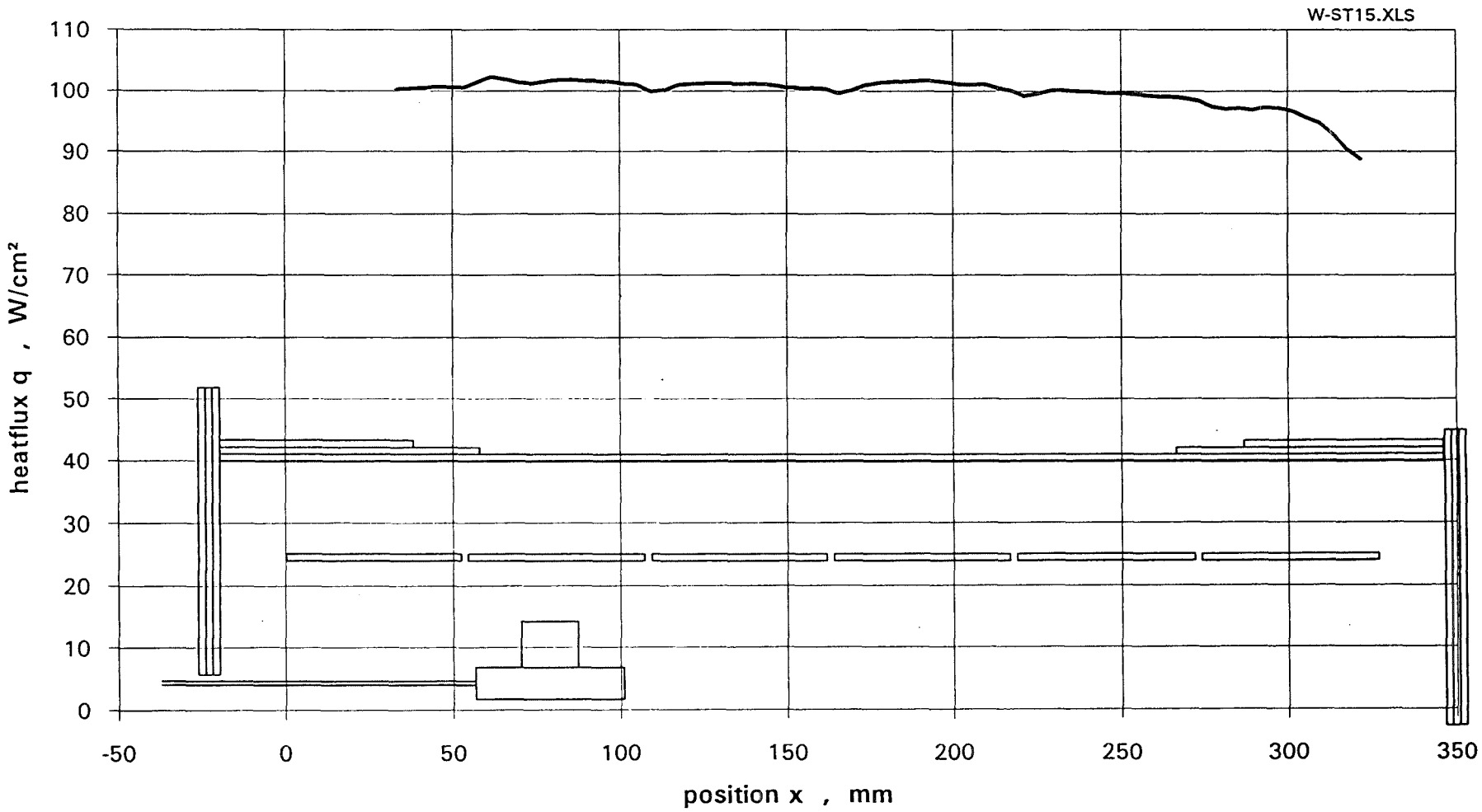

Fig. B-19 Heatflux distribution on the x-traverse for y = -538 mm at Ns = 90 kW/heater element

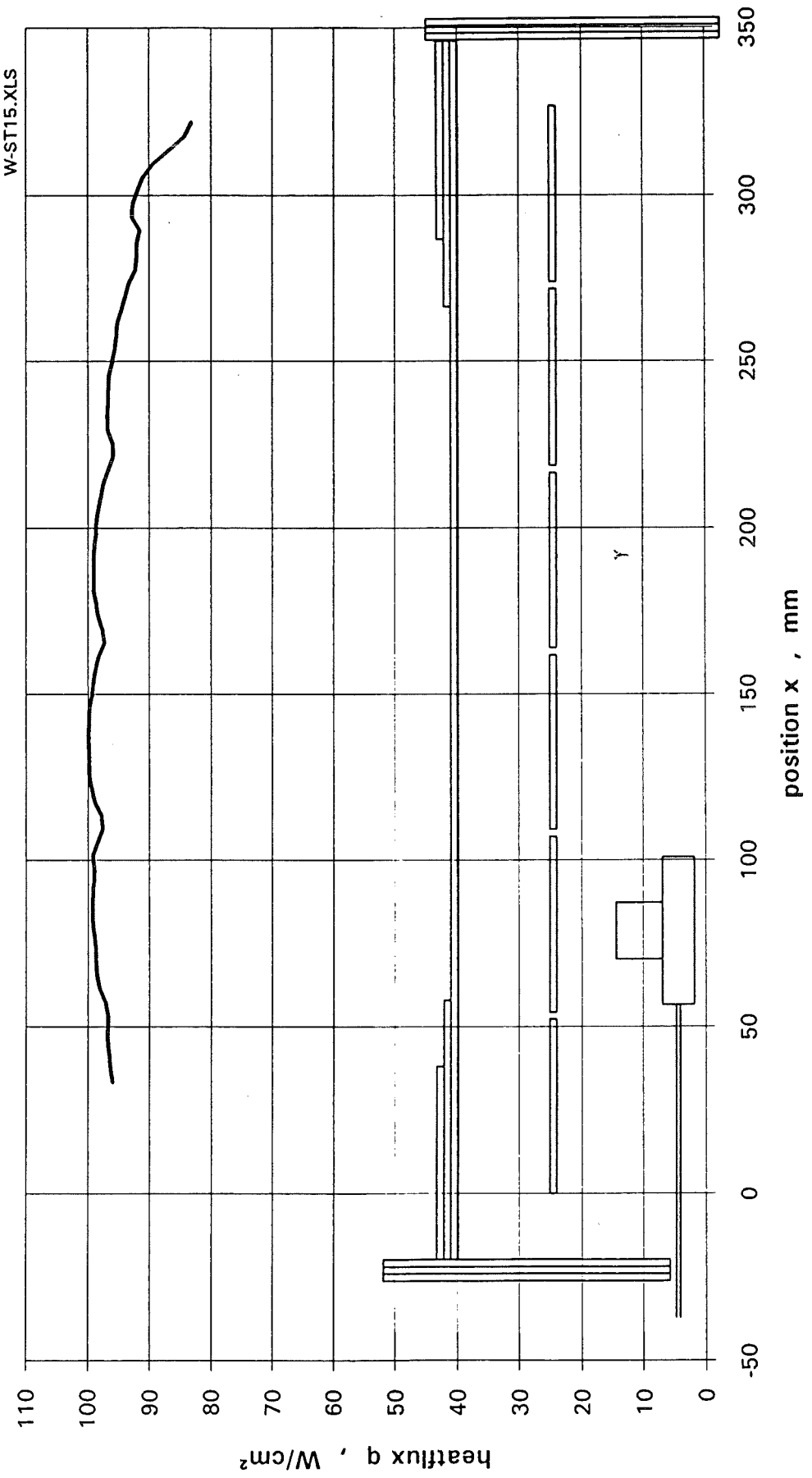

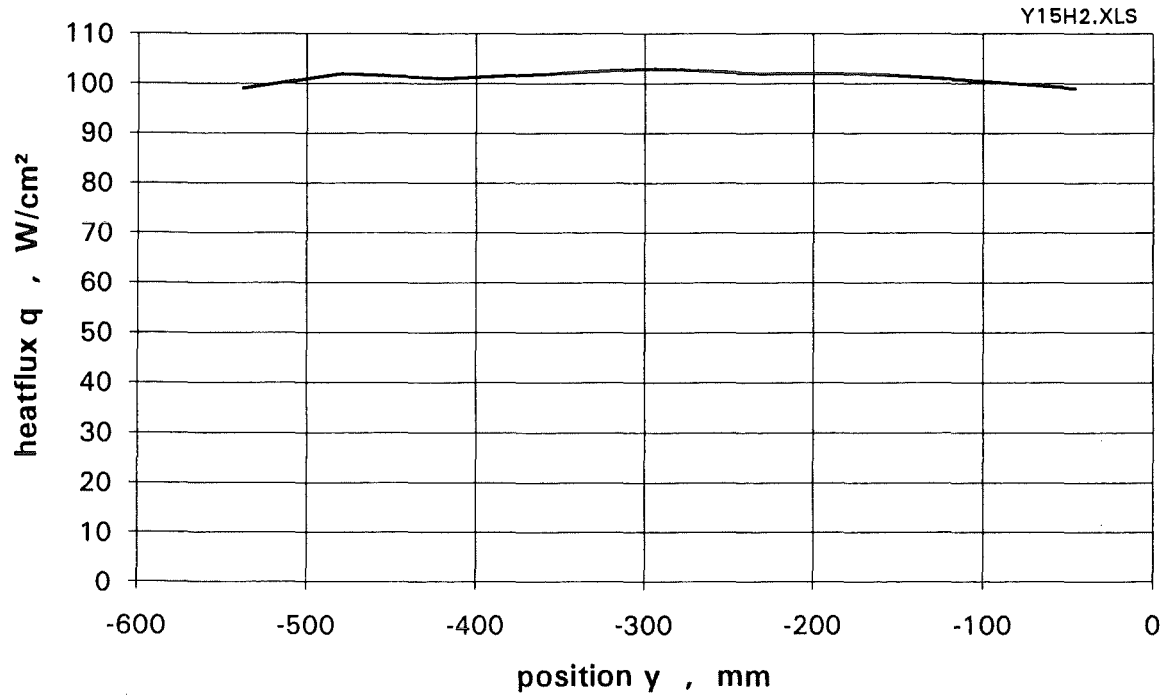

Fig. B-20 Heatflux distribution on the y-traverse
for x = 81 mm at Ns = 90 kW/heater element

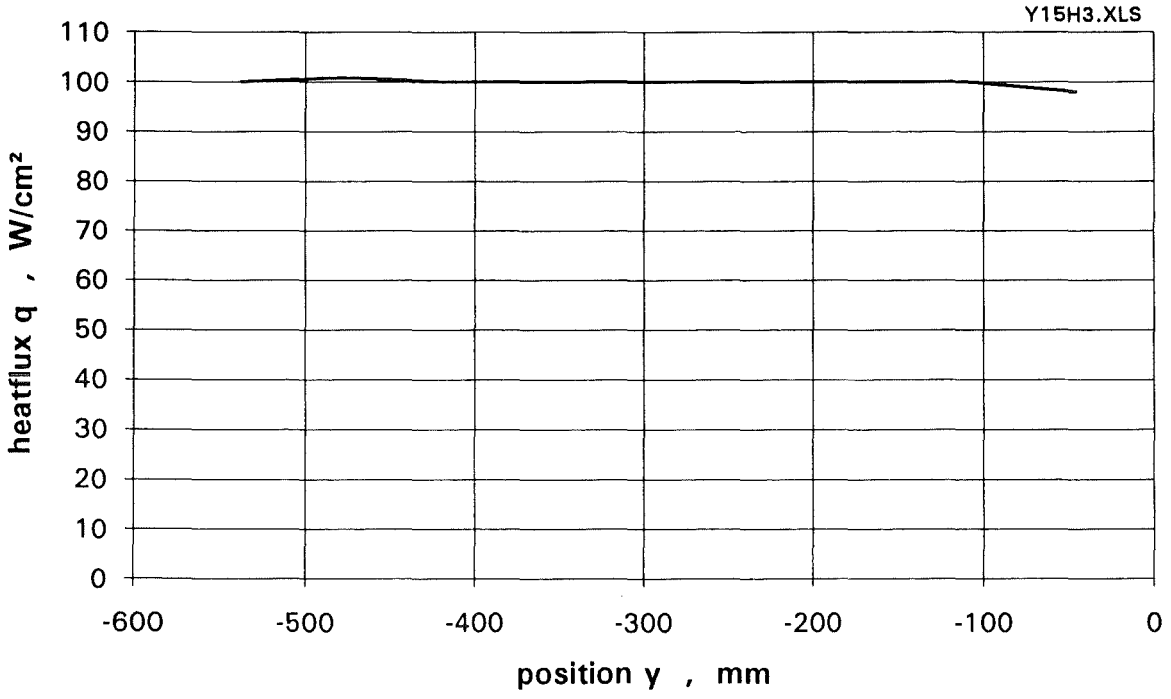

Fig. B-21 Heatflux distribution on the y-traverse
for x = 136 mm at Ns = 90 kW/heater element

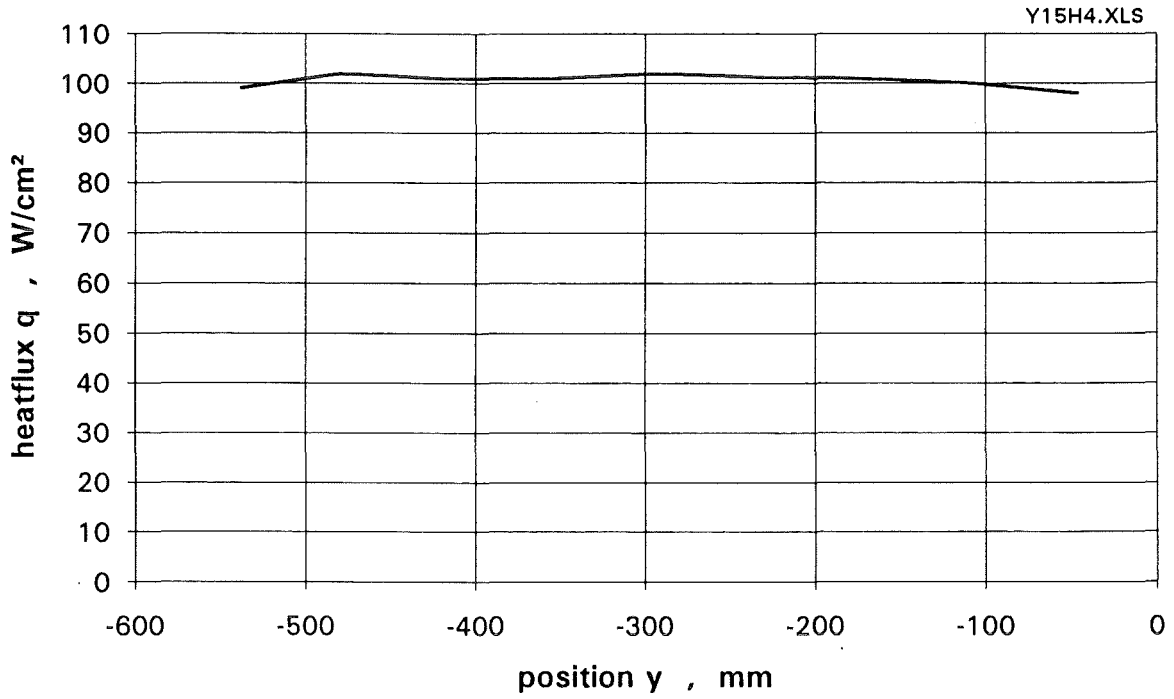

Fig. B-22 Heatflux distribution on the y-traverse for x = 191 mm at Ns = 90 kW/heater element

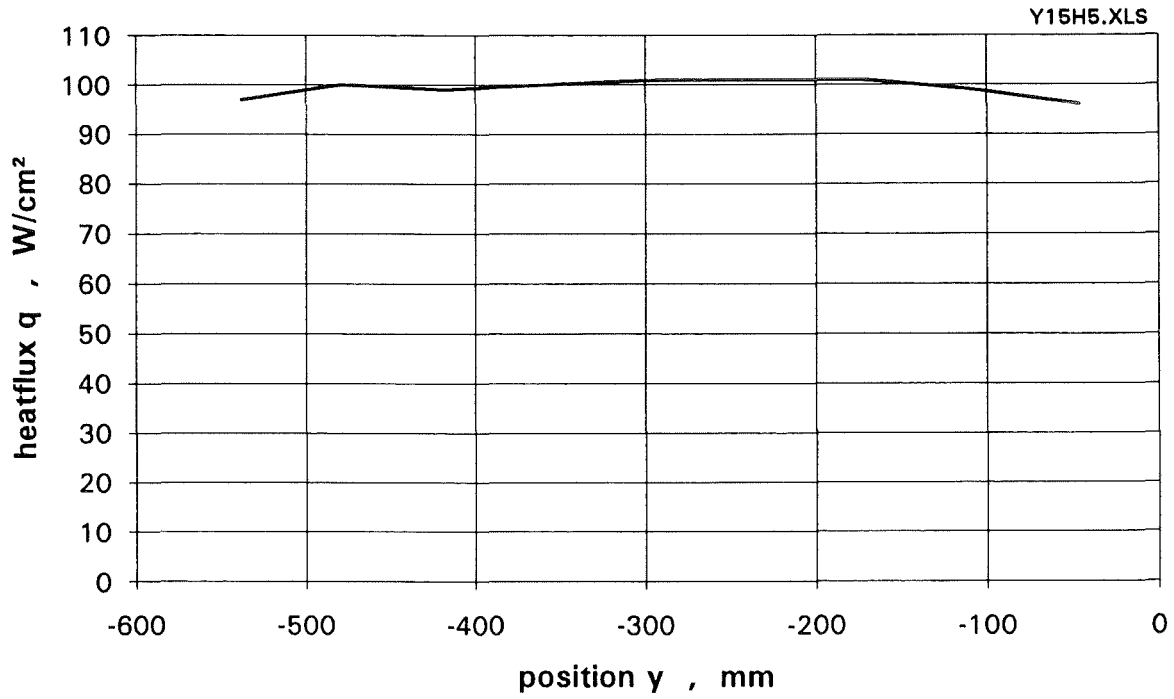

Fig. B-23 Heatflux distribution on the y-traverse for x = 246 mm at Ns = 90 kW/heater element

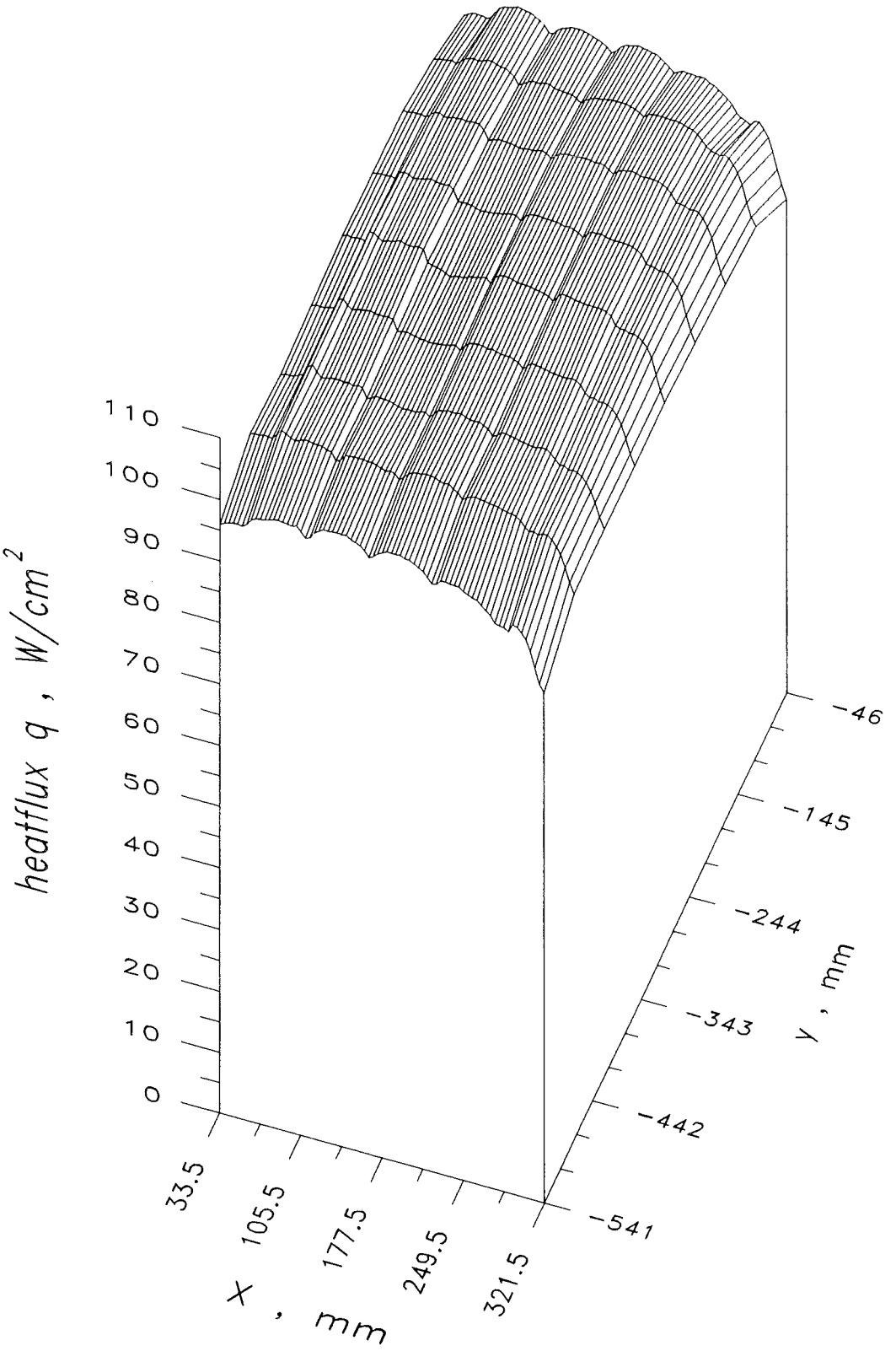

Fig. B-24 Heatflux distribution across the heater at Ns = 90 kW/heater element